

Land Cover Mapping

The use of multi-temporal and multi-sensor spaceborne SAR data

Francesco Holecz fholecz@sarmap.ch



Key objectives

- Understanding the 'object', i.e. the land cover and its dynamic
- Understanding multi-temporal
- Understanding multi-sensor
- Understanding the data
- Understanding the data processing



Content

- 1. Key SAR basics
- 2. Past, existent, forthcoming SAR systems
- 3. SAR data processing
- 4. Agriculture
 - Rice in Asia
 - Small plot agriculture in Africa
- 5. Agriculture and other land covers in Africa
- 6. Forestry
 - Natural forest
 - Forest plantation
 - Bio-physical parameters
- 7. Digital Elevation Model
 - Fusion SAR interferometry-Optical stereo



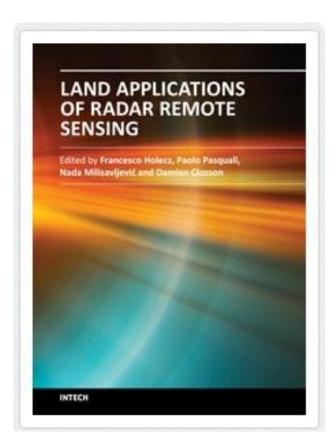
Tutorial



http://earth.eo.esa.int/download/eoedu/Earthnet-website-material/to-access-from-Earthnet/2008_Bilko-SAR-Land-Applications-Tutorial/



Book



The aim of this book is to demonstrate the use of SAR data in three application domains, i.e. land cover (Part II), topography (Part III), and land motion (Part IV). These are preceded by **Part I**, where an extensive and complete review on speckle and adaptive filtering is provided, essential for the understanding of SAR images. **Part II is dedicated to land cover mapping**. **Part III** is devoted to the generation of Digital Elevation Models based on radargrammetry and on a sensor and acquisition mode dependent fusion of interferometric and photogrammetric elevation data. **Part IV** provides a contribution to three applications related to land motion.

http://www.intechopen.com/books/land-applications-of-radar-remote-sensing



Content

1. Key SAR basics

- 2. Past, existent, forthcoming SAR systems
- 3. SAR data processing
- 4. Agriculture
 - Rice in Asia
 - Small plot agriculture in Africa
- 5. Agriculture and other land covers in Africa
- 6. Forestry
 - Natural forest
 - Forest plantation
 - Bio-physical parameters
- 7. Digital Elevation Model
 - Fusion SAR interferometry-Optical stereo



Focus on

- Understanding the 'object'
- Define the approach

Wise use of multi-temporal and multi-sensor data

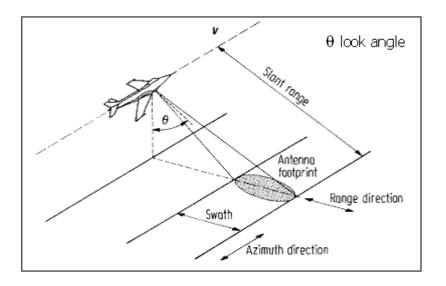


Acquisition modes and techniques

SAR		InSAR	Single-Baseline PolInSAR	Multi-Baseline PolInSAR
Scalar SAR	Vectorial SAR (PolSAR)	Scalar Interferometry	Vectorial Interferometry	
s	[s]		$[S_1][S_2]$	$\begin{bmatrix} S_2 \end{bmatrix} \begin{bmatrix} S_3 \end{bmatrix} \begin{bmatrix} S_4 \end{bmatrix}$



SAR system 1/2



Slant Range

Image direction as measured along the sequence of line-of-sight rays from the radar to each and every reflecting point in the illuminated scene.

Range (pixel) spacing
Azimuth (pixel) spacing
Incidence angle
Swath

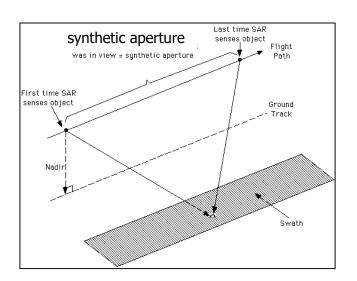
Pixel spacing <u>across</u> track
Pixel spacing <u>along</u> track
Angle from nadir at which target is viewed
Width of the imaged scene in the range direction



SAR system 2/2

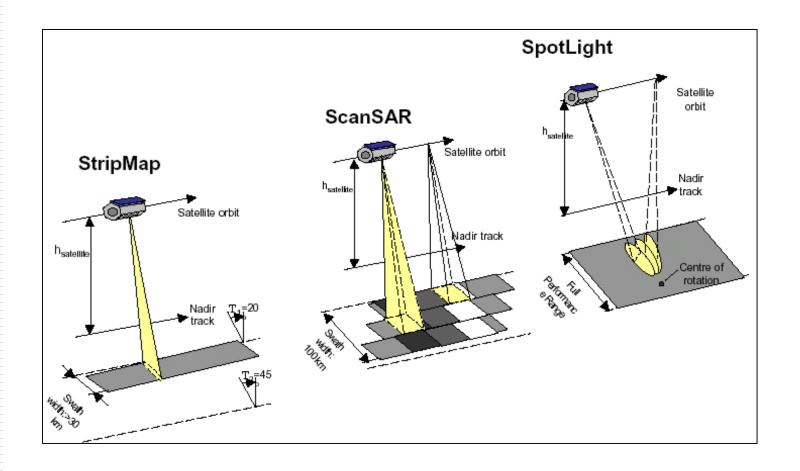
SAR takes advantage of the Doppler history of the radar echoes generated by the forward motion of the spacecraft to synthesise a large antenna. This allows high azimuth resolution in the resulting image despite a physically small antenna. As the radar moves, a pulse is transmitted at each position. The return echoes pass through the receiver and are recorded in an echo store.

SAR requires a complex integrated array of onboard navigational and control systems, with location accuracy provided by both Doppler and inertial navigation equipment. For spaceborne SAR sensors orbiting about **900km** from the Earth, the area on the ground covered by a single transmitted pulse (footprint) is about **5km** long in the along-track (azimuth) direction.





SAR acquisition modes

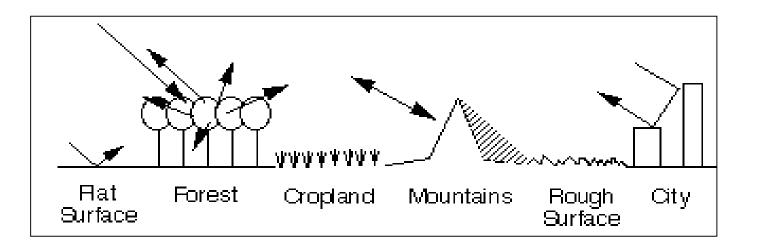




Backscattering coefficient 1/4

SAR images represent an estimate of the radar backscatter for that area on the ground.

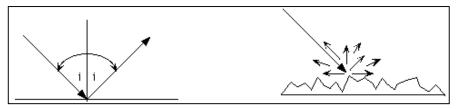
Backscatter at a particular wavelength will vary for a variety of conditions, such as the **physical size of the scatterers**, the **electrical properties** and the **moisture content**. The **wavelength** and **polarisation** of the SAR pulses, and the observation angles will also affect backscatter.





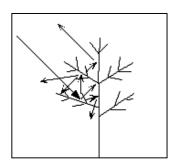
Backscattering coefficient 2/4

A useful rule-of-thumb in analysing radar images is that the higher or brighter the backscatter on the image, the rougher the surface being imaged. Flat surfaces that reflect little or no radio or microwave energy back towards the radar will always appear dark in radar images.



Surface Scattering

Vegetation is usually moderately rough on the scale of most radar wavelengths and appears as grey or light grey in a radar image.

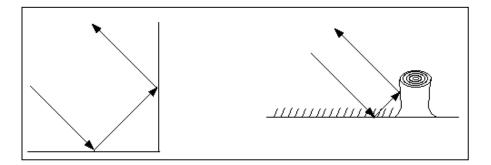


Volume Scattering



Backscattering coefficient 3/4

Surfaces inclined towards the radar will have a stronger backscatter than surfaces which slope away from the radar and will tend to appear brighter in a radar image. Some areas not illuminated by the radar, like the back slope of mountains, are in shadow, and will appear dark.



Double Bounce

When city streets or buildings are lined up in such a way that the incoming radar pulses are able to bounce off the streets and then bounce again off the buildings (called a double-bounce) and directly back towards the radar they appear very bright (white) in radar images. Roads and freeways are flat surfaces and so appear dark. Buildings which do not line up so that the radar pulses are reflected straight back will appear light grey, like very rough surfaces.



Backscattering coefficient 4/4

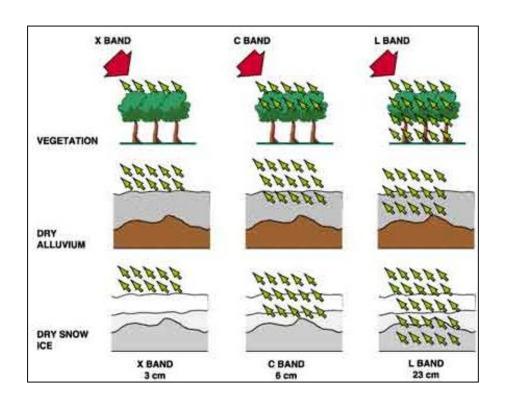
Dielectric Properties

Radar backscatter also depends on the dielectric properties of the target: for metal and water the dielectric constant is high (80), while for most other materials it is relatively low: in dry conditions, the dielectric constant ranges from 3 to 8. This means that wetness of soils or vegetated surfaces can produce a notable increase in radar signal reflectivity.

Based on this phenomenon, SAR systems are also used to retrieve the soil moisture content - primarily - of bare soils. The measurement is based on the large contrast between the dielectric properties of dry and wet soils. As the soil is moistened, its dielectric constant varies from approximately 2.5 when dry to about 25 to 30 under saturated conditions. This translates to an increase in the reflected energy. It is worth mentioning that the inference of soil moisture from the backscattering coefficient is feasible but limited to the use of polarimetric and dual frequency (C-, L-band) SAR sensors, in order to separate the effect of soil roughness and moisture.



Frequency

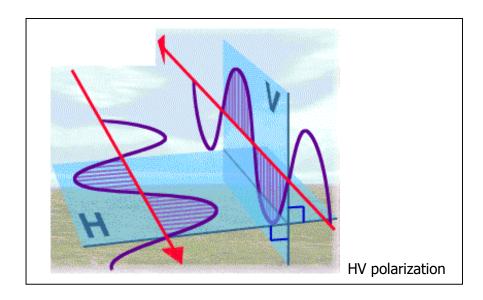


Depending on the frequency and polarization, waves can penetrate into the vegetation and, on dry conditions, to some extent, into the soil (for instance dry snow or sand). Generally, the longer the wave-length, the stronger the pene-tration into the target is. With respect to the polarization, cross-polarized (VH/HV) acquisitions have a significant weaker penetration than co-polarized (HH/VV) ones.



Polarization

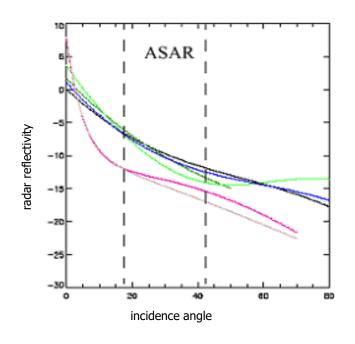
Irrespective of wavelength, radar signals can transmit horizontal (H) or vertical (V) electric-field vectors, and receive either horizontal (H) or vertical (V) return signals, or both. The basic physical processes responsible for the like-polarised (HH or VV) return are quasi-specular surface reflection. For instance, calm water (i.e. without waves) appears black. The cross-polarised (HV or VH) return is usually weaker, and often associated with different reflections due to, for instance, surface roughness.





Incidence angle

The incidence angle (θ) is defined as the angle formed by the radar beam and a line perpendicular to the surface. Microwave interactions with the surface are complex, and different reflections may occur in different angular regions. Returns are normally strong at low incidence angles and decrease with increasing incidence angle.



The plot shows the radar reflectivity variation for different land cover classes (colours), while the dashed lines highlight the swath range for ENVISAT ASAR data.

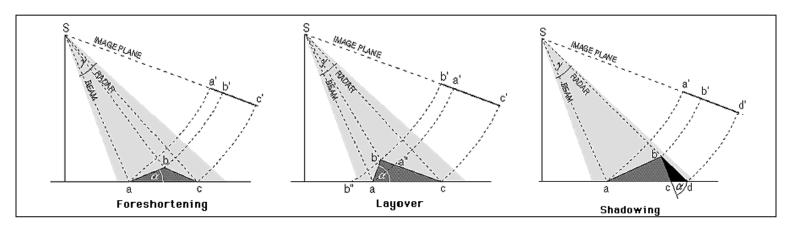
Note that this angular dependence of the radar backscatter can be exploited, by choosing an optimum configurations for different applications.



SAR Geometry

Geometry in Range

The points a,b, and c are imaged as a',b', and c' in the slant range plane (see figure). This shows how minor differences in elevation can cause considerable range distortions. These relief induced effects are called foreshortening, layover and shadow.



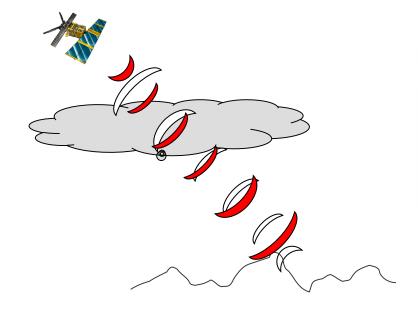
Layover is an extreme case of foreshortening, where the slope α is bigger than the incidence angle (θ). With an increasing (horizontal) distance, the slant range between sensor and target decreases.

Shadow is caused by objects, which cover part of the terrain behind them.

www.sarmap.ch June 2013



Synthetic Aperture Radar (SAR) - Intensity





SAR Intensity Image



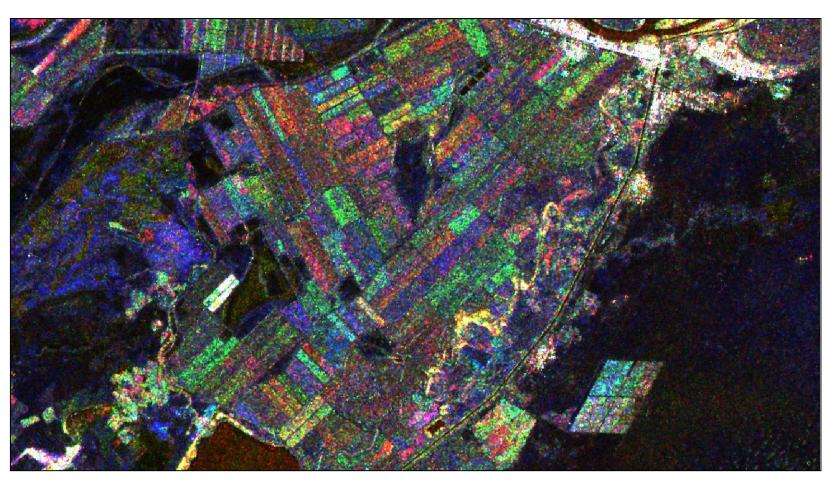
L-band HH-Polarization



19 May, 4 July, 19 August 2006



C-band HH-Polarization

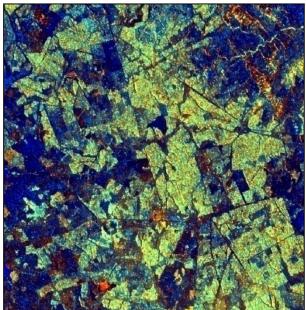


22 May, 12 July, 16 August 2006



Frequency and Polarization







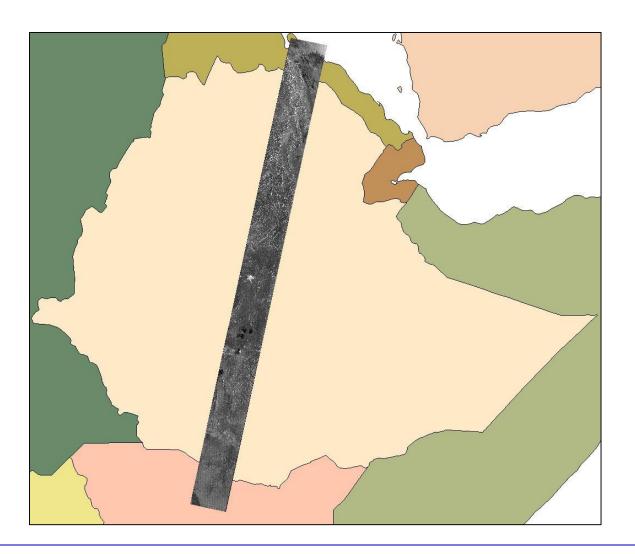
L-band HH-HV

C-band HH-HV

X-band HH-HV

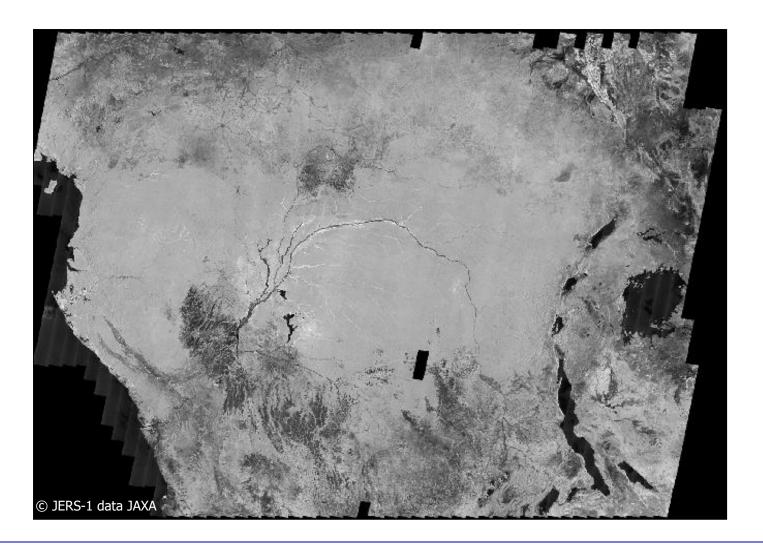


From frame to strip ...



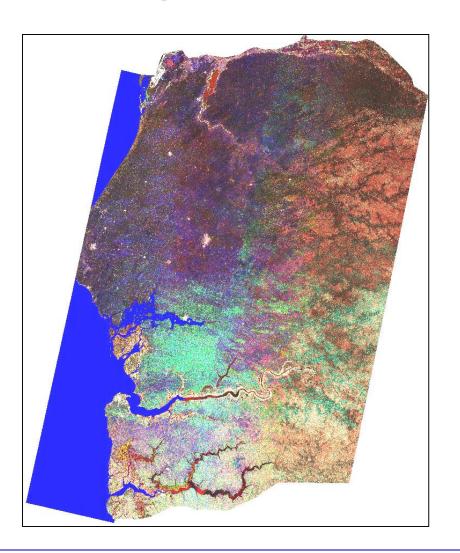


... from strips to mosaic ...





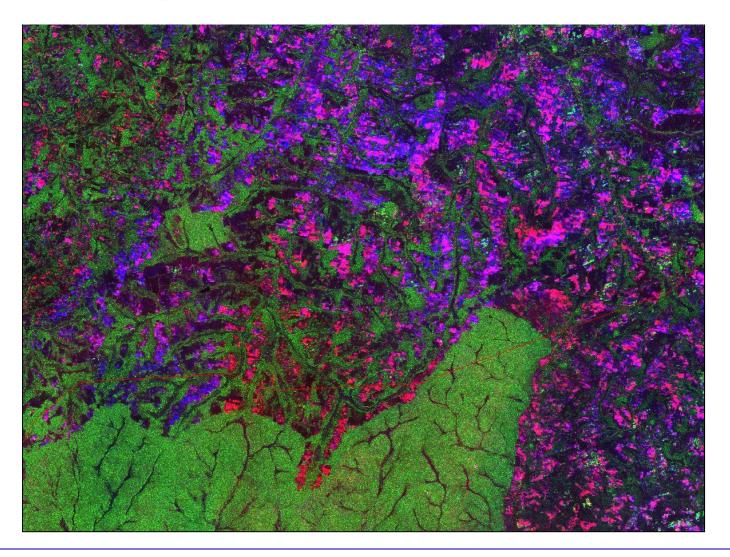
... to multi-temporal mosaic ...



This product includes around 180 **multi-temporal** ENVISAT ASAR images processed in a fully automated way.

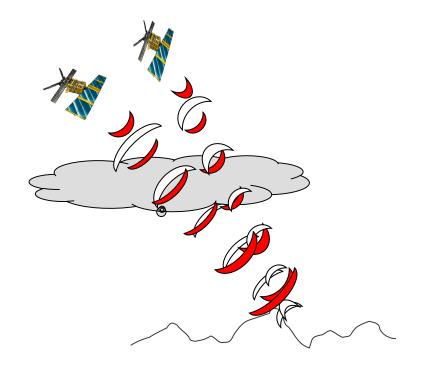


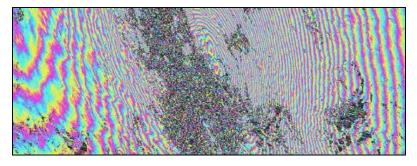
... to multi-temporal multi-sensor mosaic





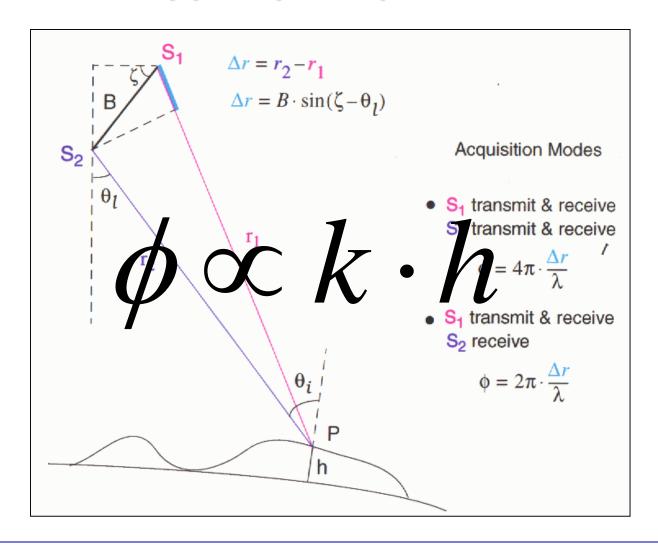
Synthetic Aperture Radar (SAR) - SAR Interferometry







SAR Interferometry (InSAR) - Principle





Coherence (interferometric correlation)

Given two co-registered complex SAR images (S_1 and S_2), one calculates the coherence (γ) as a ratio between coherent and incoherent summations:

$$\gamma = \frac{\left|\sum s_1(x) \cdot s_2(x)^*\right|}{\sqrt{\sum |s_1(x)|^2 \cdot \sum |s_2(x)|^2}}$$

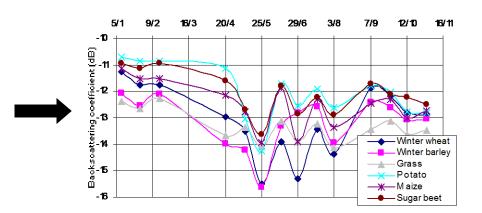
Note that the observed coherence - which ranges between 0 and 1 - is, in primis, a function of systemic spatial decorrelation, the additive noise, and the scene decorrelation that takes place between the two acquisitions.

In essence coherence has, in primis, a twofold purpose:

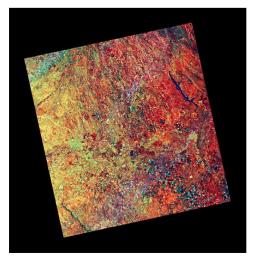
- To determine the quality of the measurement (i.e. interferometric phase). Usually, phases having coherence values lower than 0.2 should not be considered for the further processing.
- To extract thematic information about the object on the ground in combination with the backscattering coefficient (σ^{o}).

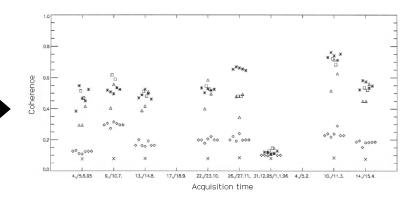


Intensity and Coherence



Intensity

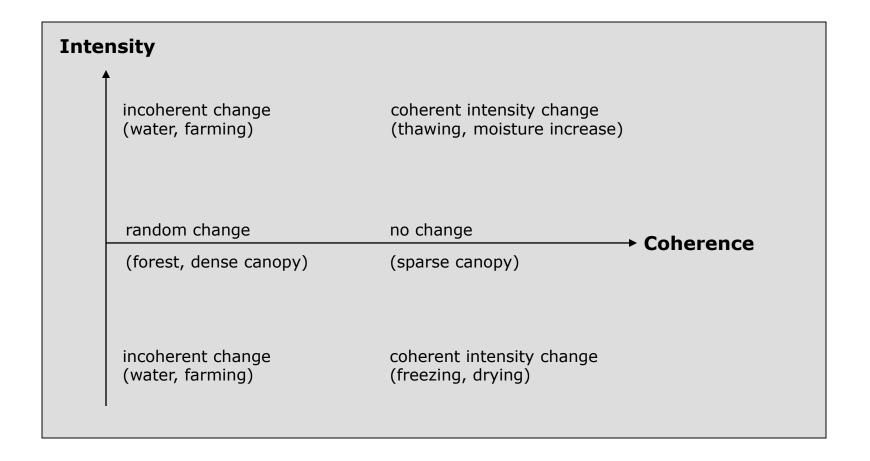




Coherence

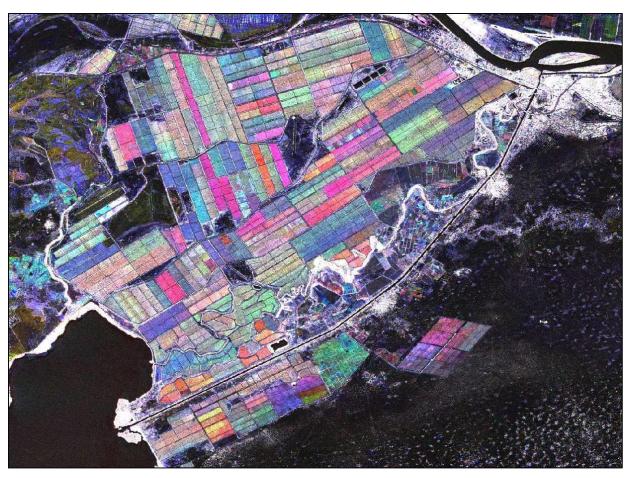


Intensity and Coherence – Information content





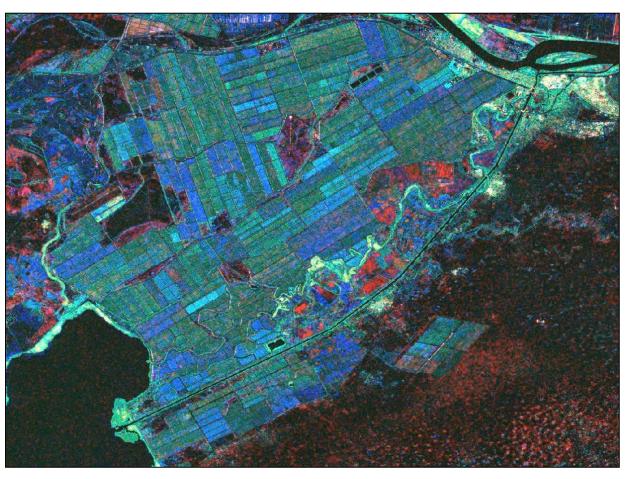
L-band HH-Polarization



19 May, 4 July, 19 August 2006



L-band Intensity & Coherence



coherence mean intensity intensity change

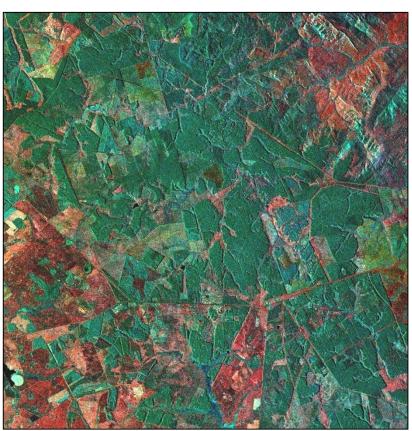
4 July -19 August 2006



Intensity vs. Coherence & Intensity



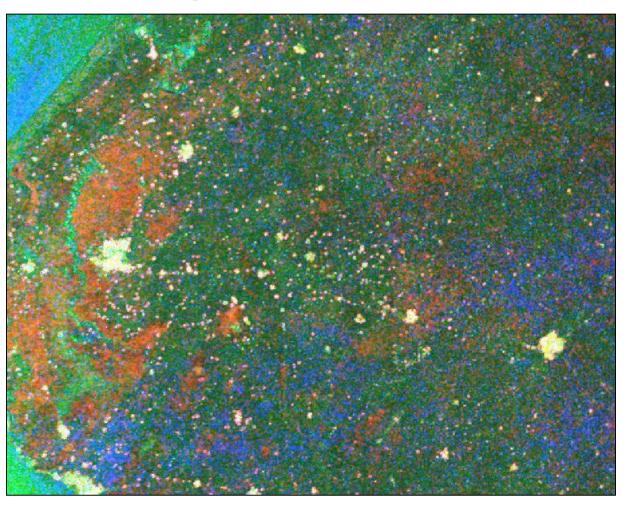




coherence mean intensity intensity change



C-band Intensity & Coherence

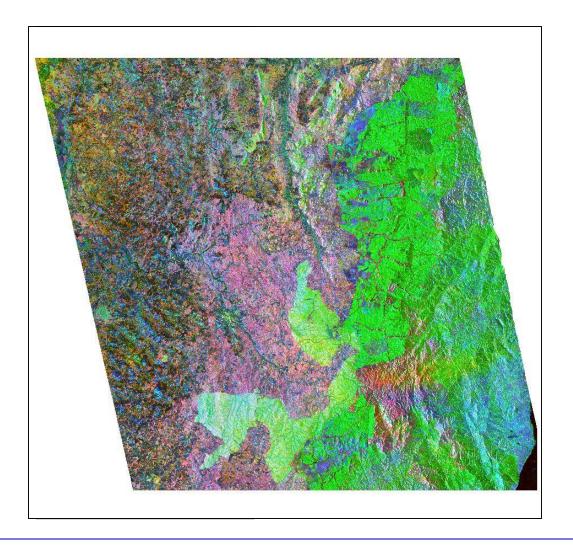


May - June 2005

Coherence Mean Intensity Intensity Change

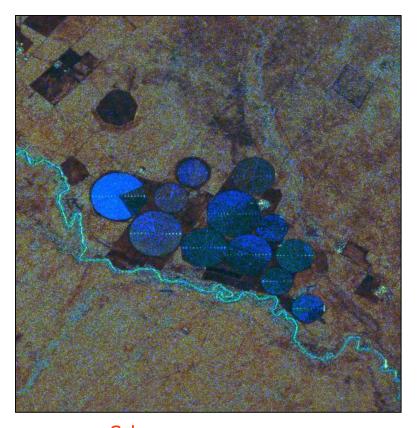


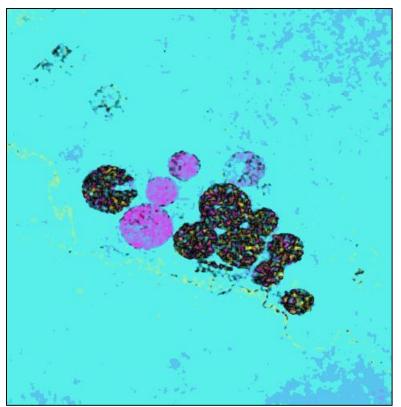
Interferometric mosaic at country level





Crop monitoring using L-HH interferometric data





Coherence Mean Intensity Intensity Change

Differential interferometric phase



Content

- 1. Key SAR basics
- 2. Past, existent, forthcoming SAR systems
- 3. SAR data processing
- 4. Agriculture
 - Rice in Asia
 - Small plot agriculture in Africa
- 5. Agriculture and other land covers in Africa
- 6. Forestry
 - Natural forest
 - Forest plantation
 - Bio-physical parameters
- 7. Digital Elevation Model
 - Fusion SAR interferometry-Optical stereo

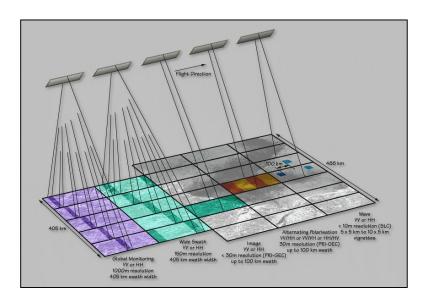


Past, existent, and forthcoming SAR systems

ERS-1/2	ESA	1991-00/1995	C-band
JERS-1 SAR	JAXA	1993-98	L-band
RADARSAT-1	CSA & MDA	1995-12	C-band
ENVISAT ASAR	ESA	2001-12	C-band
ALOS PALSAR-1	JAXA	2006-11	L-band
TerraSAR-X-1/2	Germany	2007/10	X-band
RADARSAT-2	MDA	2007	C-band
COSMO-SkyMed-1/2/3/4	ASI	2008/10	X-band
RISAT-1	ISRO	2012	C-band
KOMPSAT-5	KARI	2013	X-band
PAZ-1	INTA	2013	X-band
Sentinel-1 A	ESA	2014	C-band
ALOS-2	JAXA	2014	L-band
Sentinel-1 B	ESA	2016	C-band
COSMO-SkyMed-5/6/7/8	ASI	2016	X-band
ASNARO constellation	JAXA	2016	X-band
SAOCOM-1/2	CONAE	2016/17	L-band
PAZ-2	INTA	2017	X-band
JV-LOTUSat-1/2	Vietnam	2017/21	X-band
BIOMASS SAR	ESA	2020	P-band



ENVISAT ASAR



Agency

Acquisition Modes

Frequency

Polarization

Ground Resolution 15 to 100 m

Swath

Repeat cycle

Mission Duration

European Space Agency

StripMap and Wide Swath

C-band

Single and Dual

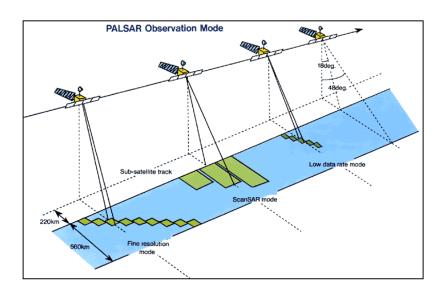
100 to 405 km

35 / 30 (after December 2010) days

2001-2012



ALOS PALSAR-1



Agency

Acquisition Modes

Frequency

Polarization

Ground Resolution 7 to 100 m

Swath

Repeat Cycle

Mission Duration

Japan Aerospace Exploration Agency

StripMap and ScanSAR

L-band

Single, Dual, Full

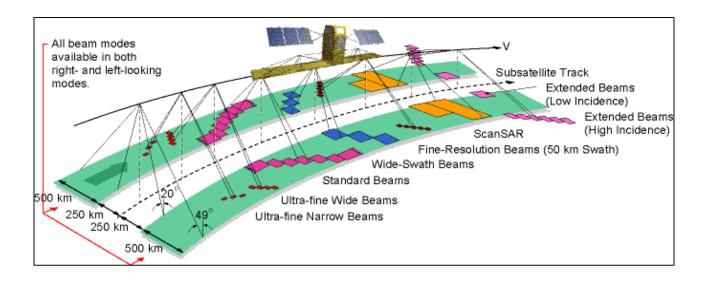
70 to 350 km

44 days

2006-2011



RADARSAT-2



Agency Canadian Space Agency and MacDonald Dettwiler (MDA)

Acquisition Modes SpotLight, Stripmap and ScanSAR

Frequency C-band

Polarization Single, Dual, Full

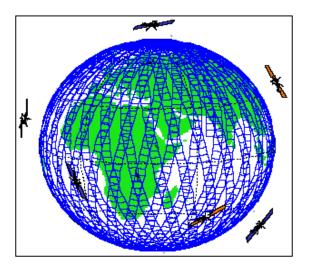
Ground Resolution **1 to 160 m**Swath 18 to 500 km

Repeat cycle 24 days

Launch 2007



Cosmo-SkyMed-1-2-3-4



Agency Italian Space Agency (ASI)

Acquisition Modes SpotLight, StripMap and ScanSAR

Frequency X-band

Polarization HH, VV, HV

Ground Resolution 1 to 15 m

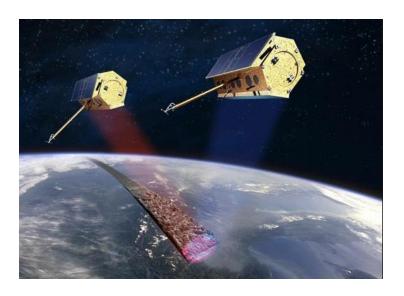
Swath 10 to 220 km

Repeat cycle 16 days

Launch 2008-2010



TerraSAR-X-1/2 (TanDEM-X)



Agency

Acquisition Modes

Frequency

Polarization

Ground Resolution 1 to 16 m

Swath

Repeat cycle

Launch

Infoterra, Germany

Stripmap, ScanSAR and Spotlight

X-band

Single Pol, Dual Pol, Full Pol

15 to 60 km

11 days

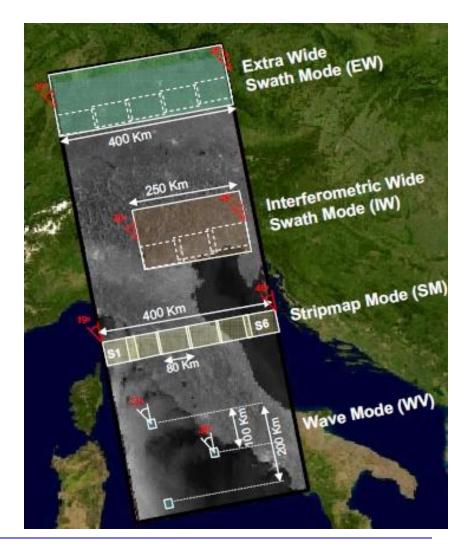
2006/2011





Agency Acquisition Modes Frequency Polarization Ground Resolution 5 to 50 m Swath Repeat Cycle A Repeat Cycle A+B Launch

ESA SM, IW, EW **C-band** Dual 80 to 400 km 12 days 6 days 2014 / 2016



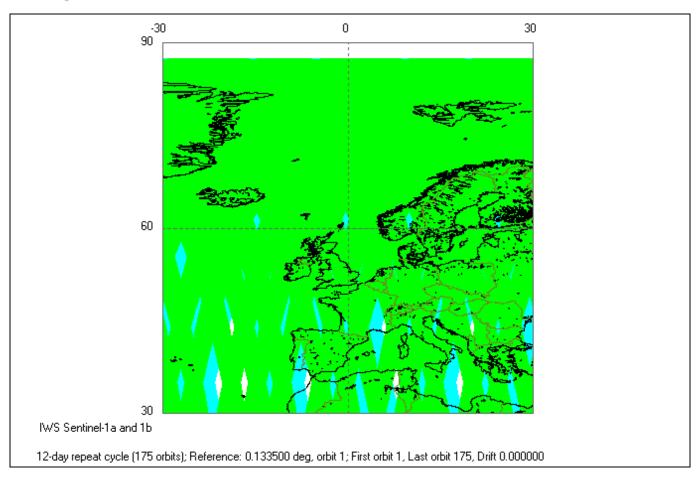


Mode	Access Angle	GR <u>Single Look</u> Resolution	Swath Width	Polarisation
Strip Map	20-45 deg.	Range 5 m Azimuth 5 m	> 80 km	HH or VV or HH+HV or VV+VH
Interferometric Wide Swath	> 25 deg.	Range 5 m Azimuth 20 m	> 250 km	HH or VV or HH+HV or VV+VH
Extra Wide Swath	> 20 deg.	Range 20 m Azimuth 40 m	> 400 km	HH or VV or HH+HV or VV+VH
Wave mode	23 deg. & 36.5 deg.	Range 5 m (TBC) Azimuth 5 m (TBC)	> 20 x 20 km Vignettes at 100 km intervals	HH or VV



Acq. Mode	Product Type	Resolution Class	Resolution [Rng x Azi] [m]	Pixel Spacing [Rng x Azi]	No. Looks [Rng x Azi]	ENL
	SLC	-	1.7 x 4.3 to 3.6 x 4.9	1.5 x 3.6 to 3.1 x 4.1	1 x 1	1
SM GRD		FR	9 x 9	4 x 4	2 x 2	3.9
	HR	23 x 23	10 x10	6 x 6	34.4	
	MR	84 x 84	40 x 40	22 x 22	464.7	
•		•		•	•	
	SLC	-	2.7 x 22 to 3.5 x 22	2.3 x 17.4 to 3 x 17.4	1	1
IW GRD	HR	20 x 22	10 x 10	5 x 1	4.9	
	GRD	MR	88 x 89	40 x 40	22 x 5	105.7
•				•	•	
	SLC	-	7.9 x 42 to 14.4 x 43	5.9 x 34.7 to 12.5 x 34.7	1 x 1	1
EW GRD	HR	50 x 50	25 x 25	3 x 1	3	
	MR	93 x 87	40 x 40	6 x 2	12	
<u> </u>				•		
WV	SLC	-	2.0 x 4.8 and 3.1 x 4.8	1.7 x 4.1 and 2.7 x 4.1	1 x 1	1
	GRD	MR	52 x 51	25 x 25	13 x 13	139.7

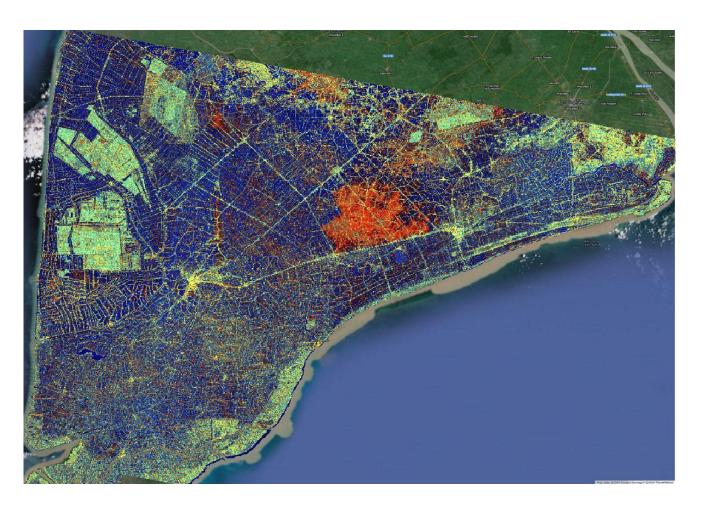




Global coverage every 6 days (1A & 1B) at a resolution of 20 meter



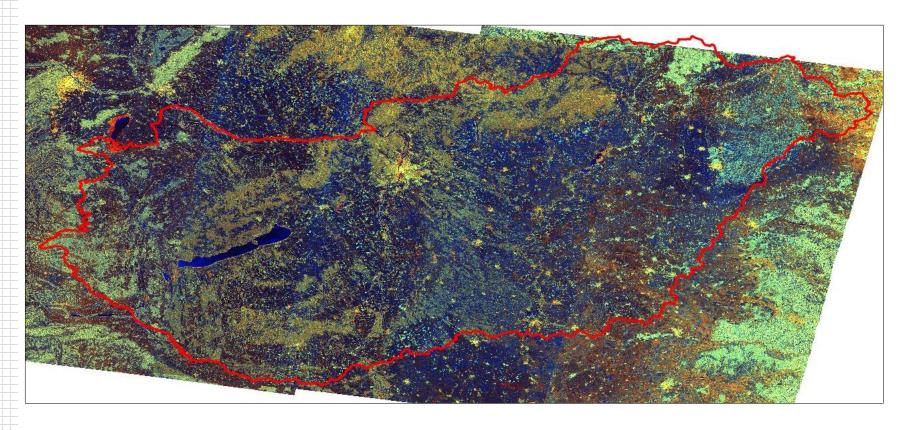
Mekong River – Sentinel-1A



6 October 2014 VV VH VV-VH



Sentinel-1A 12-days cycle, national scale



VV VH VV-VH

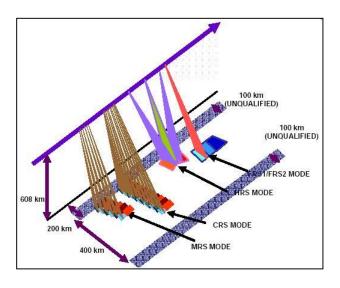


Sentinel-1A 12-days cycle, sub-continental scale





RISAT-1



Agency Indian Space Research Organization

Acquisition Modes SpotLight, StripMap and ScanSAR

Frequency C-band

Polarization Single, Dual, Full

Ground Resolution 3 to 55 m

Swath 30 to 220 km

Repeat cycle 25 days

Launch 2012



ALOS-2



Agency Japan Aerospace Exploration Agency

Acquisition Modes SpotLight, StripMap and ScanSAR

Frequency L-band

Polarization Single, Dual, Full

Ground Resolution **3 to 100 m**Swath 25 to 490 km

Repeat Cycle 14 days Launch 2014

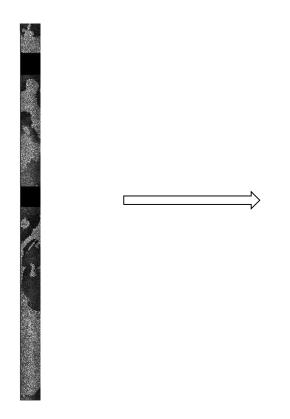


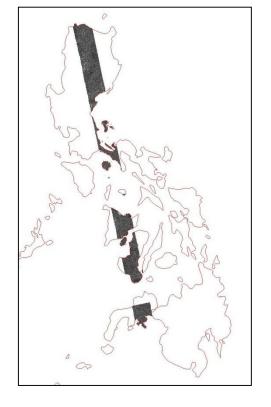
Content

- 1. Key SAR basics
- 2. Past, existent, forthcoming SAR systems
- 3. SAR data processing
- 4. Agriculture
 - Rice in Asia
 - Small plot agriculture in Africa
- 5. Agriculture and other land covers in Africa
- 6. Forestry
 - Natural forest
 - Forest plantation
 - Bio-physical parameters
- 7. Digital Elevation Model
 - Fusion SAR interferometry-Optical stereo



SAR Intensity – From raw data to sigma nought





Input

Single Look Complex data (1-look Intensity displayed)

Output

Terrain geocoded backscattering coefficient (sigma nought)



SAR Intensity – Processing steps

It is assumed the availability of **multi-temporal SAR Intensity data** acquired with the same geometry and mode over the same area.

- 1. Co-registration including Digital Elevation Model (DEM)
- 2. Time series speckle filtering
- 3. Terrain geocoding and radiometric calibration
- 4. Radiometric normalisation
- 5. Anisotropic Non-Linear Diffusion filtering



SAR Intensity – Co-registration

Aim

When multiple images (acquired with the same observation geometry and mode) cover the same area, they can be precisely and automatically co-registered to achieve a sub-pixel accuracy overlap in the satellite viewing geometry; the co-registration is mandatory to apply afterwards the time-series speckle filtering.

Method

- A gross shift estimation is computed based on the orbital data parameters.
- A set of sub-windows is selected automatically based on the reference image and on the image(s) to be co-registered.
- The cross-correlation function is computed between the pixels of corresponding sub-windows in the two images.
- The maximum of the cross-correlation function indicates the proper shift for the selected location.
- The shift to be applied in azimuth direction and range direction is calculated by a polynomial depending on the pixel position respectively in azimuth and range.



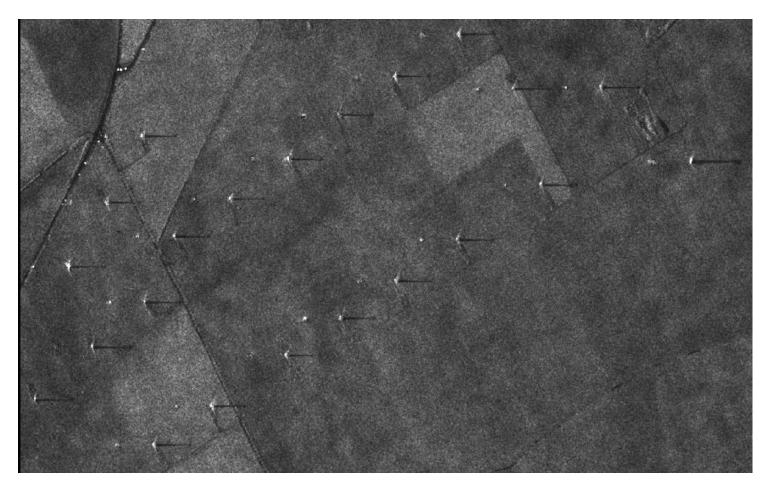
Aim

Images obtained from coherent sensors such as SAR system are characterized by speckle. This is a spatially random multiplicative noise due to coherent superposition of multiple backscatter sources within a SAR resolution element. In other words, the speckle is a statistical fluctuation associated with the radar reflectivity (brightness) of each image pixel.

Method

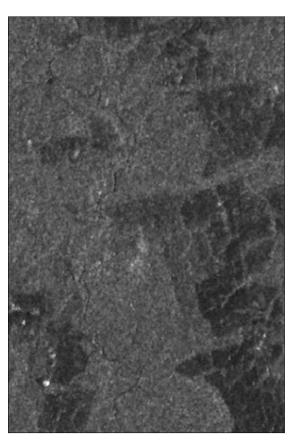
Within the multi-temporal filtering an optimum weighting filter is introduced to balance differences in reflectivity between images at different times. It has to be pointed out that multi-temporal filtering is based on the assumption that the same resolution element on the ground is illuminated by the radar beam in the same way, and corresponds to the same coordinates in the image plane (sampled signal) in all images of the time series. The reflectivity can of course change from one time to the next due to a change in the dielectric and geometrical properties of the elementary scatters, but should not change due to a different position of the resolution element with respect to the radar.

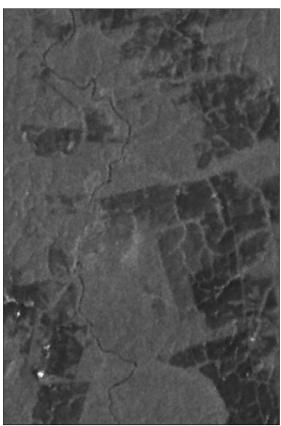




Cosmo-SkyMed StripMap image







Original

Multi-temporal speckle filtered

ALOS PALSAR-1 ScanSAR image





Sentinel-1A IWS data



SAR Intensity – Terrain <u>geocoding</u> and radiometric calibration

Aim

Geocoding, georeferencing, geometric calibration, mapping and ortho-rectification are synonyms. All these definitions correspond to the conversion of SAR images from the original slant range geometry into a map coordinate system (e.g. cartographic reference system).

Method

The geometric correction has to consider the sensor and processor characteristics and thus must be based on a rigorous range-Doppler approach. For each pixel the following two relations must be fulfilled:

$$R = S - P$$
 Range equation
$$f_D = \frac{2f_0(v_p - v_s)R_s}{c|R_s|}$$
 Doppler equation

where

 R_s = Slant range

 \vec{S} , P = Spacecraft and backscatter element position

 v_{s} , v_{n} = Spacecraft and backscatter element velocity

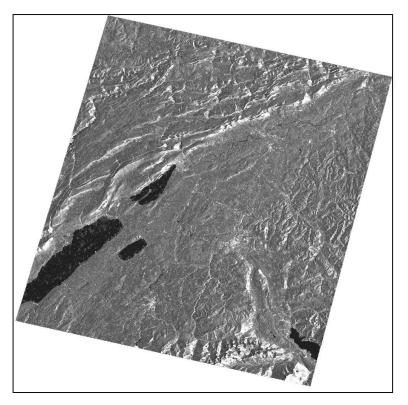
 f_0 = Carrier frequency

c = Speed of light

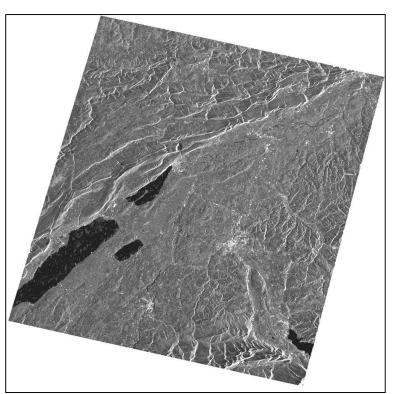
 f_D = Processed Doppler frequency



SAR Intensity – Terrain <u>geocoding</u> and radiometric calibration



Terrain geocoded ERS-2 image



Ellipsoidal geocoded ERS-2 image



SAR Intensity – Terrain geocoding and <u>radiometric</u> calibration

Aim

Radars measure the ratio between the power of the pulse transmitted and that of the echo received. This ratio is called the backscatter. Calibration of the backscatter values is necessary for intercomparison of radar images acquired with different sensors, or even of images obtained by the same sensor if acquired in different modes or generated with different processors.

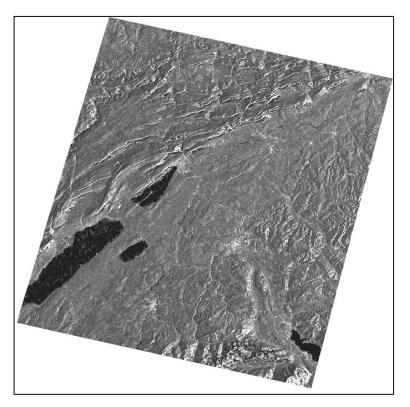
Method

The radiometric calibration of the SAR images involves corrections for:

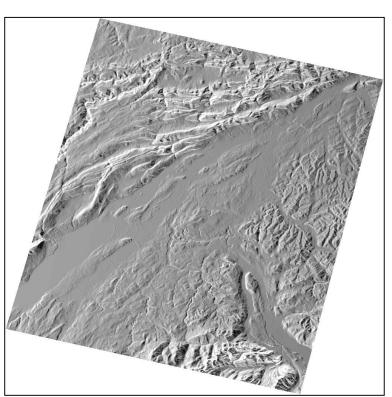
- The scattering area (A): each output pixel is normalised for the actual illuminated area of each resolution cell, which may be different due to varying topography and incidence angle.
- The antenna gain pattern (G): the effects of the variation of the antenna gain (the ratio of the signal, expressed in dB, received or transmitted by a given antenna as compared to an isotropic antenna) in range are corrected, taking into account topography (DEM) or a reference height.
- The range spread loss (R^3): the received power must be corrected for the range distance changes from near to far range.



SAR Intensity – Terrain geocoding and <u>radiometric</u> calibration



Terrain geocoded ERS-2 backscattering coefficient



Local incidence angle map



SAR Intensity — Anisotropic Non-Linear Diffusion Filtering

Aim

The Anisotropic Non-Linear Diffusion Filter (ANLD) enables to significantly smooth homogeneous distributed targets, enhancing at the same time the discontinuities between different areas.

Method

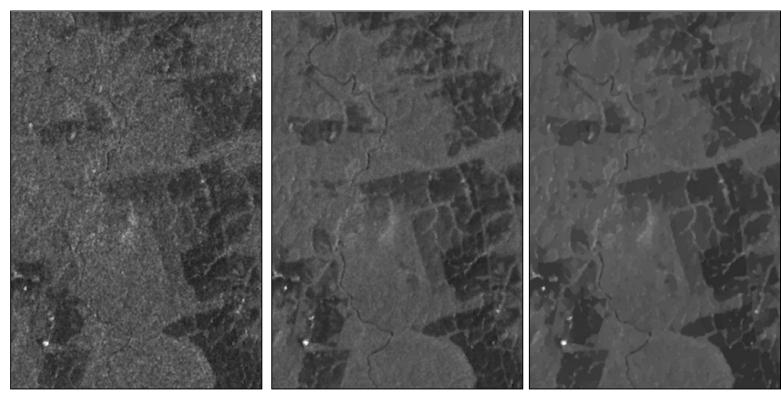
First introduced for single optical images, this particular type of filtering allows a high level of regularization in homogenous areas while preserving the relevant features ultimately used for segmentation (edges or more generally discontinuities). For a continuous image, diffusion on image may be enacted by the partial differential equation:

$$\frac{\partial \mathbf{I}}{\partial t} = \operatorname{div}[c(\|\nabla \mathbf{I}_{\sigma}\|) \cdot \nabla \mathbf{I}_{\sigma}]$$

where ∇ is the gradient , div is the divergence operator, and c, the conduction coefficient is a matrix of diffusion coefficients of the same size as I. c is designed to be a non-linear function of the smoothed image gradient magnitude $\nabla \cdot I_s$).



SAR Intensity – Anisotropic Non-Linear Diffusion Filtering



Original

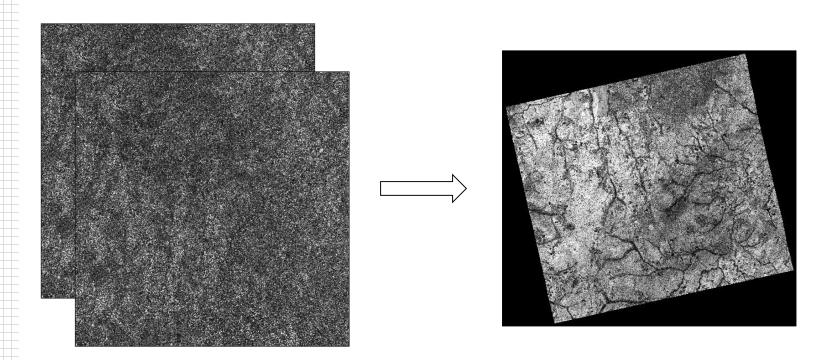
Multi-temporal De Grandi

Anisotropic Non-Linear Diffusion

ALOS PALSAR-1 ScanSAR image



SAR Coherence – From SLC data pair to coherence



Input

Single Look Complex data (1-look Intensity displayed)

Output

Terrain geocoded coherence



SAR Coherence – Processing Steps

It enables the generation of coherence (interferometric correlation, γ) from Single Look Complex (SLC) data.

In includes the following steps:

- 1. Co-registration including DEM
- 2. Generation of coherence including DEM
- 3. Terrain geocoding
- 4. Anisotropic Non-Linear Diffusion filtering



SAR Coherence – Generation of Coherence

Aim

To estimate coherence from Single Look Complex SAR data pair.

Method

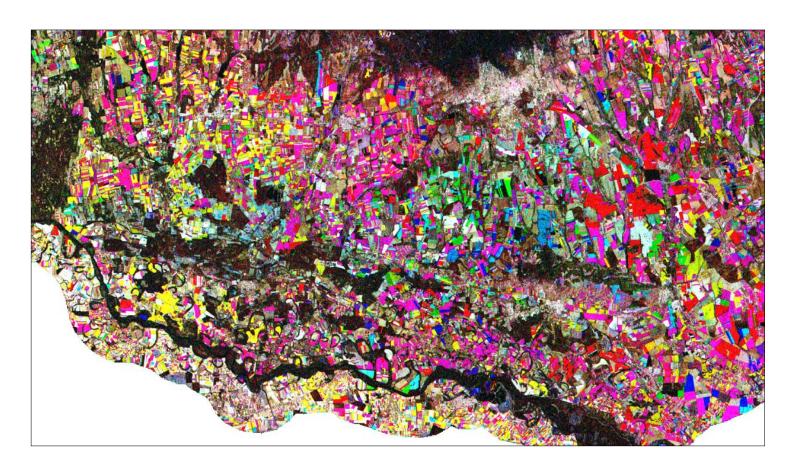
Given two co-registered Single Look Complex images (S_1 and S_2), one calculates the interferometric coherence (γ) as a ratio between coherent and incoherent summations:

$$\gamma = \frac{\left|\sum s_1(x) \cdot s_2(x)^*\right|}{\sqrt{\sum |s_1(x)|^2 \cdot \sum |s_2(x)|^2}}$$

Note that the observed coherence - which ranges between 0 and 1 - is, in primis, a function of systemic spatial decorrelation, the additive noise, and the scene decorrelation that takes place between the two acquisitions.

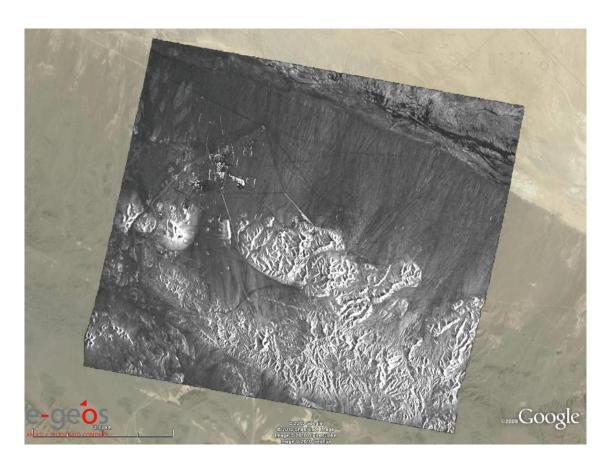


SAR Coherence – Multi-temporal coherence



Sentinel-1A IWS data





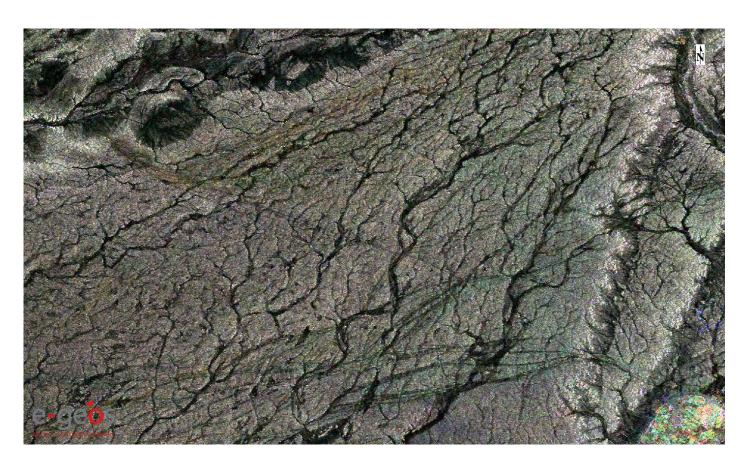
Cosmo-SkyMed Intensity





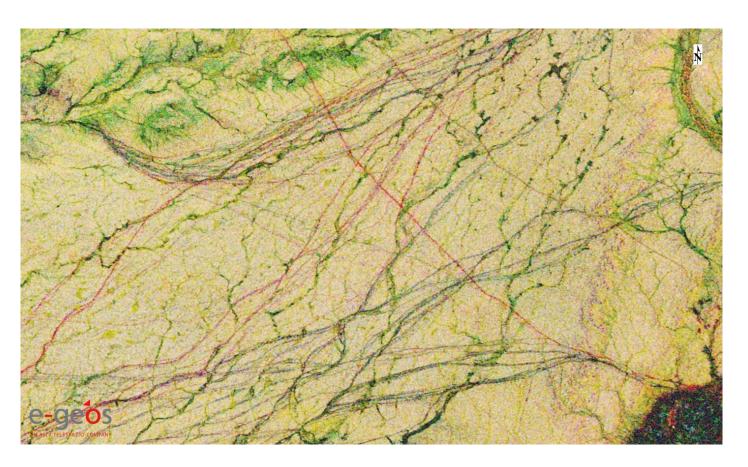
Cosmo-SkyMed Coherence





Cosmo-SkyMed Multi-temporal Intensity





Cosmo-SkyMed Multi-temporal Coherence

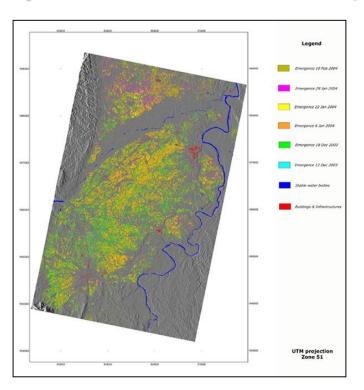


Content

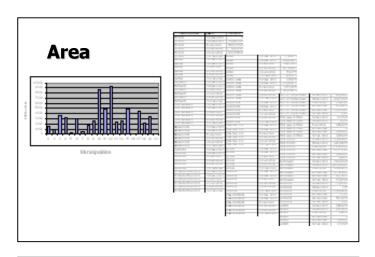
- 1. Key SAR basics
- 2. Past, existent, forthcoming SAR systems
- 3. SAR data processing
- 4. Agriculture
 - Rice in Asia
 - Small plot agriculture in Africa
- 5. Agriculture and other land covers in Africa
- 6. Forestry
 - Natural forest
 - Forest plantation
 - Bio-physical parameters
- 7. Digital Elevation Model
 - Fusion SAR interferometry-Optical stereo

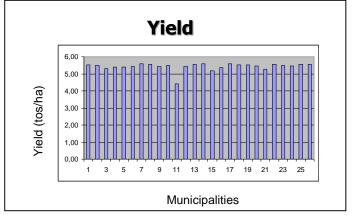


Requested information: where, when, how much



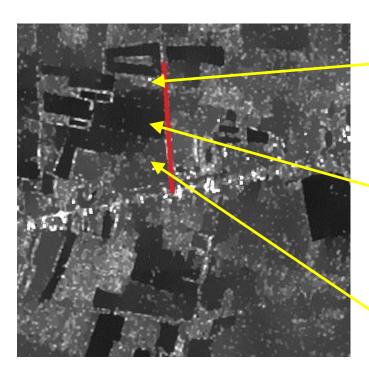
The different colors represent the rice area including the dates of the start of season (rice emergence). The tables list the rice area at municipality level for each acquisition date, while yield is estimated at the peak of season.







Rice imaged by SAR — single-date image



The gray values in this <u>single-date image</u> correspond to the different soil preparation and rice phenological moments, as recorded in the terrestrial pictures taken on the same acquisition day.

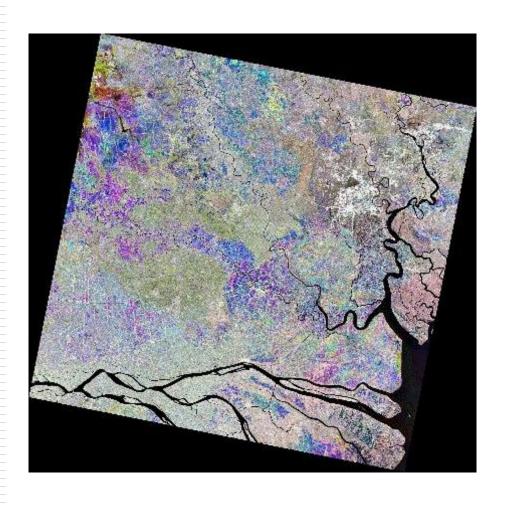


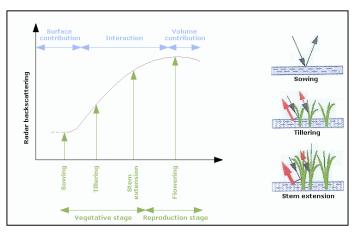






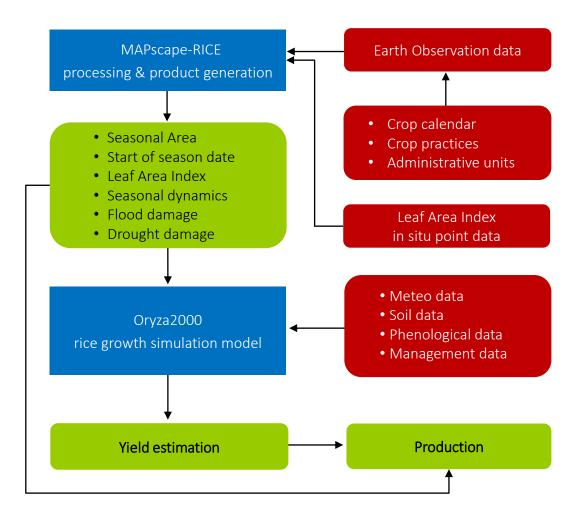
Rice - Seasonal signature





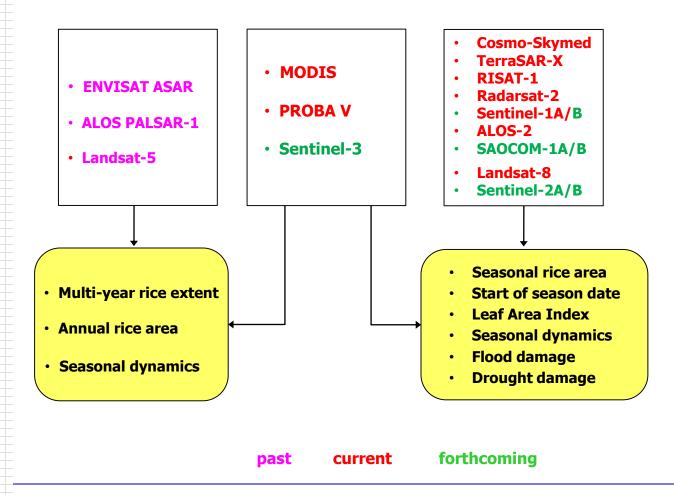


Methods and products



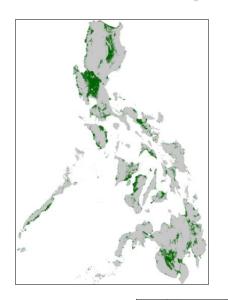


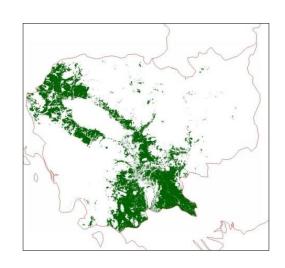
Remote sensing data and products

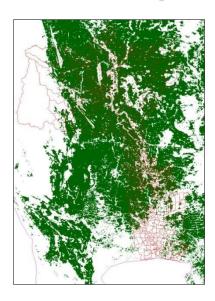




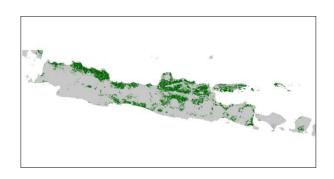
National scale products based on multi-annual ASAR — Examples





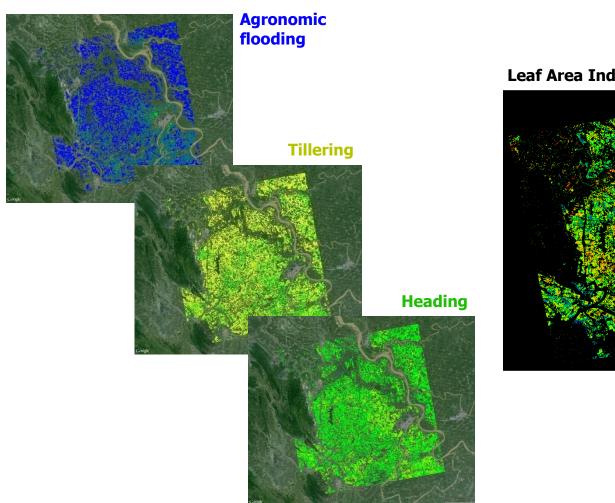




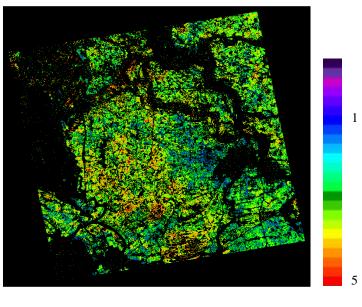




Local scale products based on seasonal Cosmo-SkyMed – Examples

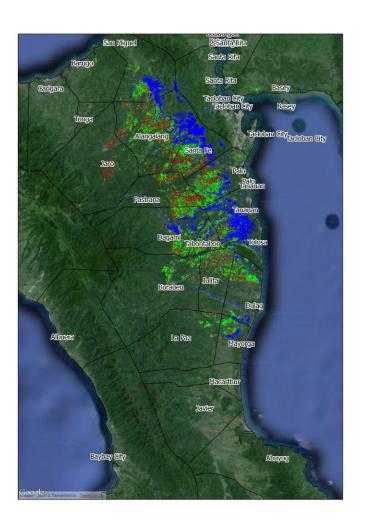


Leaf Area Index





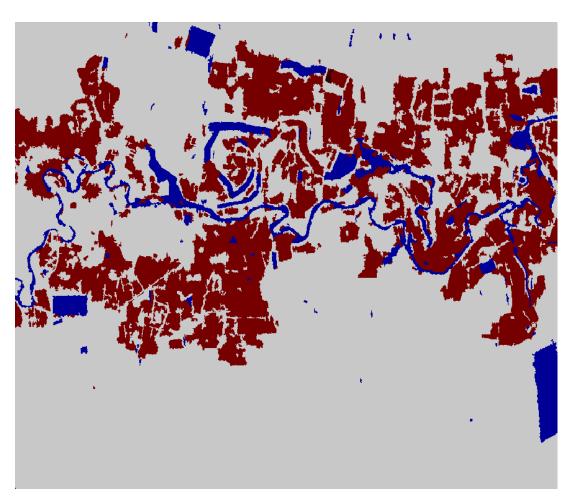
Typhoon crop area losses – Philippines, 2013



Municipality	Rice area	Flooded area
Alangalang	3,079	939
Albuera	58	2
Burauen	570	124
Dagami	1,757	681
Dulag	1,055	370
Jaro	400	14
Julita	1,017	140
La Paz	209	17
Mayorga	395	199
Ormoc City	0	1
Palo	2,104	402
Pastrana	1,427	71
San Miguel	711	611
Santa Fe	1,715	781
Tabontabon	861	227
Tanauan	1,628	1,545
Tolosa	286	376
Total	17,272	6,501



Flood damage map - Thailand, 2013



stable water flooded rice fields



Rice area/extent — Two approaches

Two possible approaches:

- **1.** Temporal descriptors are derived from sigma nought time series.
 - → Unsystematic SAR acquisitions can be also used;
 - → A priori information is not required.
- 2. The temporal evolution of the backscattering coefficient is analyzed from an agronomic perspective (Dedicated crop detection algorithm).
 - → Systematic SAR acquisitions during the whole crop season;
 - → A priori knowledge is existent (crop type, calendar, phenology, duration, practices).



The object - Rice

Rice from an agronomic perspective

- Rice production systems are unique and the longevity of rice farming speaks for itself. Irrigated lowland rice, which makes up three-quarters of the world rice supply, is the only crop that can be grown continuously without the need for rotation and can produce up to four harvests a year — literally for centuries, on the same plot of land. Farmers also grow rice in rainfed lowlands, uplands, mangroves, and deepwater areas.
- Rice systems are characterized by seasonal-dependent space-temporal variations.
 Off crop season, rice areas are often bare soil on which crop will grow later on.
 After field preparation, irrigation, and transplanting/sowing phase, crop starts developing their plant structure. Month later, after the vegetative and reproduction stage, plants dry before harvesting.



The object - Rice

Rice from a remote sensing perspective

- Due to the fact that <u>rice systems are not subject to seasonal rotations</u>, an accurate rice extent/area map derived from remote sensing data has a high value, because it enables, by combining it with archived daily medium resolution optical data, to provide an estimation of variations of the cultivated extent/area and to assess shortages, due to drought or flood events.
- Fields soil change and their evolution over time are not casual whenever <u>multitemporal</u> remote sensing data are analysed. In fact, <u>knowledge of crop calendar and land practices</u>, multi-temporal remote sensing data offer valuable information to determine at the earliest stage of the crop season, when and where fields are prepared and irrigated, and later, the phenological crop's status such as flowering, tillering, plant drying and harvesting. In summary: assuming that <u>data are/have been appropriately acquired</u>, key information is the <u>temporal signature</u> and <u>not spectral and/or polarimetric one</u>. One image or randomly acquired scenes, even if very high resolution, are not at all suitable and hardly useful. On the contrary, multi-temporal SAR data, due to the all weather condition acquisition capabilities, is a perfect candidate.

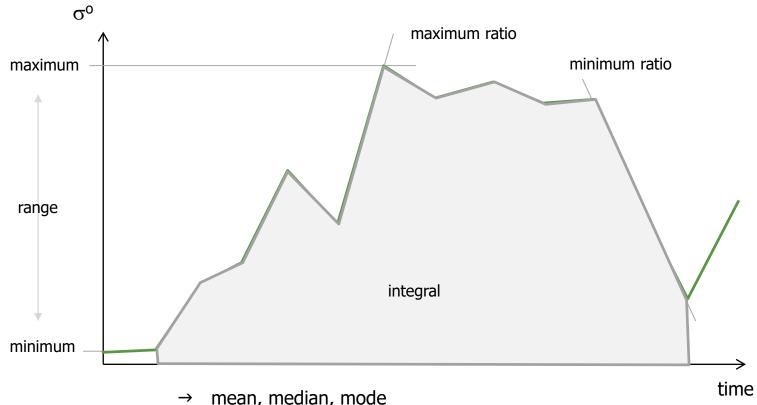


Approach 1 – Temporal descriptors

From multi-temporal sigma nought, <u>temporal descriptors (or features)</u> are calculated, as for instance minimum, maximum, mean, span, minimum and maximum ratio between two subsequent images, etc.



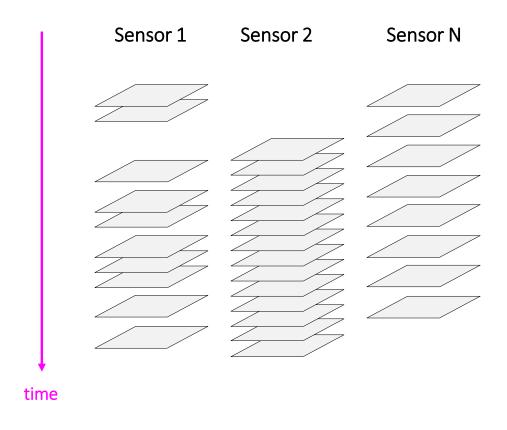
Temporal descriptors



- mean, median, mode
- corresponding dates
- selection of time range (seasonal, annual, etc.) is crucial

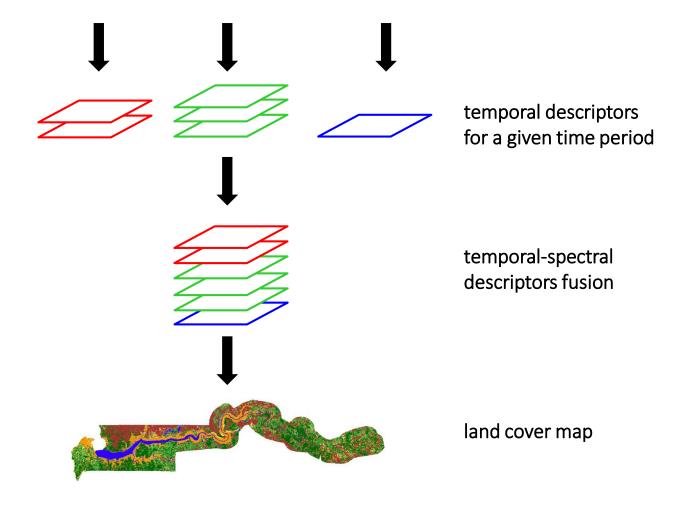


Temporal spectral descriptors 1 of 2



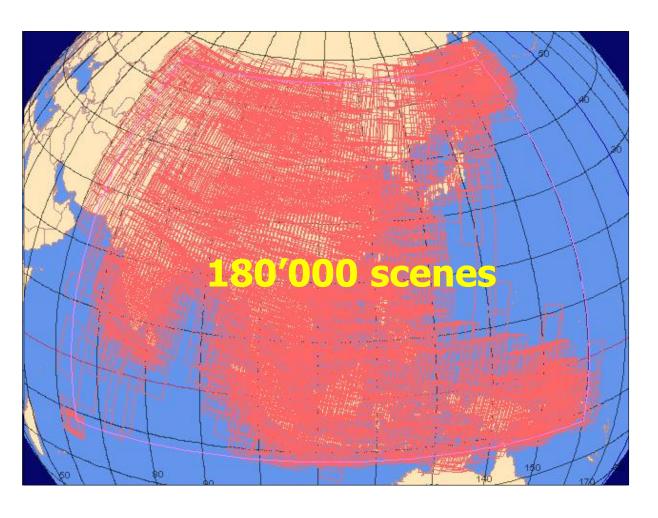


Temporal spectral descriptors 2 of 2





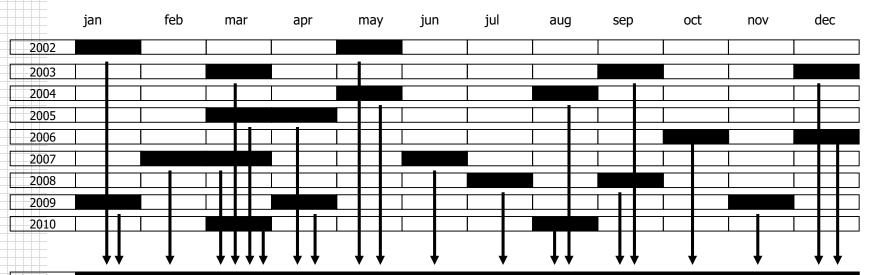
ENVISAT ASAR Wide Swath data archive



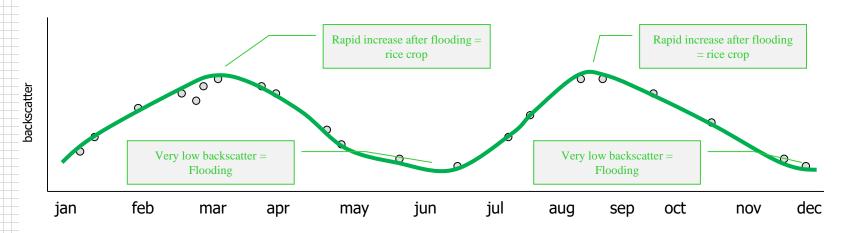
descending



What we can do with multi-annual ENVISAT ASAR data?



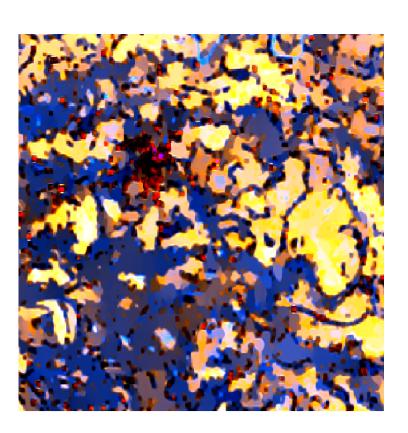






Temporal descriptors derived from multi-annual ASAR WS data



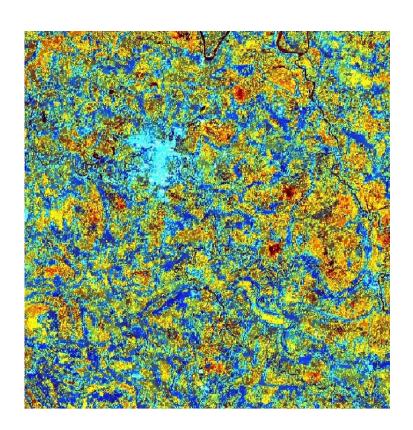


ASAR Mosaic (100 m) of temporal features based on ENVISAT ASAR Wide Swath data acquired from 2002 to 2010. Red is the maximum variation, green is the relative maximum, and blue is the relative minimum.



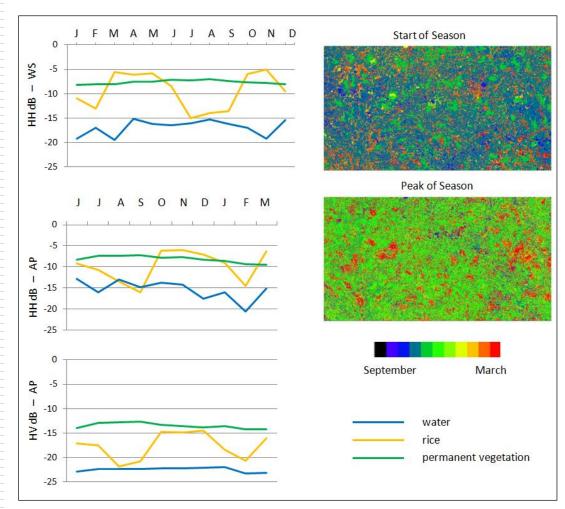
Temporal descriptors derived from multi-annual ASAR WS data

Temporal features (15 m) based on ENVISAT ASAR Alternating Polarization data acquired from June 2011 to March 2012. Red is the maximum variation, green is the relative maximum, and blue is the relative minimum.





Multi-annual vs. seasonal rice signature



Top left: Temporal signatures derived from ENVISAT ASAR Wide Swath HH data acquired from 2002 to 2010.

Middle left: Temporal signatures derived from ENVISAT ASAR Alternating Polarization HH data acquired from June 2011 to March 2012.

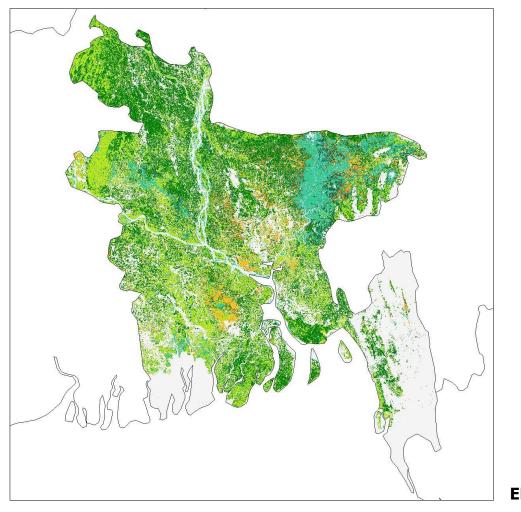
signatures derived from ENVISAT ASAR Alternating Polarization HV data acquired from June 2011 to March 2012.

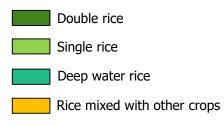
Right: Detected start of season and peak of season based on

and peak of season based on ENVISAT ASAR Alternating Polarization HH data acquired from June 2011 to March 2012.



Rice Extent - Bangladesh (1ha)

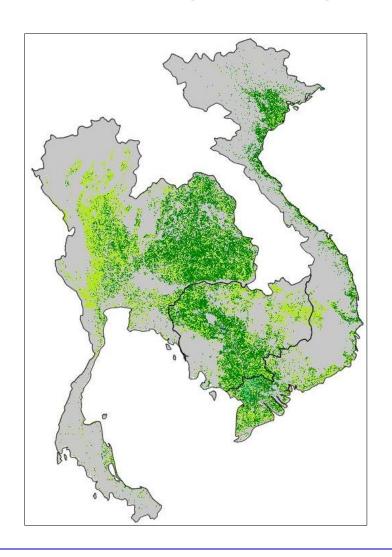




ENVISAT ASAR Wide Swath



Rice Extent - Thailand, Cambodia, Vietnam (1ha)



Baseline map, 1ha



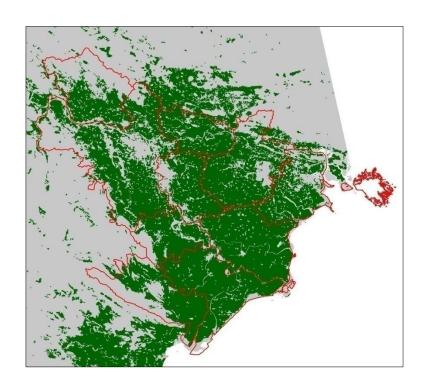
Double rice

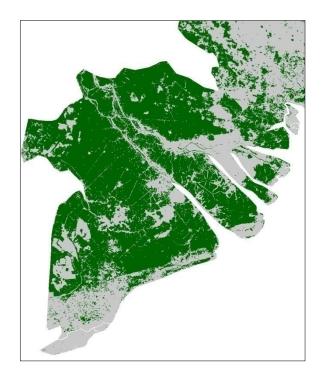


Single rice



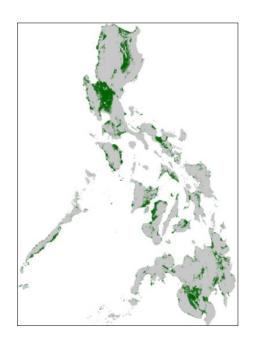
Rice Extent – Red River and Mekong River Delta

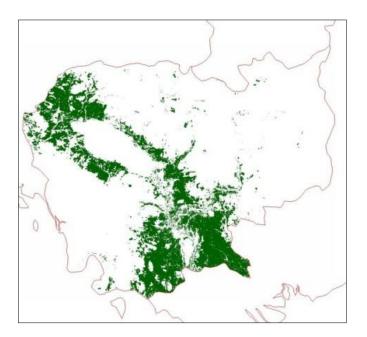


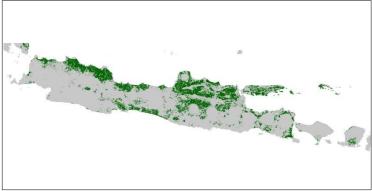




Rice Extent - Philippines, Cambodia, Java









Country-wide rice extent and area – Accuracy

	average rice extent, 1ha	annual rice area 2011, 15m
Thailand	84%	Insufficient data
Red River	83%	86%
Mekong River	93%	90%
Cambodia	91%	Insufficient data
Tamil Nadu	Insufficient data	Validation not possible
Philippines	73%	76%
Java	Insufficient data	Validation not possible

Note, based on ENVISAT ASAR archive data

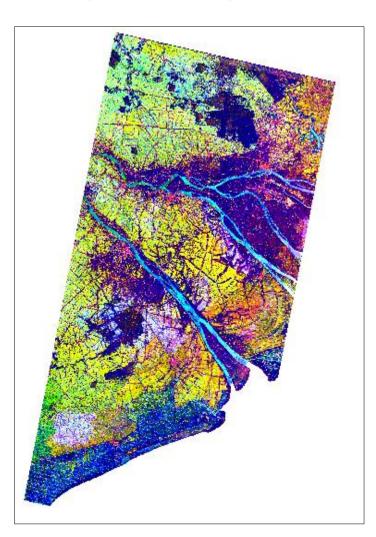


Mekong River Delta – Data set

- ASAR HH-VV data acquired every 35 days in 2007;
- PALSAR-1 HH-HV data irregularly acquired from 2008 to 2010;
- CSK-SM data regularly acquired every 16 days during three rice seasons: September 2012-January 2013; June-September 2013; June-September 2014;
- Radarsat-2 HH-HV ascending and descending data acquired every 24 days during the rice season May-August 2014.
- Sentinel-1A VV-VH acquired every 12 days from October 2014 to April 2015.



Mekong River – Temporal descriptors ASAR HH

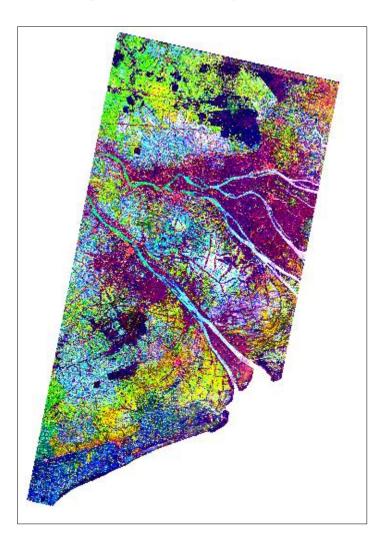


2007, regular acquisitions

maximum span maximum between two dates



Mekong River – Temporal descriptors ASAR VV

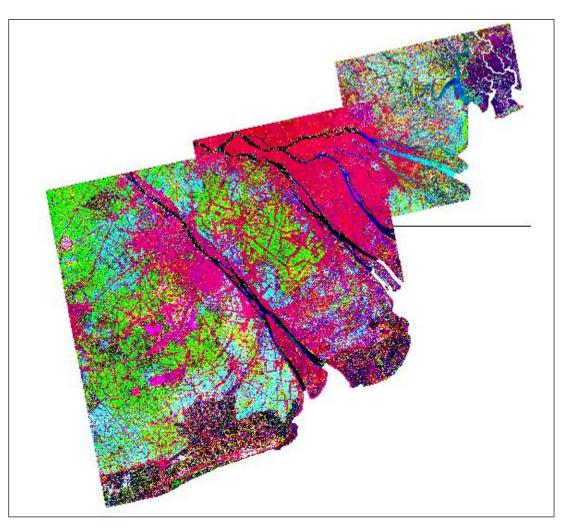


2007, regular acquisitions

maximum span maximum between two dates



Mekong River – Temporal descriptors PALSAR-1 HH



2008-2010, irregular acquisitions

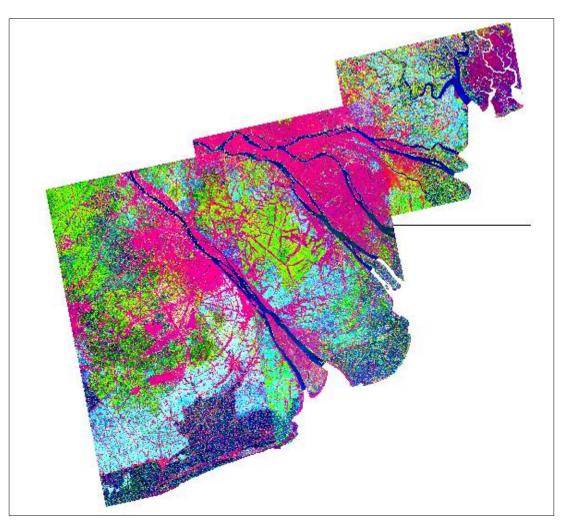
maximum

span

maximum between two dates



Mekong River – Temporal descriptors PALSAR-1 HV



2008-2010, irregular acquisitions

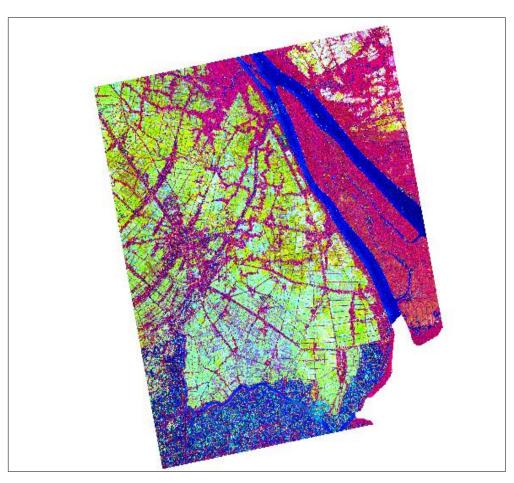
maximum

span

maximum between two dates



Mekong River – Temporal descriptors CSK HH



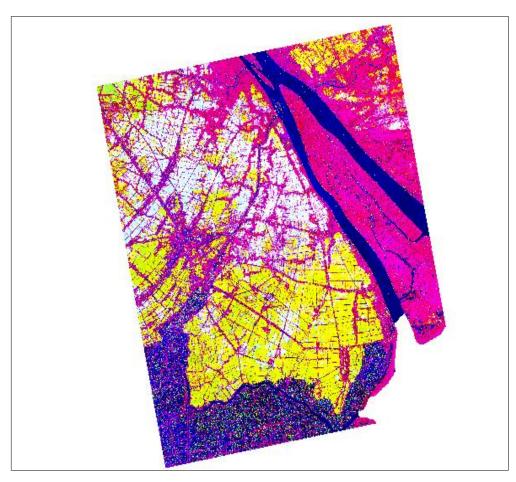
2012 – Sept-Dec, regular acquisitions

maximum

span



Mekong River – Temporal descriptors CSK HH



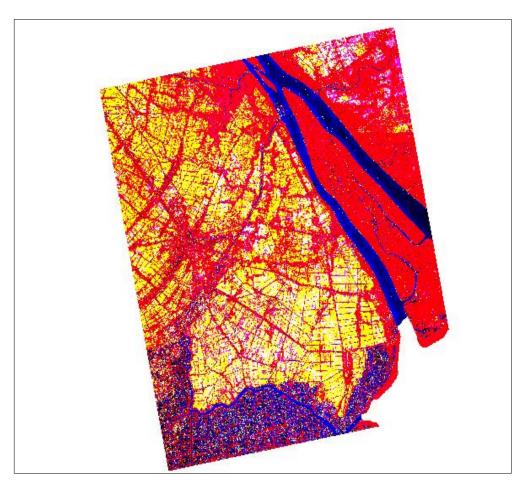
2013 – June-Sept, regular acquisitions

maximum

span



Mekong River – Temporal descriptors CSK HH

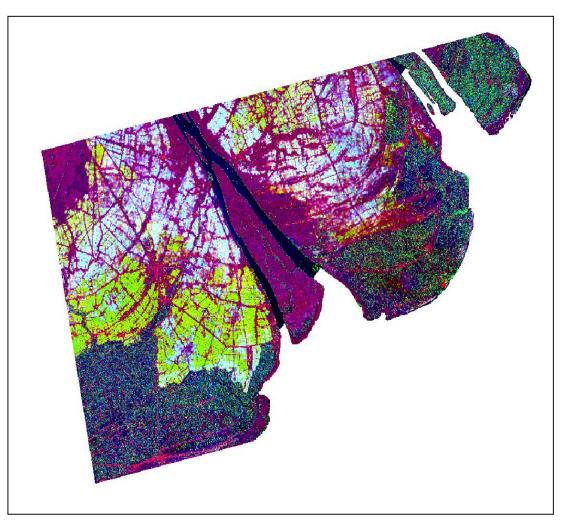


2012-2013, regular acquisitions during 3 seasons

maximum span maximum between two dates



Mekong River – Temporal descriptors RSAT-2 HH Ascending



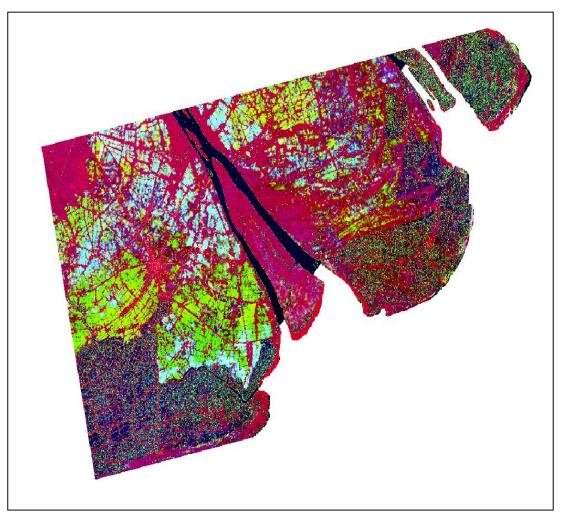
2014 – May-Sept, regular acquisitions

maximum

span



Mekong River – Temporal descriptors RSAT-2 HV Ascending



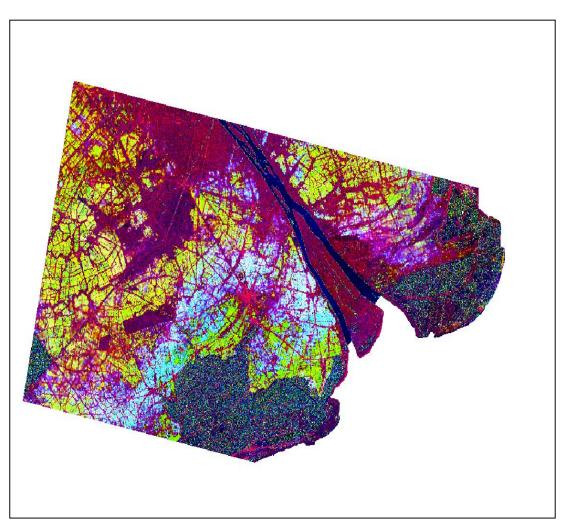
2014 – May-Sept, regular acquisitions

maximum

span



Mekong River – Temporal descriptors RSAT-2 HH Descending

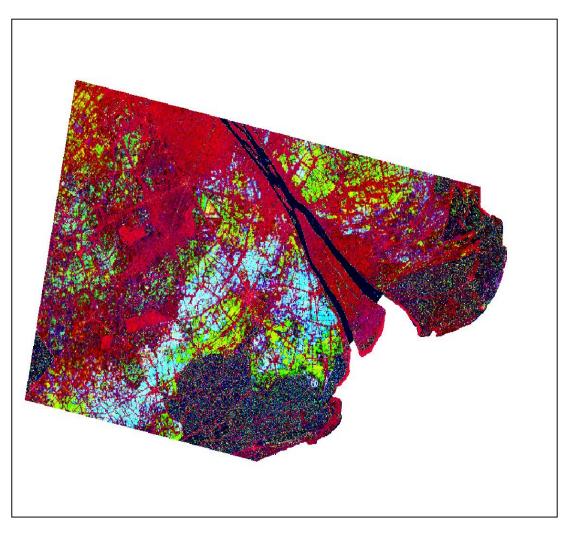


2014 – May-Sept, regular acquisitions

maximum span



Mekong River – Temporal descriptors RSAT-2 HV Descending

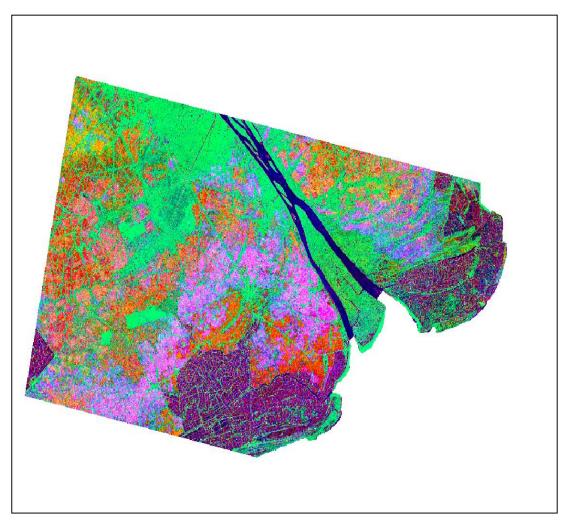


2014 – May-Sept, regular acquisitions

maximum span



Mekong River – Temporal descriptors RSAT-2 HH+HV Descending

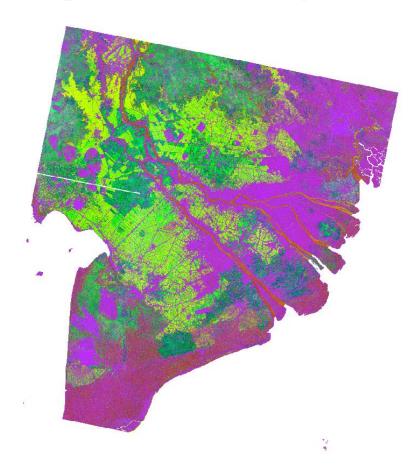


2014 – May-Sept, regular acquisitions

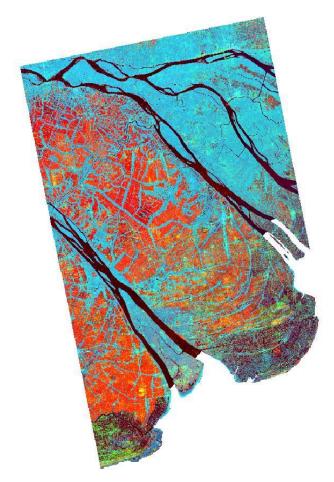
HH span
HV median
HH minimum



Mekong River Delta – Temporal descriptors



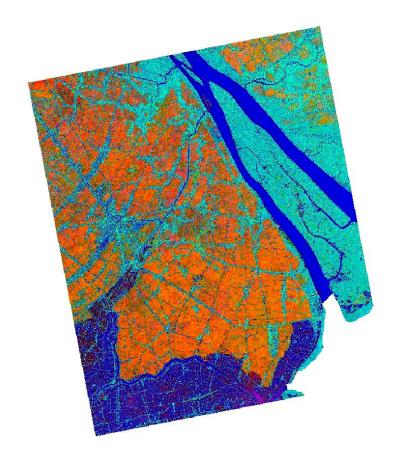
S-1A VHminR VVspan VHmin



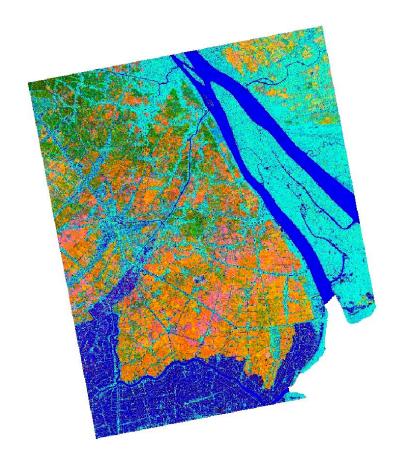
PALSAR-1 HVspan HHmed HVmin



Mekong River Delta – Temporal descriptors



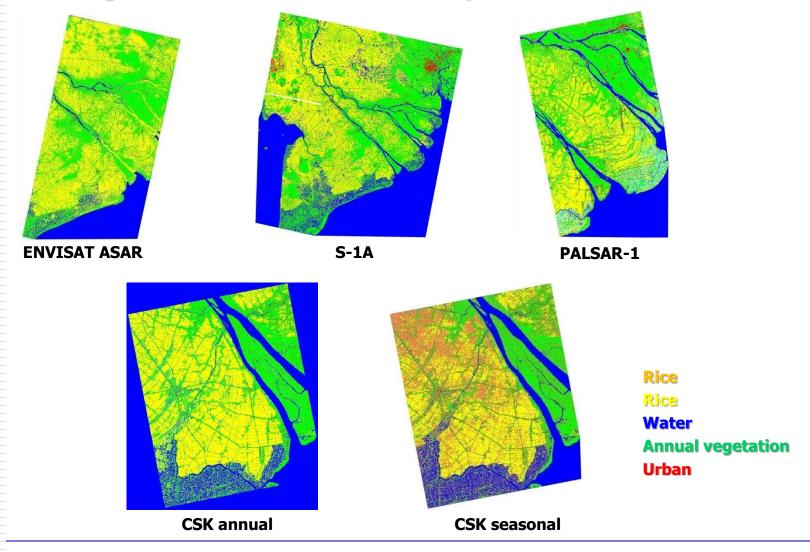
CSK annual VHminR VVspan VHmin



CSK seasonal HVspan HHmed HVmin



Mekong River Delta – Land cover maps vs. sensors





Mekong River Delta – TD versus sensors

	PALSAR	ASAR	CSK annual	CSK seasonal	RSAT-2	S-1A
min	L1- HV		L1- HH	L1- HH	L2- HH	L1- VH
max	L2,3- HH	L1,3- HH	L2- HH	L2- HH	L2,3- HH	L2- VV
span	L2- HV					
maxR			L3- HH	L3- HH		
minR		L2- VV				
mean					L1- HH	



Mekong River Delta – Validation

	overall accuracy	kappa	temporal descripotors
ASAR	87.3	0.81	maxHH minRHH
PALSAR-1	87.8	0.83	minHV spanHV maxHH
CSK seasonal	97.7	0.97	minHH maxHH maxRHH
CSK annual	95.1	0.94	minHH maxHH maxRHH
RSAT-2	94.6	0.92	meanHH maxHH minHH
S-1A	97.7	0.97	minVH maxVH maxVV



Publication – IGARSS'15

ON THE USE OF TEMPORAL-SPECTRAL DESCRIPTORS FOR CROP MAPPING, MONITORING AND CROP PRACTICES CHARACTERIZATION

Francesco Holecz, Luca Gatti, Francesco Collivignarelli, Massimo Barbieri sarmap – Cascine di Barico 10, 6989 Purasca, Switzerland – www.sarmap.ch fholecz@sarmap.ch – phone +41 91 600 9366

Abstract — Irrespective if remote sensing data are acquired by active or passive sensors, high or medium resolution, key information is the temporal signature. This is particularly true — but not limited to — agriculture, where the spatio-temporal dynamic is significant. Spectral (here meant in frequency and polarimetric terms) information, definitely, complements the temporal one. In this paper, temporal-spectral descriptors are derived from sigma nought time series acquired from various Synthetic Aperture Radar (SAR) systems over different agroecological zones in Senegal, The Gambia, Vietnam. It is shown that:

- a limited set of temporal descriptors is sufficient to generate a reliable crop map;
- -the selection of the appropriate time period is crucial;
- the temporal combination of wavelengths and polarizations may enhance the level of detail and product's reliability;
- the use of temporal descriptors derived from multiannual, annual, and seasonal time series data provides, from an agronomic perspectives, complementary information;

time series data sets is demonstrated in different agroecological zones in Senegal, The Gambia, Vietnam.

II. METHOD

Time series data can be interpreted in two ways:

- The temporal evolution of the backscattering coefficient is analyzed from an agronomic perspective by means of a dedicated crop detection algorithm [4,5]. Pre-requisite is that the data have been systematically acquired, and a priori knowledge of crop type, calendar, duration and crop practices during the whole season is well known.
- 2. From sigma nought time series, temporal descriptors (or features) are derived [2,4,6]. Even if this approach does not allow to derive all specific information as the previous one, it provides, in a rather simple way, valuable information on the crop location, and, depending on the temporal spacing of the remote sensing acquisitions, knowledge on the crop seasonal dynamics, crop practices and, to some extent, type. The advantage is that it does not require a priori information of the underlying agriculture as long as temporal descriptors are not interpreted from an agronomic perspective. Crop

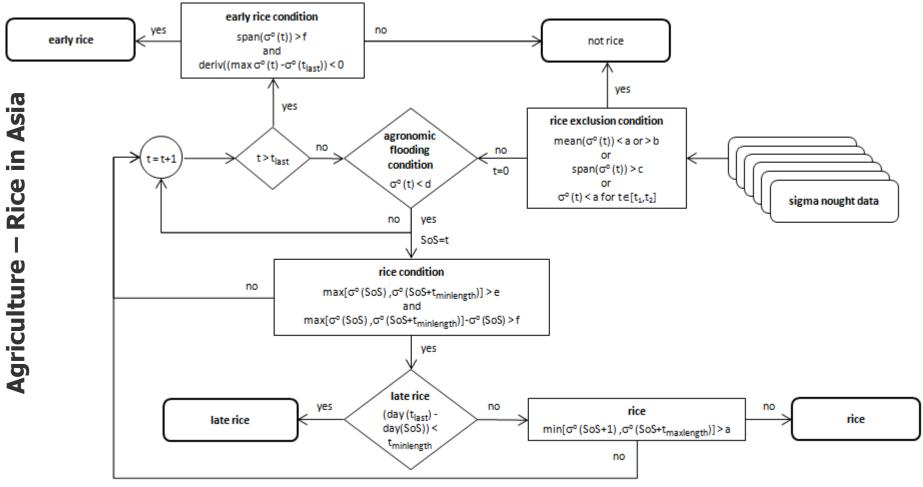


Approach 2 – Regular (or systematic) acquisitions

From multi-temporal sigma nought the temporal evolution is analyzed from an agronomic perspective. This approach enables to map the actual cultivated rice area AND to provide information of the seasonal dynamics, in particular the identification of the Start of Season, essential for crop yield modeling purposes.



The rice knowledge based algorithm





Algorithm's input parameters

a = lowest mean

b = highest mean

c = maximum variation

d = maximum value at SoS

e = minimum value at maximum peak

f = minimum variation

t = time

 t_1,t_2 = maximum time under water

 $t_{minlenght}$ = minimum number of days of season length

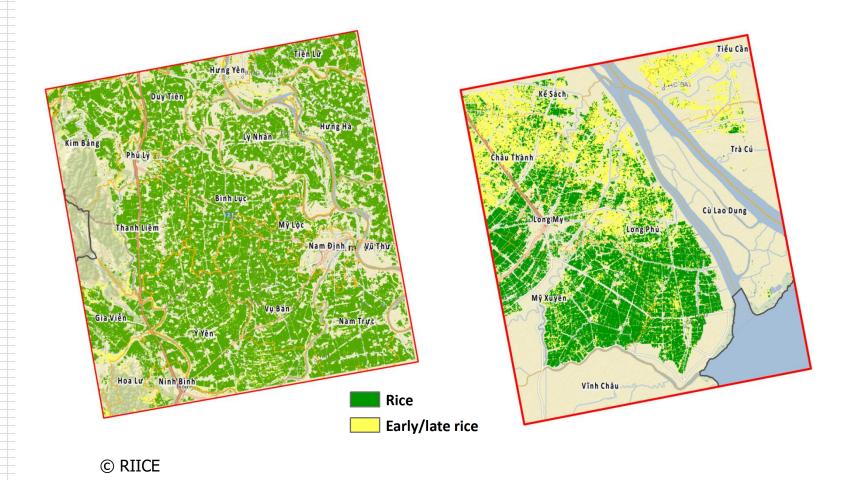
 $t_{maxlenght}$ = maximum number of days of season length

 t_{last} = date of the last acquisition

SoS = Start of Season

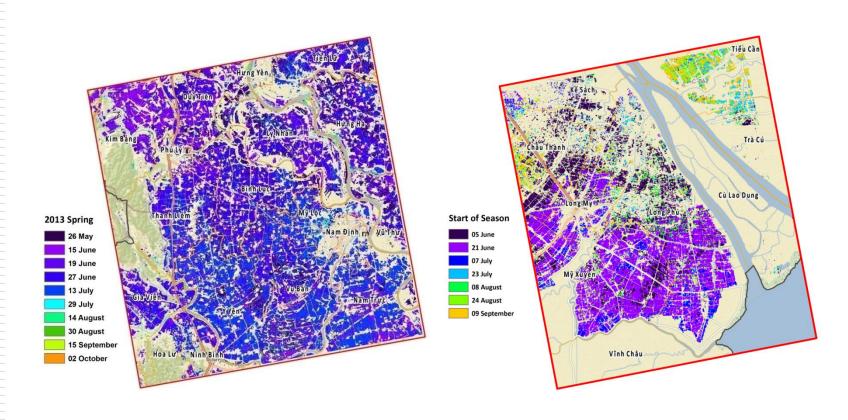


Seasonal rice area — Red River and Mekong River Delta, 2013





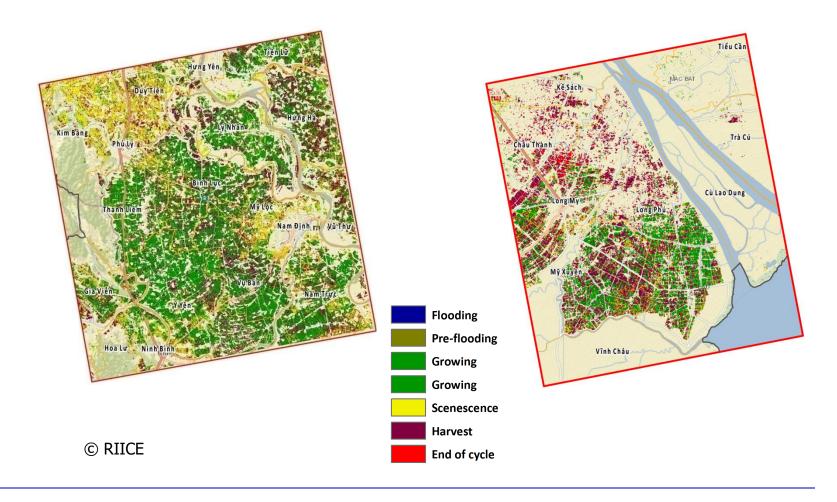
Start of Season – Red River and Mekong River Delta, 2013



© RIICE

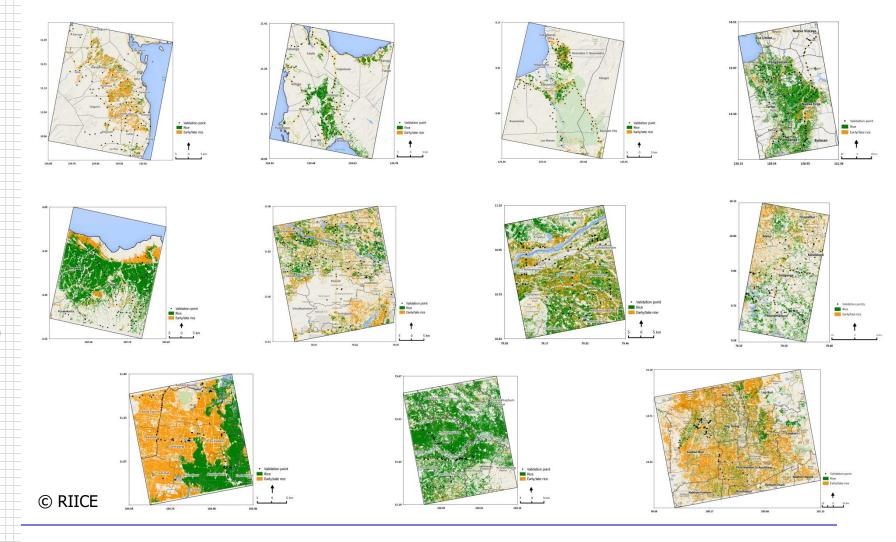


Seasonal rice dynamics—Red River and Mekong River Delta, 2013



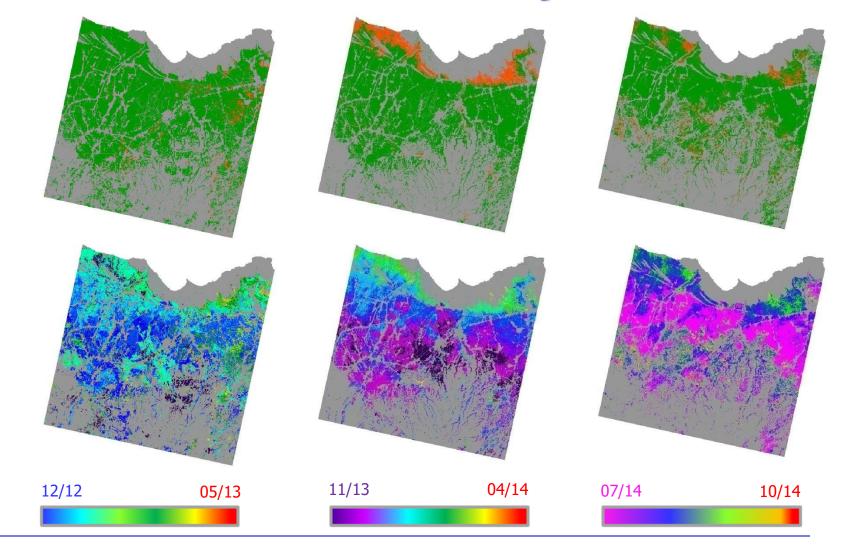


Seasonal rice area – Philippines, Java, Tamil Nadu, Cambodia, Thailand





Seasonal rice area and start of season during 3 seasons — Java



Seasonal rice area based on CSK data – Accuracy

Site	Season	Period	Fields & visits	Establishment	Maturity (days)	Water source	Validation points & date(s)	Rice area (ha)	Accuracy kappa
Camobodia, Takeo	Dry	Oct to Apr	4 fields, 20 visits	Direct seeding (DS)	95	Irrigated (IR)	100 08 & 22-04,11-09-2013	150,026	85% 0.70
Philippines, Leyte East	Wet	May to Sep	20 fields 200 visits	Transplanting (TP)	114	IR	99 24 to 26-09-2013	17,817	87% 0.74
Philippines, Leyte West	Wet	May to Sep	20 fields 200 visits	TP	110-112	IR	85 27 to 28-09-2013	15,229	89% 0.79
Philippines, Agusan del Norte	Dry	May to Oct	18 fields 182 visits	TP & DS	107-123	IR & some rainfed (RF)	100 14 to 16-10-2013	13,163	89% 0.78
Vietnam, Soc Trang	Summer- autumn	Jun to Sep	12 fields 66 visits	TP & DS	95-120	IR	108 25-09-2013	55,216	87% 0.74
Vietnam, Nam Dinh	Summer	Jul to Nov	20 fields 160 visits	TP	125-134	IR	100 30-08 and 05-09-2013	108,733,	89% 0.78
Indonesia, Subang	Wet	Nov to Apr	20 fields 160 visits	TP	115-135	IR	115 10 to 13-02-2014	64,533	95% 0.90
India, Cuddalore	Samba	mid-Jul to Jan	20 fields 160 visits	TP	130-160	IR	111 12-02 and 03-03-2014	26,015	92% 0.85
India, Thanjavur	Samba	Aug to Dec	20 fields 162 visits	TP & DS	135-160	IR	102 31-01, 01-02 & 07-03-2014	83,871	91% 0.82
India, Sivaganga	Samba	Sep to Jan	18 fields 110 visits	TP & DS	100-110	Semi-dry rice	110 14 and 21-02-2014	41,825	87% 0.73
Thailand, Muang Yang	Wet	May to Nov	16 fields 130 visits	DS	150-178	RF	109 17-10 and 12-12-2013; 12-02, 28-02-2014	91,908	86% 0.72
Thailand, Suphan Buri	Wet	Jun to Oct	20 fields 172 visits	DS	92-120	IR	100, 25-09, 25-10, 14-12- 2013; 22-01-2014	555,317	87% 0.74
Philippines, Nueva Ecija	Wet	Jul to Nov	20 fields 200 visits	TP	114	IR	100 19-09, 03-10 and 04-10-2013	424,801	86% 0.72
© RIICE			228 fields 1,922 visits	DS – 7 TP - 10	92-160	IR – 11 RF – 2 Other - 1	1,339 points	1.65M ha	



On accuracy and rice management practices

Crop establishment method	Number of sites	Avg. Accuracy
Transplanting	6	89.7
Transplanting / Direct Seeding	4	88.5
Direct seeding	3	86.0

Water management	Number of sites	Avg. Accuracy
Irrigated	10	88.8
Irrigated / Rainfed	1	89.0
Rainfed	100	86.0
Semi Dry	1	87.0

Maturity / duration	Number of sites	Avg. Accuracy		
Long	3	89.7		
Medium	7	88.9		
Short to Medium	1	87.0		
Short	2	85.0		

© RIICE



On rice management practices and algorithm's parameters a X-band

Study site	а	b	С	d	е	f
Takeo (short rice only)	-18	-6	20	-11	-13	4
Leyte East	-14	-7.5	20	-11	-10.5	3
Leyte West	-14	-7.5	20	-11	-10.5	3
Agusan del Norte	-14	-7.5	20	-8	-10.5	3
Soc Trang	-15.5	-7.5	20	-10.5	-10	3
Nam Dinh	-15.5	-7.5	20	-10.5	-11	3
Subang	-17.5	-6	20	-12	-12	4
Cuddalore	-14	-8	20	-12	-11	3
Thanjavur	-14	-8	20	-11	-11	3
Sivaganga	-14	-9	20	-12	-12	3
Mueang Yang	-14	-4	20	-8	-10.5	3
Suphan Buri	-15.5	-7.5	20	-10.5	-10.5	3
Nueva Ecija	-14	-7.5	20	-11	-10.5	3

a = lowest mean

b = highest mean

c = maximum variation

d = maximum value at start of season

e = minimum value at maximum peak

f = minimum variation



Publication – Remote Sensing

Remote Sens. 2014, 6, 10773-10812; doi:10.3390/rs61110773

OPEN ACCESS

remote sensing

ISSN 2072-4292

www.mdpi.com/journal/remotesensing

Article

Towards an Operational SAR-Based Rice Monitoring System in Asia: Examples from 13 Demonstration Sites across Asia in the RIICE Project

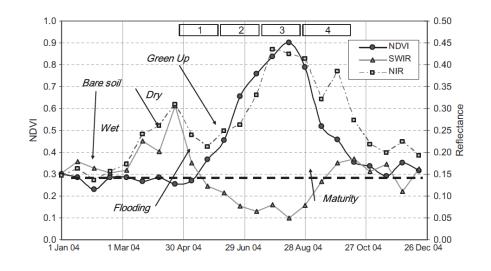
Andrew Nelson ^{1,*}, Tri Setiyono ^{1,*}, Arnel B. Rala ¹, Emma D. Quicho ¹, Jeny V. Raviz ¹, Prosperidad J. Abonete ¹, Aileen A. Maunahan ¹, Cornelia A. Garcia ¹, Hannah Zarah M. Bhatti ¹, Lorena S. Villano ¹, Pongmanee Thongbai ¹, Francesco Holecz ², Massimo Barbieri ², Francesco Collivignarelli ², Luca Gatti ², Eduardo Jimmy P. Quilang ³, Mary Rose O. Mabalay ³, Pristine E. Mabalot ³, Mabel I. Barroga ³, Alfie P. Bacong ³, Norlyn T. Detoito ³, Glorie Belle Berja ³, Frenciso Varquez ³, Wahyunto ⁴, Dwi Kuntjoro ⁴, Sri Retno Murdiyati ⁴, Sellaperumal Pazhanivelan ⁵, Pandian Kannan ⁵, Petchimuthu Christy Nirmala Mary ⁵, Elangovan Subramanian ⁵, Preesan Rakwatin ⁶, Amormrat Intrman ⁷, Thana Setapayak ⁷, Sommai Lertna ⁷, Vo Quang Minh ⁸, Vo Quoc Tuan ⁸, Trinh Hoang Duong ⁹, Nguyen Huu Quyen ⁹, Duong Van Kham ⁹, Sarith Hin ¹⁰, Touch Veasna ¹⁰, Manoj Yadav ¹¹, Chharom Chin ¹² and Nguyen Hong Ninh ¹³



Phenological Monitoring using MODIS time-series

8- or 16-days MODIS composites are used to identify peculiar behavior of agronomic practices and phenological dynamics. Following information with respect to the rice development can be identified from the temporal signature:

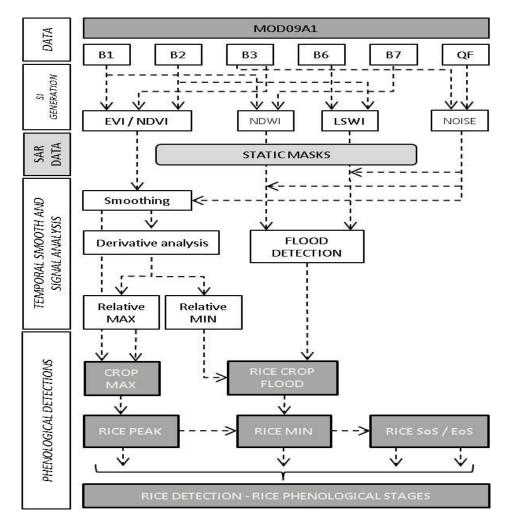
- Flood condition
- Crop Rapid growth
- Phenological stages



- [1] emergence and tillering
- [2] stem elongation
- [3] peak LAI and flowering
- [4] grain filling and maturity



Phenological Monitoring – CNR-IREA



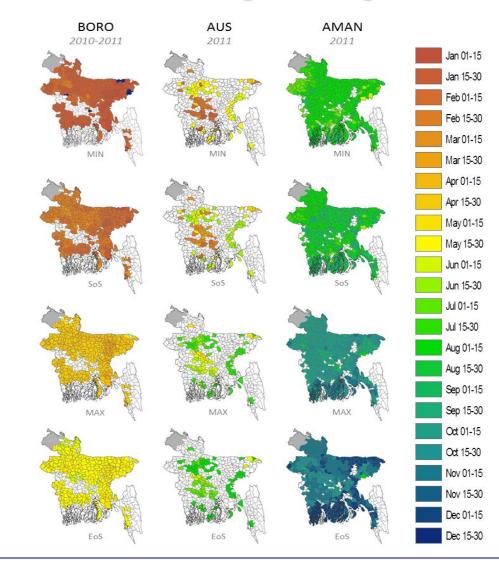
Rice transplanting/seeding
(MIN point) is identified when a
local EVI minima occurs at the
same time as a flood (NDWI,
LSWI), and a series of positive EVI
derivative values (indicating plant
growth) occur shortly after.

Rice heading/flowering (MAX point) is detected when there is a local absolute maxima in the EVI time-series.

Rice emergence [start of season (SoS)] and maturity [end of season (EoS)]. These metrics are identified for each rice pixel, when EVI values match pixel-specific relative thresholds.



Rice Extent including Phenological Monitoring – CNR-IREA





Lessons learned

- Temporal signature is conditio sine qua non for the identification of rice and a correct interpretation of rice phenology.
- For irregular acquisitions the use of temporal descriptors is an efficient way to derive the most significant information. If regularly acquired data are available the use of knowledge based algorithms is doubtless more appropriate.
- The proposed methodology applied to Sentinel-1A and B data will enable to map and monitor rice at continental level.
- MODIS data are useful to quantify annual variations. However, only if in combination with accurate baseline maps (rice extent or rice area).
- Large unused remote sensing data archive exists.



Content

- 1. Key SAR basics
- 2. Past, existent, forthcoming SAR systems
- 3. SAR data processing
- 4. Agriculture
 - Rice in Asia
 - Small plot agriculture in Africa
- 5. Agriculture and other land covers in Africa
- 6. Forestry
 - Natural forest
 - Forest plantation
 - Bio-physical parameters
- 7. Digital Elevation Model
 - Fusion SAR interferometry-Optical stereo



The 'object'





The still pending answers

$Production = Area \times Yield$

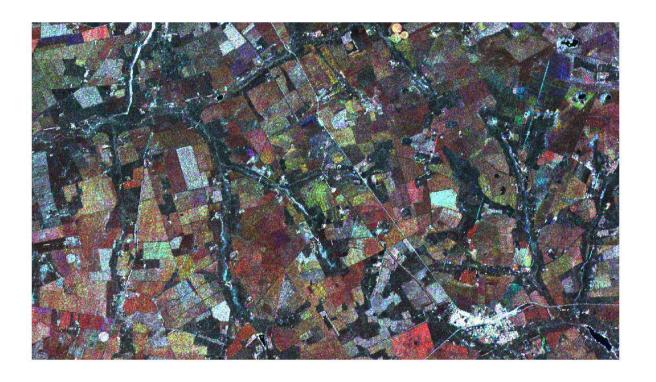
- How many <u>hectares</u> have been prepared at the begin of the crop season?
- How many hectares have been harvested?



The use of HIGH RESOLUTION data



Maize - Temporal signature

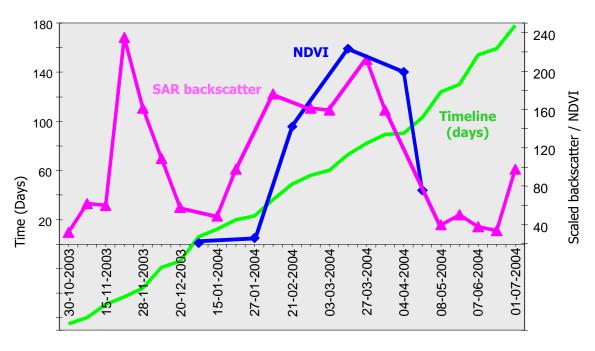


ENVISAT ASAR IM and RADARSAT-1 FB



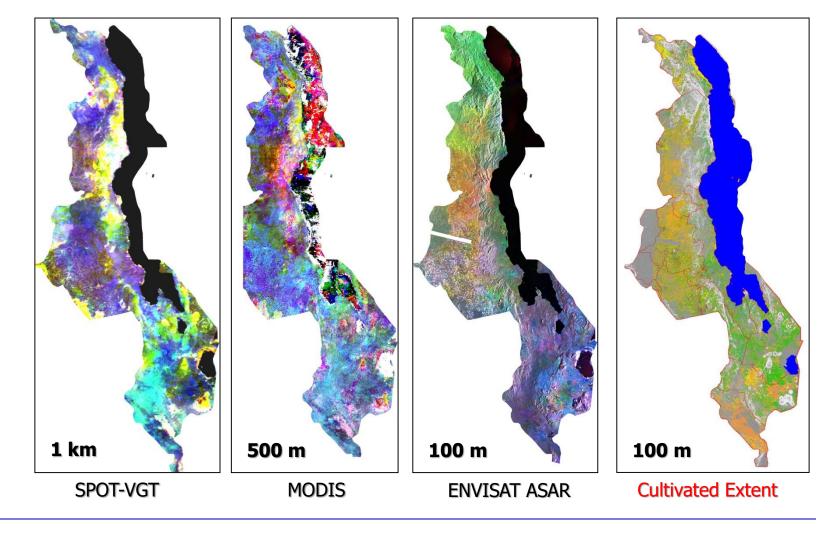
Maize – Temporal signature at C-HH



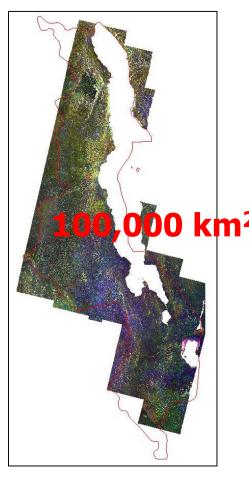




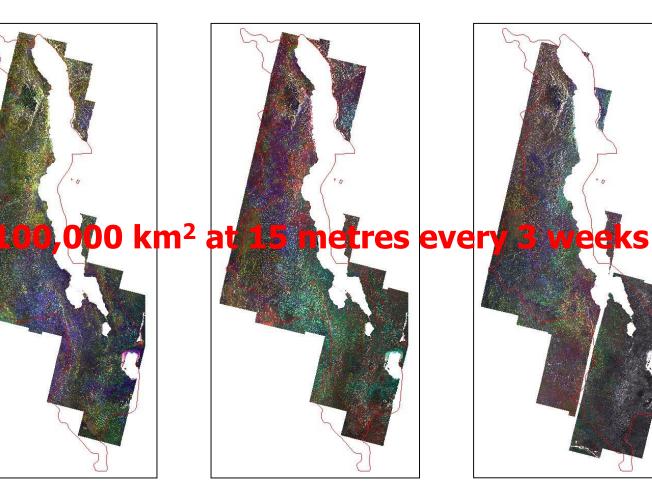
From low (1km) to medium (100m) resolution ...



... to the monitoring at high resolution (15m)



120 scenes ASAR sept-oct-nov



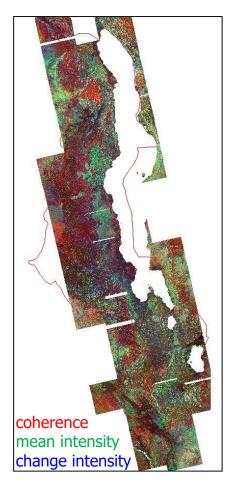
120 scenes ASAR oct-dec-jan



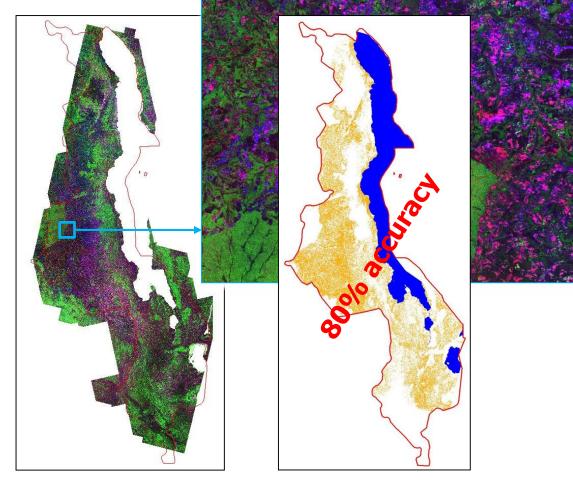
120 scenes ASAR jan-feb-mar

Sarna pour information gateway

... to the monitoring at high resolution (15m)



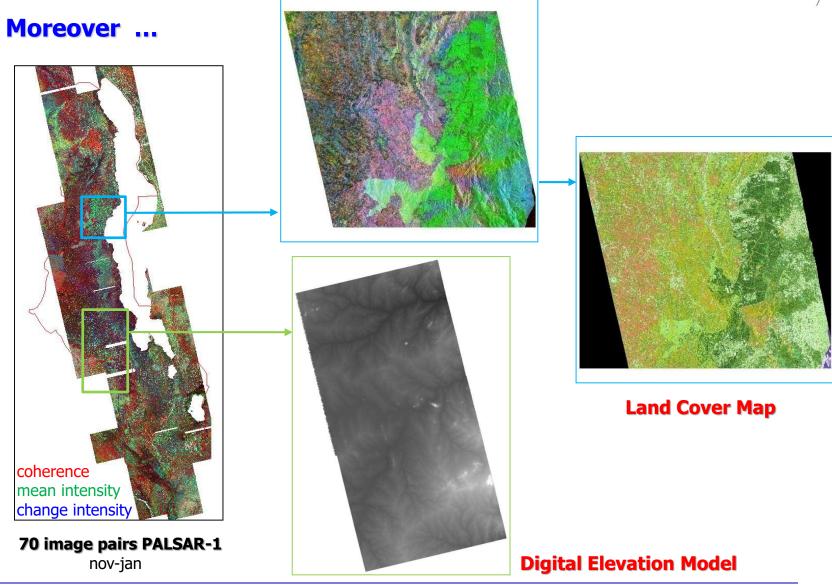
70 image pairs PALSAR-1 nov-jan



ASAR-PALSAR-ASAR

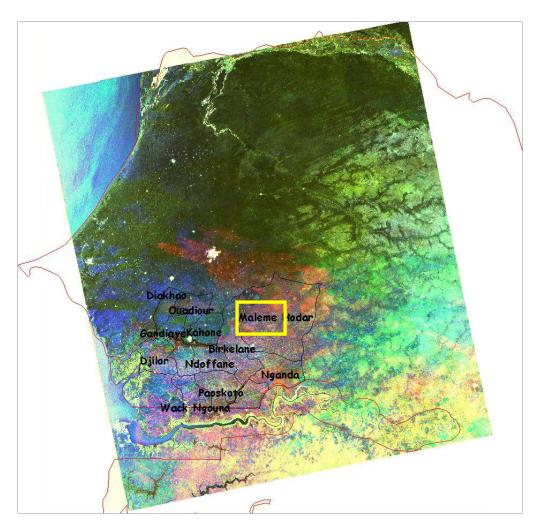
Cultivated area (15 m)



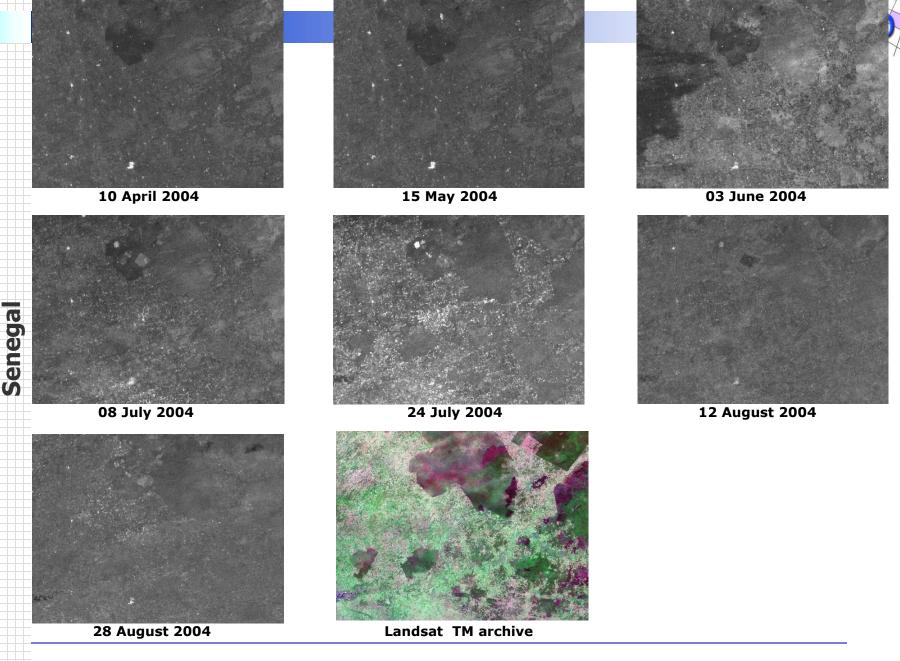


Sarma your information gateway

ENVISAT ASAR Wide Swath (100m)

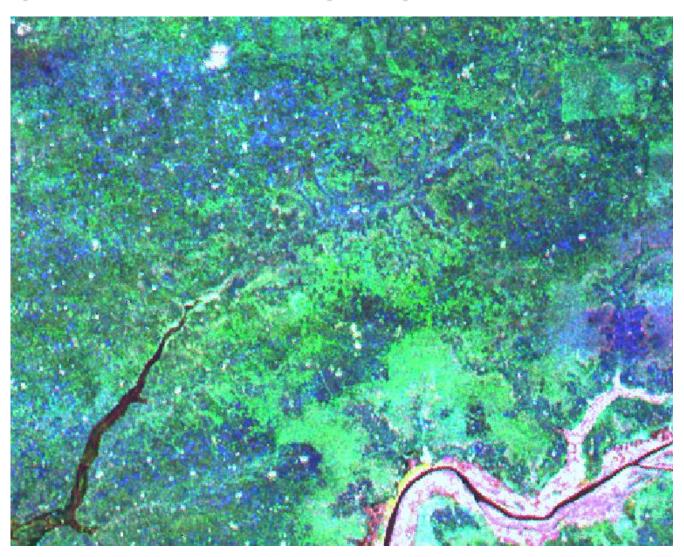


03 June 2004 08 July 2004 24 July 2004





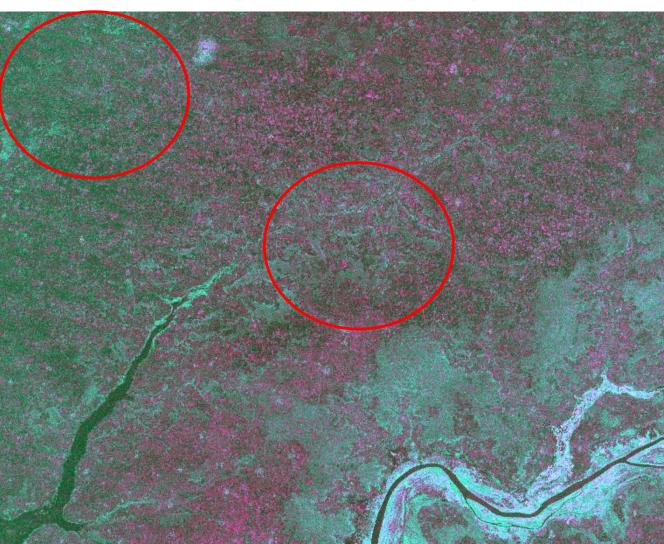
Multi-temporal ASAR Wide Swath (100m)



15 May 2004 03 Jun 2004 08 July 2004

Sarna pour information gateway

Single-date ASAR Alternating Polarization (15m)

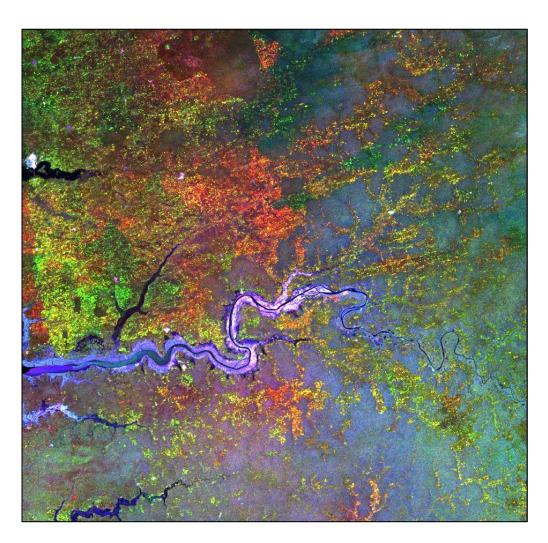


07 July 2005

HH-HV HV HH

Sarma your information gateway

SPOT-VGT vs. ENVISAT ASAR Wide Swath

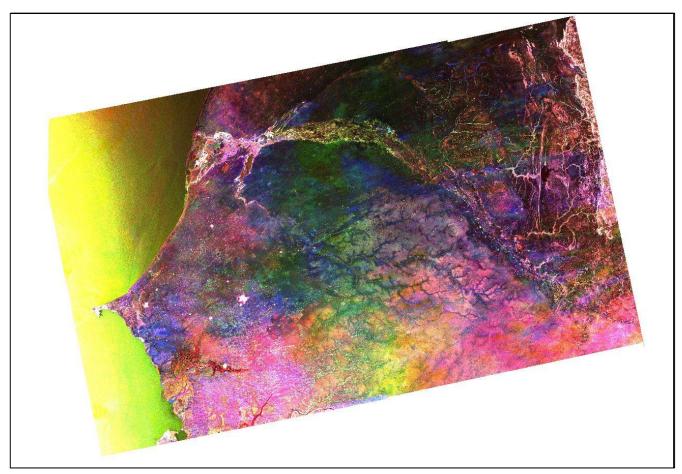


2005

May July August



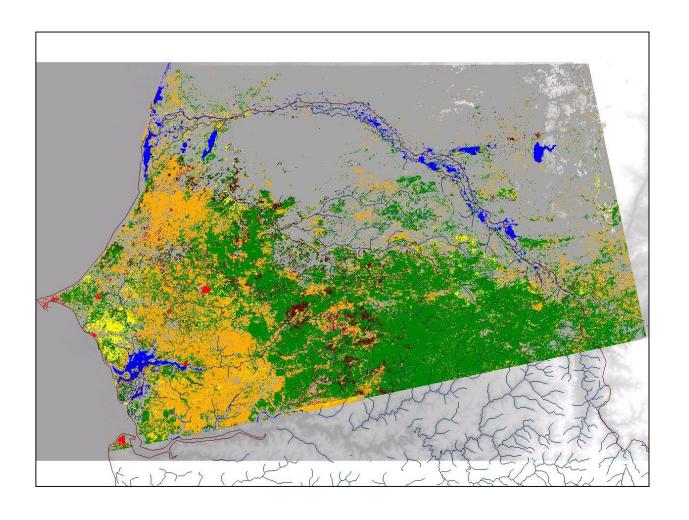
ENVISAT ASAR Wide Swath – May-August 2005



July-August

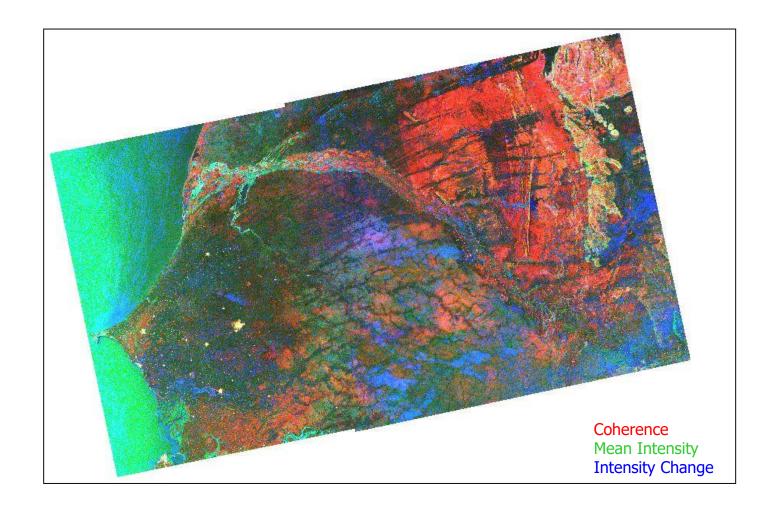


Crop Extent, May-August 2005



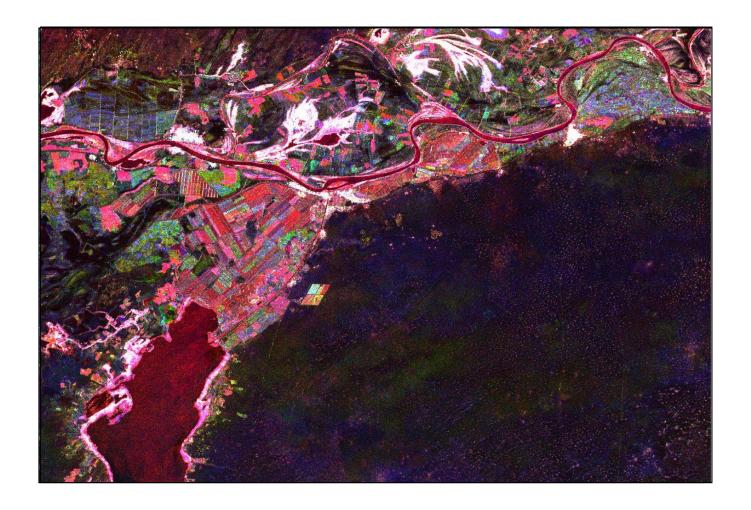


ASAR Wide Swath Interferometry, May-June 2005



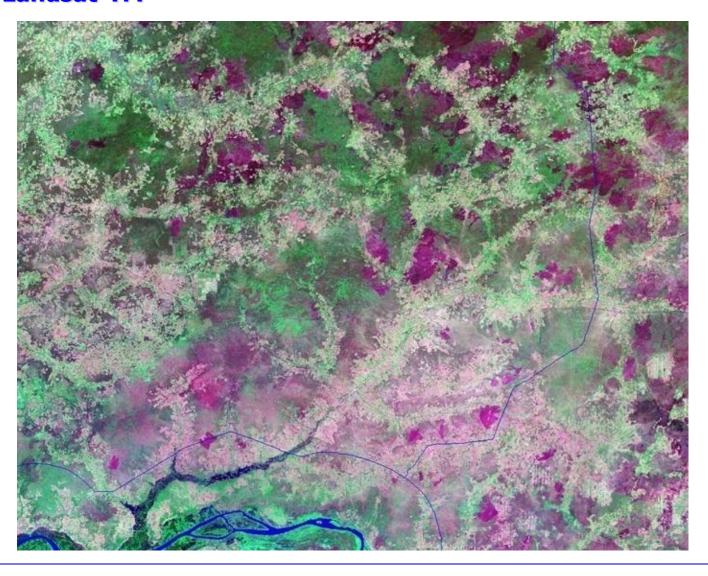


ENVISAT ASAR Alternating Polarization – June-July-August 2005



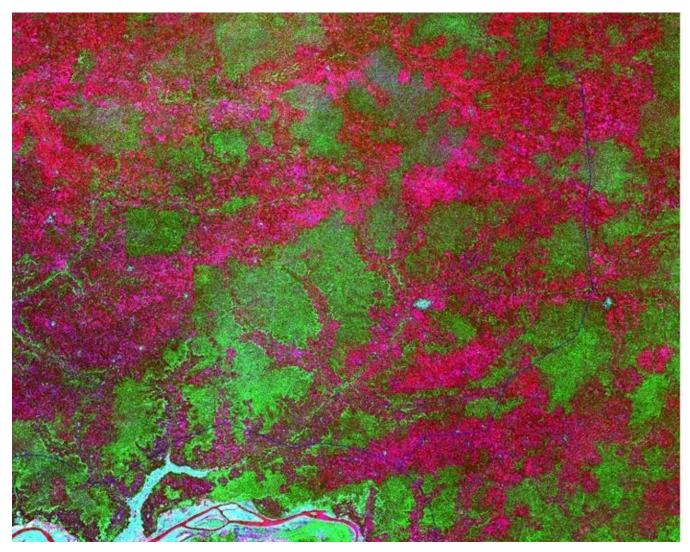
Sarmap your information gateway

Landsat-TM



Sarma your information gateway

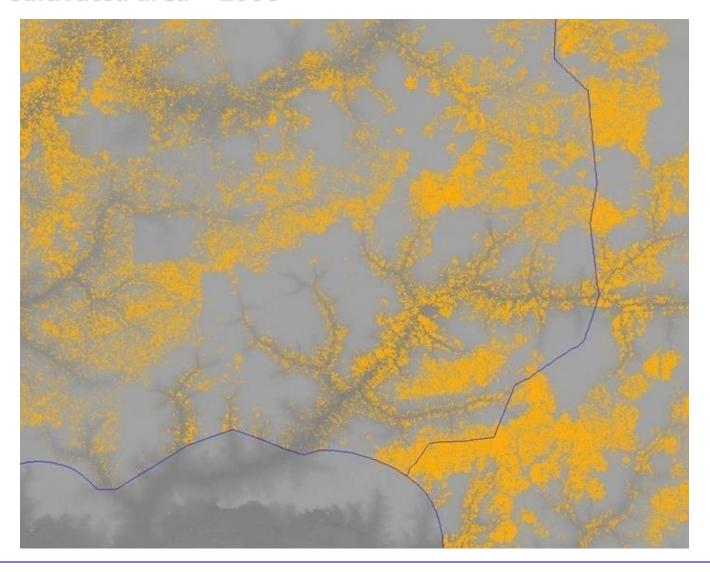
ENVISAT ASAR Alternating Polarization – 2006



HH max ratio
HV pre-crop mean
HH max difference

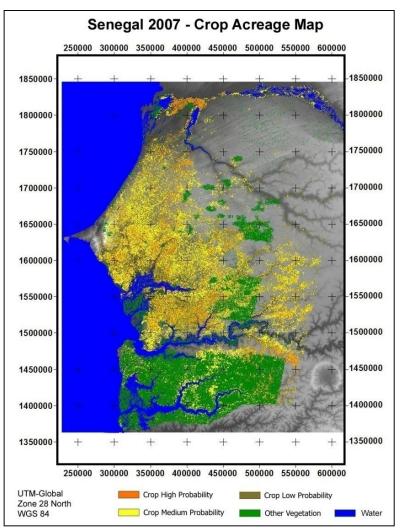
Sarmapour information gateway

Cultivated area – 2006





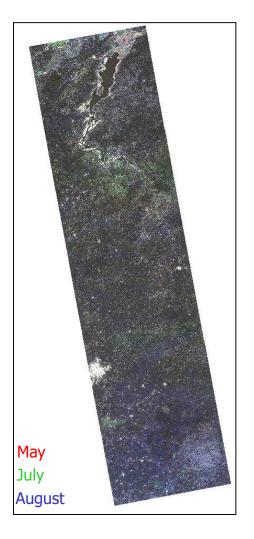
Senegal 2007 - Cultivated Area

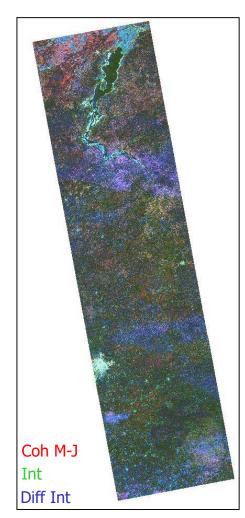


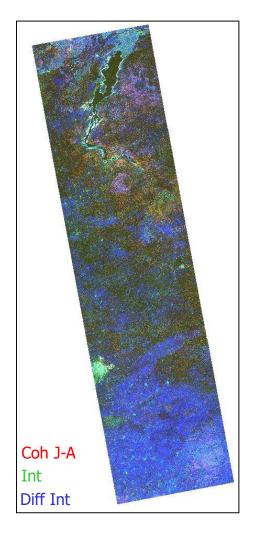
ASAR Alternating Polarization

Sarmapour information gateway

PALSAR-1 - 2006

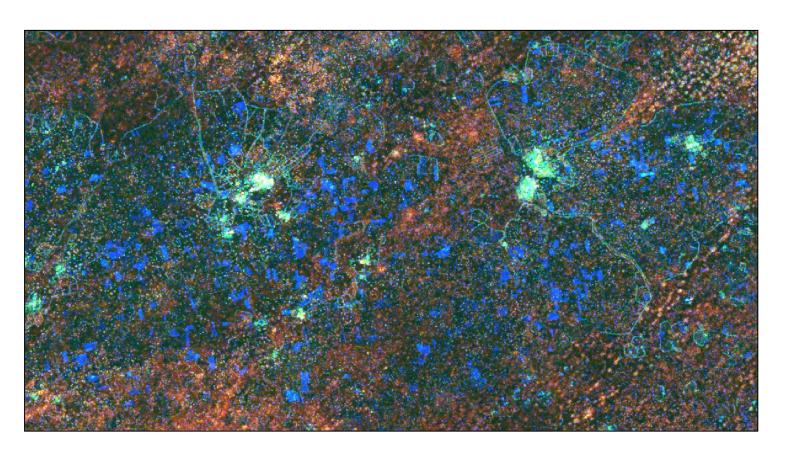






Sarmap your information gateway

PALSAR-1 HH - 2006



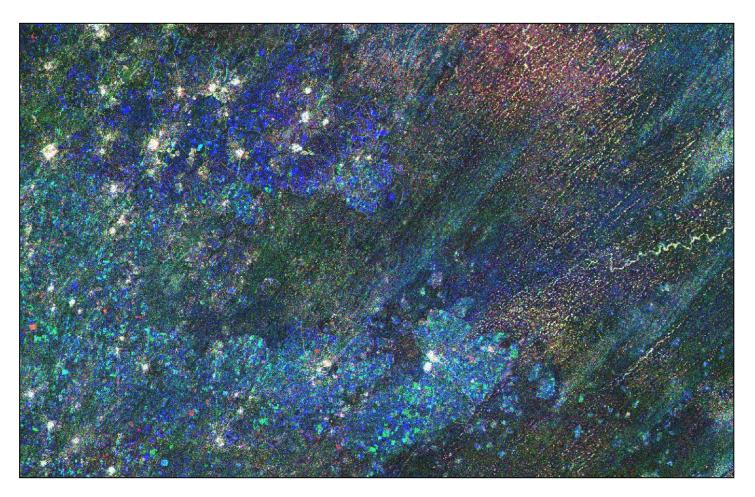
Coherence

Mean Intensity

Intensity Difference

Sarmap your information gateway

PALSAR-1 HH and ASAR HH - 2006



PALSAR HH AS

ASAR HH

ASAR HH



Lessons learned

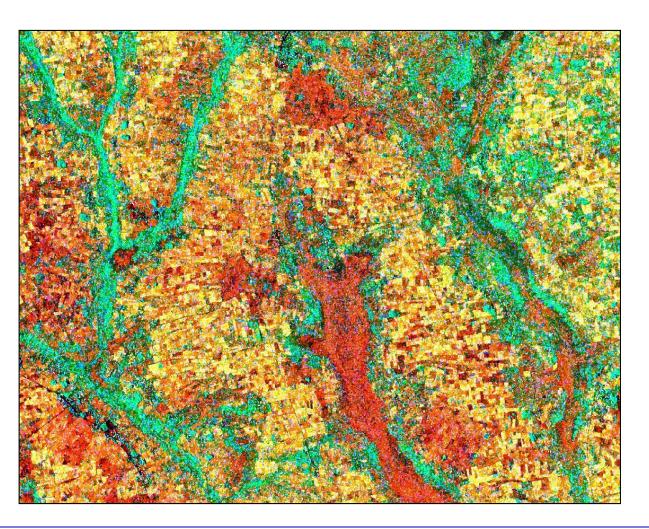
- The key factors are acquisition time and interval and spatial resolution
 -> Make use of all existing multi-temporal data.
- Crop in wet conditions is usually well discriminated.
- Crop in dry conditions is very difficult to detect with optical and SAR Intensity
 - -> **Coherence** can contribute, but today not available -> Sentinel 1A/B.
- Data synergy is conditio sine qua non
- Small plot agriculture in Africa requires the use of very high resolution data in order to identify the fields.



The use of VERY HIGH RESOLUTION data



The impact of coherence and very high resolution SAR data

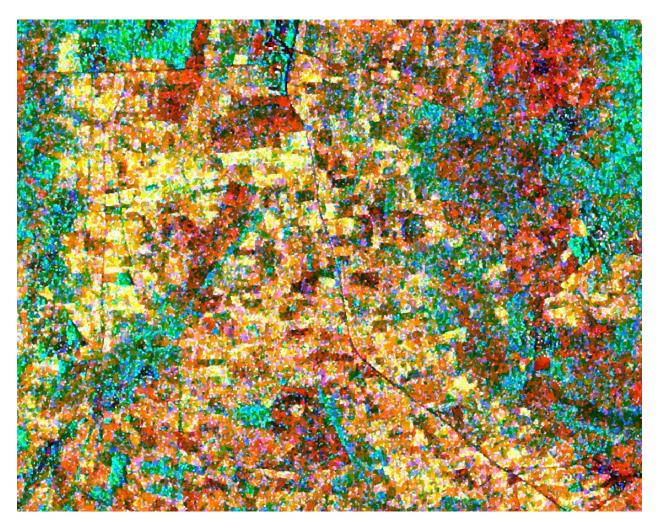


Cosmo-SkyMed (3m)

coherence mean intensity difference intensity

Sarma your information gateway

Cosmo-SkyMed (3m)

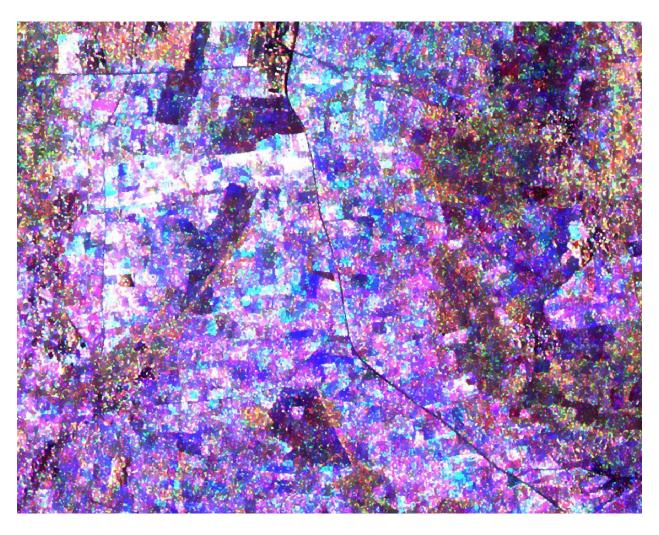


December 2009

coherence mean intensity difference intensity



Multi-temporal Cosmo-SkyMed (3m)



December January January



Cultivated area – Approach

It is meant the effective crop growth (i.e. cultivated) area during the rainfed crop season.

The method consists in the generation of three independent and complementary products, which, in turn, they are fused enabling the provision of the cultivated area. Each intermediate product has a clear meaning, i.e.

- i) the potential crop extent prior to the rainfed crop season;
- ii) the potential area at start of the rainfed crop season;
- iii) the crop growth extent during the rainfed crop season.



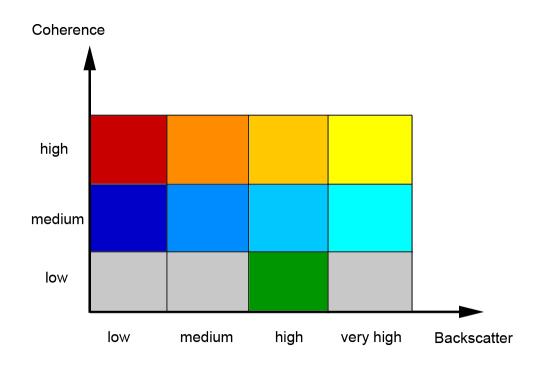
Cultivated area – Approach

	Multi-temporal ALOS PALSAR-1	Interferometric Cosmo-SkyMed StripMap	Multi-temporal ENVISAT
Potential crop extent prior to the start of crop season	PotCropExt once every n years		
Potential cultivated area at start of crop season		PCA-SoS once every m years	
Crop growth extent			CropGrowthExt every crop season

Cultivated Area = PotCropExt \cap PCA-SoS \cap CropGrowthExt

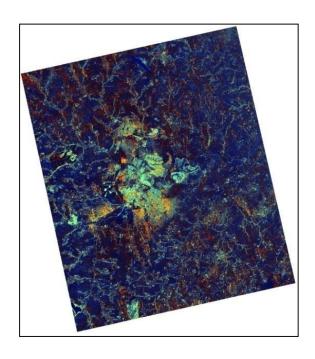


Cultivated area – The use of coherence



Sarmapour information gateway

Crop season 2010/11



Potential Crop Extent
ALOS PALSAR-1 (15m)

July-Sept 2008,2009,2010

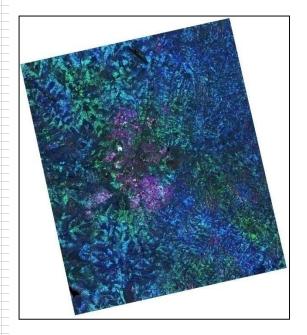


Potential Cultivated Area at SOS

1-day interferometric Cosmo-SkyMed StripMap (3m)
December 2010

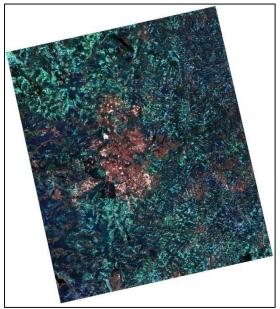
Sarmap your information gateway

Crop season 2010/11

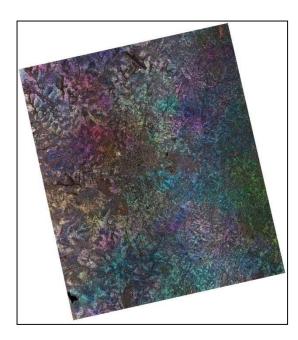


Crop Growth Extent

Multi-temporal ENVISAT ASAR (15m)
October 2010-April 2011



Crop Growth Extent
Multi-temporal ALOS PALSAR-1 (8m)
October 2010-April 2011



Crop Growth Extent

Multi-temporal Cosmo-SkyMed (3m)

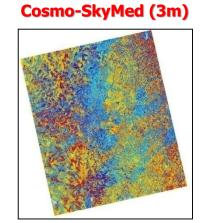
December 2010-February 2011



Lilongwe - Crop season 2010/11



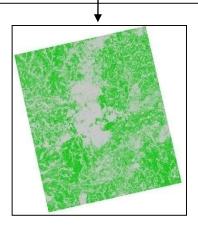
Potential Crop Extent



Potential crop area at SoS



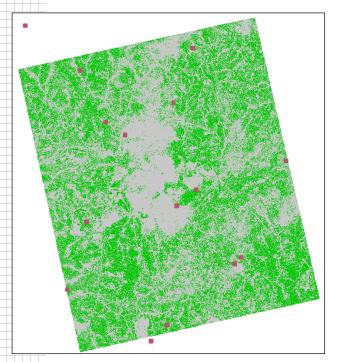
Crop Extent during the crop season



Cultivated Area (15m)



Lilongwe - Crop season 2010/11



	Other	Crop	Total	Omission error (%)
Other - A	32	0	32	0
Crop - B1-6	8	94	102	8
Other - B7	4	0	4	0
Other - C	0	0	0	0
Other - D	4	0	4	0
Other - E	0	0	0	0
Other - F	15	1	16	6
Other - G	0	0	0	0
Other - H	13	0	13	0
Total	76	95	171	K-coeff 0.9
Commission error (%)	11	1	Overall accuracy 95%	



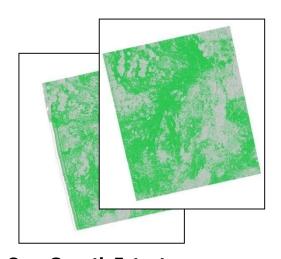
Rumphi - Crop season 2010/11



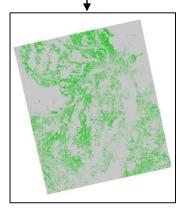
Potential Crop Extent



Potential Crop Area at SoS



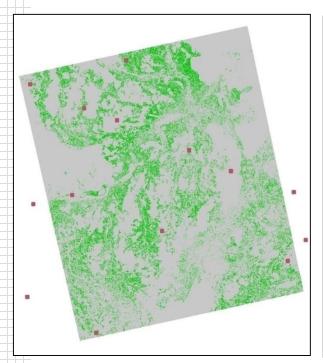
Crop Growth Extent



Cultivated Area



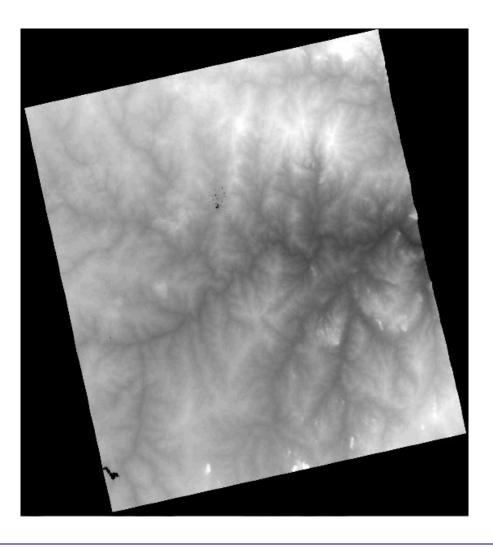
Rumphi - Crop season 2010/11



	Other	Crop	Total	Omission error (%)
Other - A	1	0	1	0
Crop - B1-6	2	26	28	7
Other - B7	8	1	9	11
Other - C	7	0	7	0
Other - D	33	0	33	0
Other - E	7	0	7	0
Other - F	26	0	26	0
Other - G	0	0	0	0
Other - H	1	0	1	0
Total	85	27	112	K-coeff 0.9
Commission error (%)	2	4	Overall accuracy 97%	



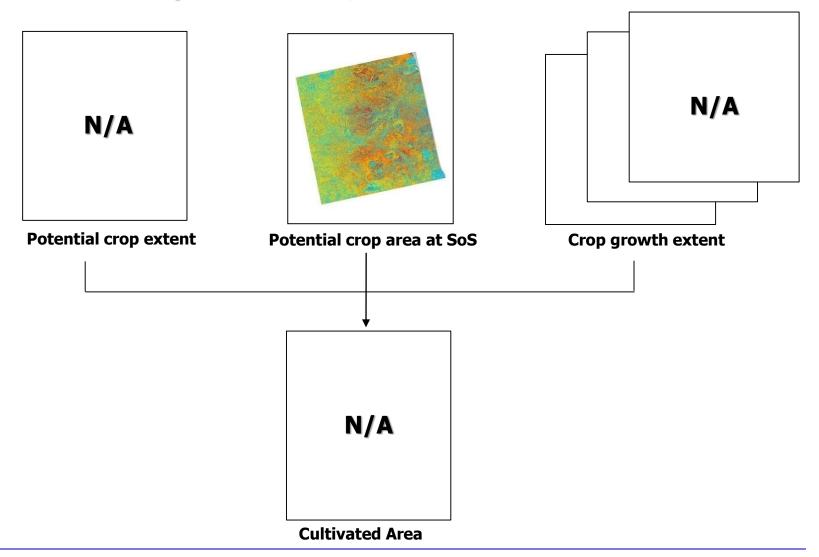
Rumphi – A 'side' product ... Digital Elevation Model



Based on 1-day interferometric
Cosmo-SkyMed StripMap data (3m) acquired in December 2010.

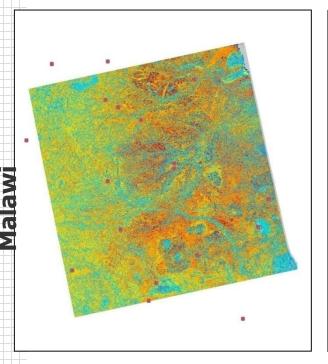


Zomba – Crop season 2010/11



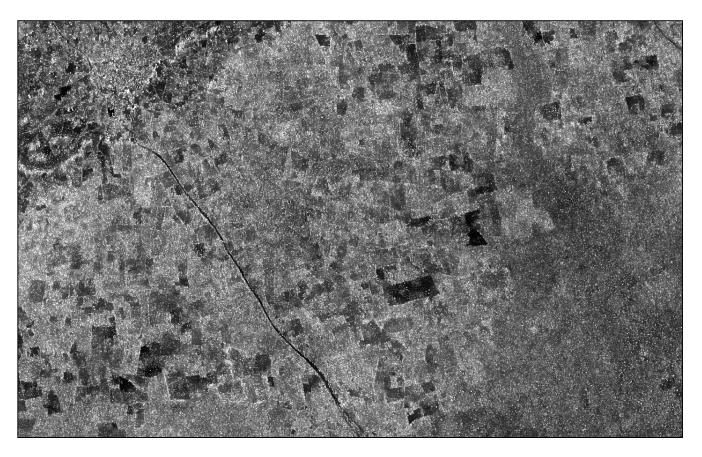


Zomba - Crop season 2010/11



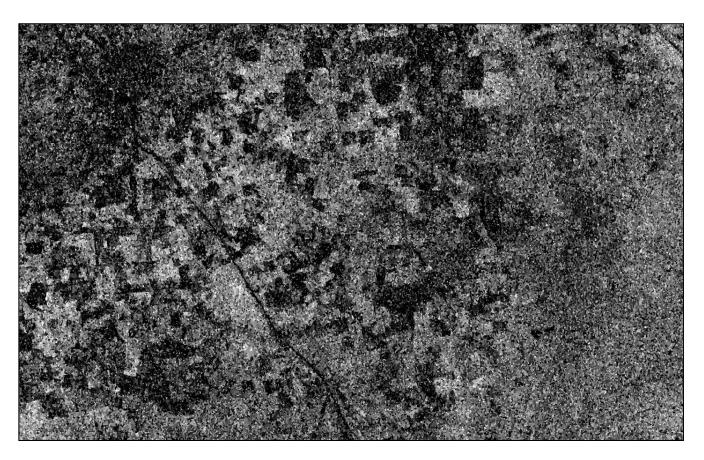
	Other	Crop	Total	Omission error (%)
Other - A	12	6	18	33
Crop - B1-6	19	114	133	14
Other - B7	1	9	10	90
Other - C	0	0	0	0
Other - D	4	0	4	0
Other - E	8	2	10	20
Other - F	16	10	26	38
Other - G	1	1	2	50
Other - H	1	1	2	50
Total	62	143	205	K-coeff 0.5
Commission error (%)	31	20	Overall accuracy 77%	





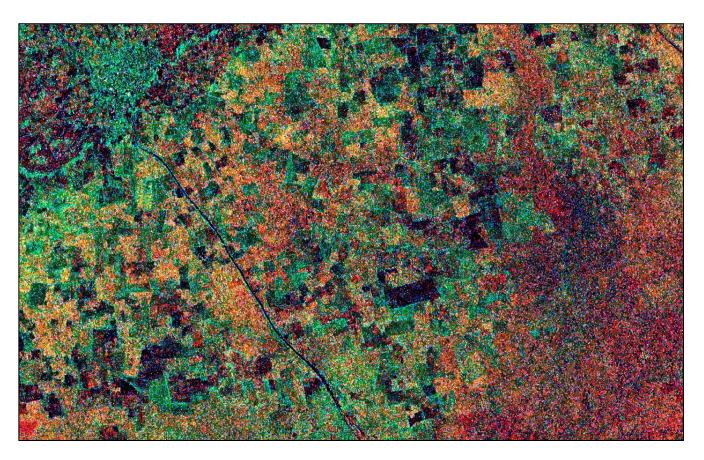
Cosmo-SkyMed Intensity - September 2011





Cosmo-SkyMed Coherence - September 2011





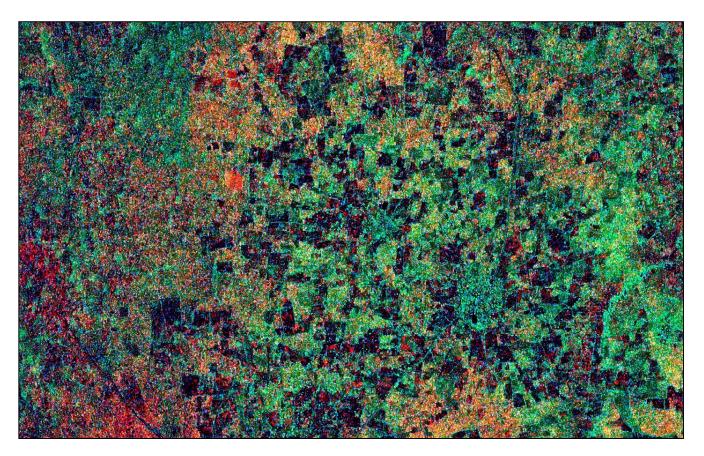
Cosmo-SkyMed Coherence & Intensity - September 2011





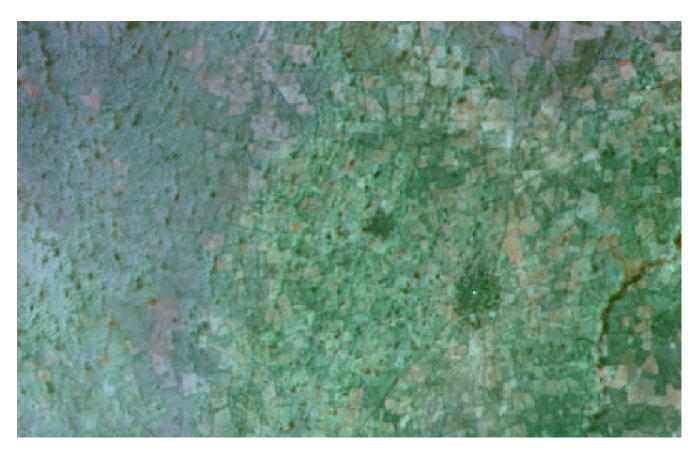
SPOT-2 - October 2010

Crop in dry condition



Cosmo-SkyMed Coherence & Intensity - September 2011



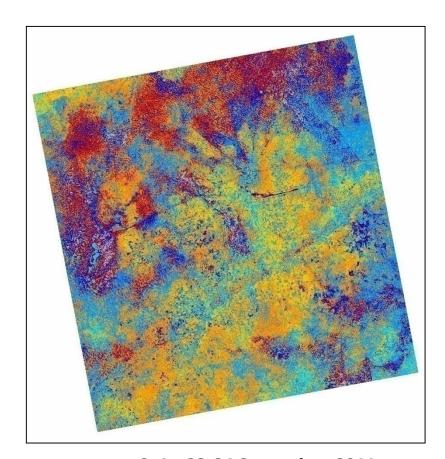


SPOT-2 - October 2010

Crop in dry condition



CSK – 23-24 September 2011

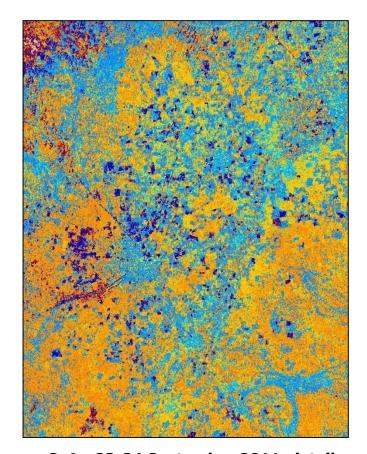


CuA - 23-24 September 2011

Crop in dry condition

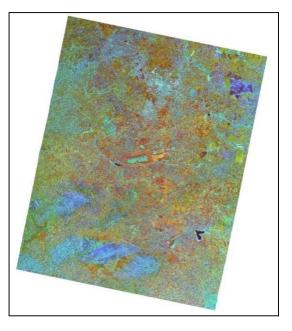


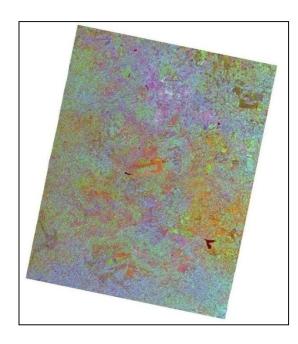
CSK - 23-24 September 2011, detail



CuA - 23-24 September 2011, detail

Crop growth monitoting





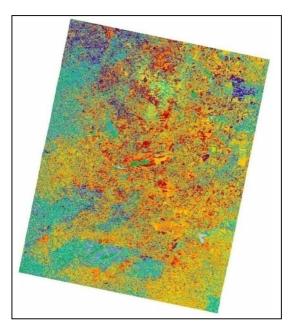
CSK - 06-07 March

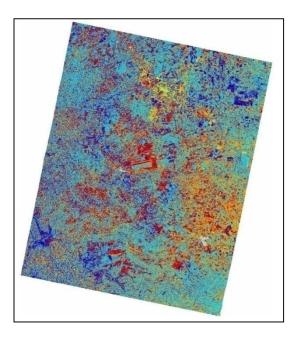
CSK - 07-08 April

CSK - 28-29 July



Crop growth monitoting



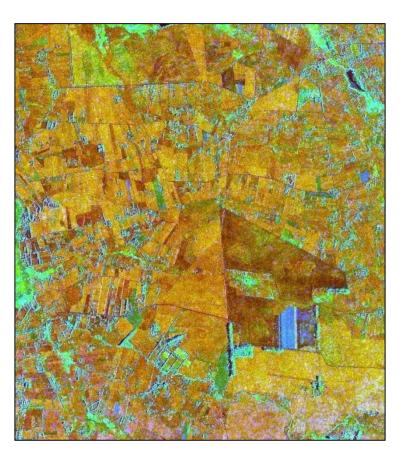


CuA - 06-07 March

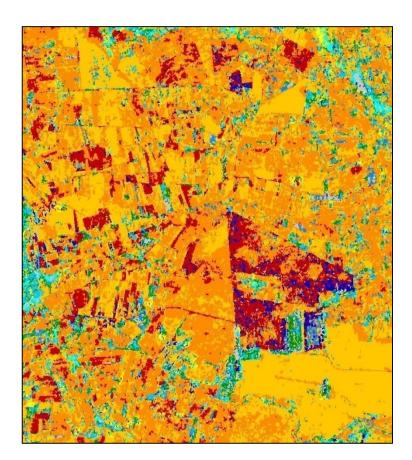
CuA - 07-08 April

CuA - 28-29 July

Crop growth monitoting

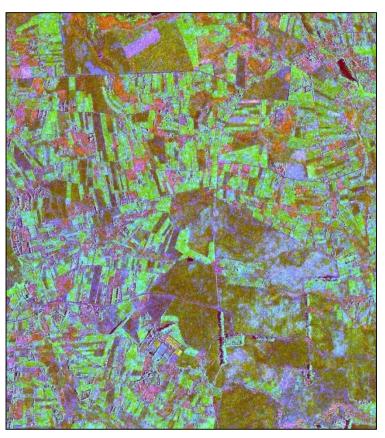


CSK - 07-08 April, detail

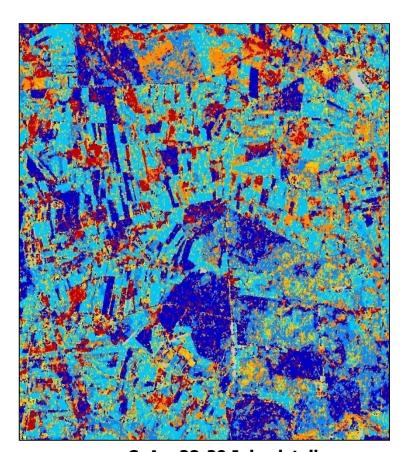


CuA - 07-08 April, detail

Crop growth monitoting

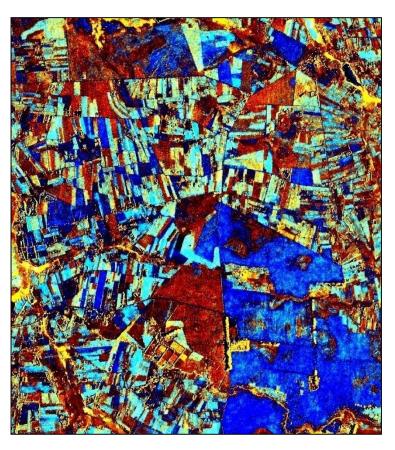


CSK - 28-29 July, detail

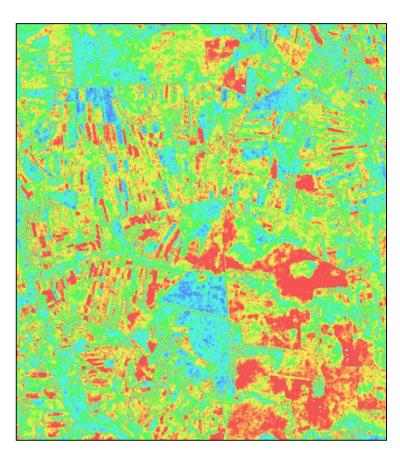


CuA - 28-29 July, detail

Crop growth monitoting



CSK - min max span, detail



Crop Development March-July





Lessons learned

- The use of very high resolution data is conditio sine qua non in small plot agriculture in Africa.
- Coherence plays a key role in crop in dry conditions.
- Data synergy is fundamental in order to
 - provide appropriate time-series;
 - improve information content.



Content

- 1. Key SAR basics
- 2. Past, existent, forthcoming SAR systems
- 3. SAR data processing
- 4. Agriculture
 - Rice in Asia
 - Small plot agriculture in Africa
- 5. Agriculture and other land covers in Africa
- 6. Forestry
 - Natural forest
 - Forest plantation
 - Bio-physical parameters
- 7. Digital Elevation Model
 - Fusion SAR interferometry-Optical stereo



How land cover maps are generated?

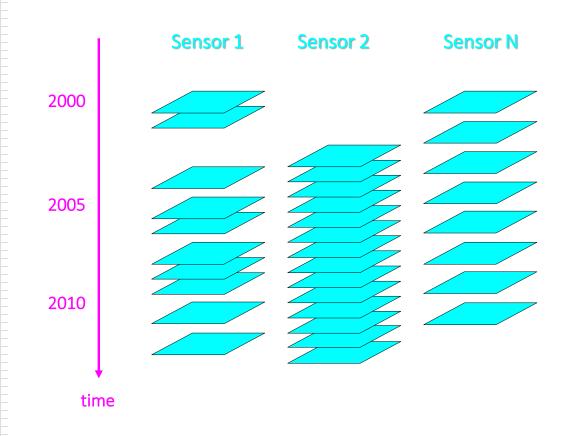
- Each sensor has its own peculiarity
 - ⇒ Extract the selected information from the most suitable sensor

- Each land cover has a different temporal evolution
 - Extract the requested information within the most suitable time period

⇒ Multi-annual, multi-sensor approach

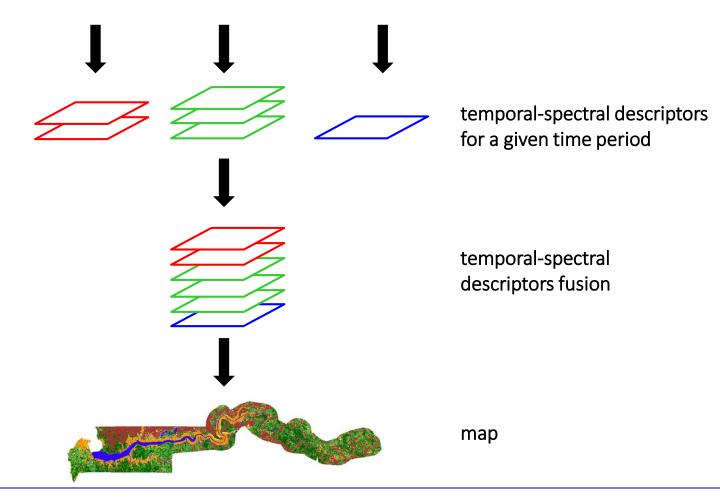


Multi-annual, multi-sensor data analysis



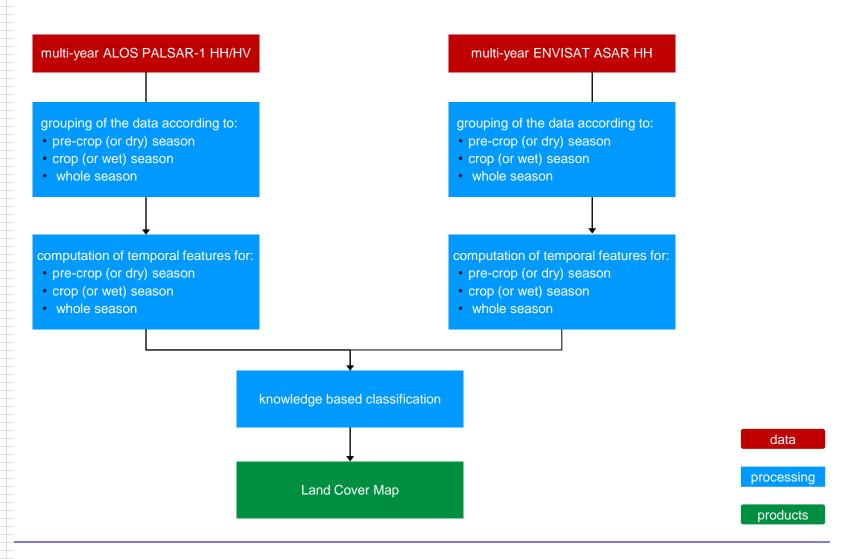


Multi-annual, multi-sensor data analysis





Method





Data set

- 21 ENVISAT ASAR WS scenes (400x400km, 100m) <u>irregularly</u> acquired from 2004 to 2006.
- 17 ALOS PALSAR-1 SS scenes (350x350km, 100m) <u>irregularly</u> acquired from 2006 to 2010.
- 280 ENVISAT ASAR AP scenes (100x100km, 15m) <u>irregularly</u> acquired from 2003 to 2010.
- 156 ALOS PALSAR-1 FBD scenes (70x70km, 15m) regularly acquired during given periods of the year from 2007 to 2010.
- 11 Cosmo-SkyMed Stripmap scenes (40x40km, 3m) <u>regularly</u> acquired from May to December 2013.
- 506 MODIS Terra (MOD13Q1) and Aqua (MYD13Q1) 16-days composite at 250m from 2002 to 2012.



Multi-year ENVISAT ASAR Wide Swath, 100m



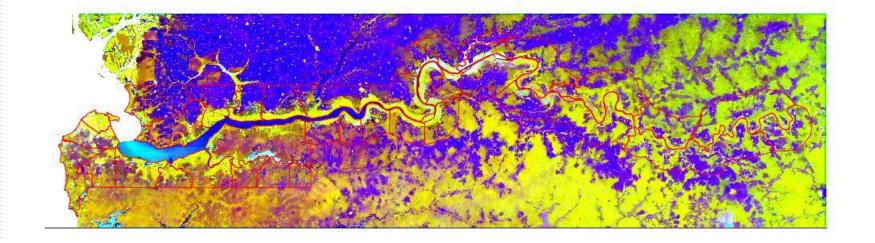
ENVISAT ASAR WS C-HH maximum

ENVISAT ASAR WS C-HH span

ENVISAT ASAR WS C-HH minimum



Multi-annual ASAR WS and PALSAR-1 ScanSAR, 100m



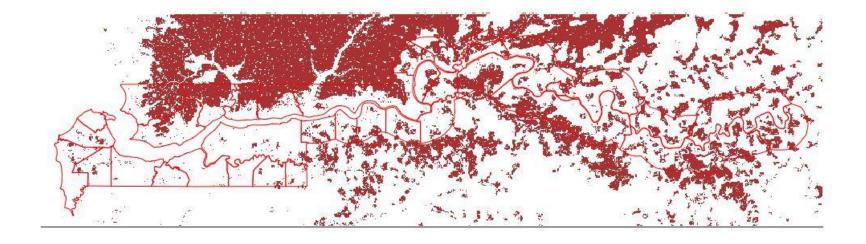
ALOS PALSAR-1 L-HH pre-crop

ENVISAT ASAR C-HH pre-crop

ENVISAT ASAR C-HH span

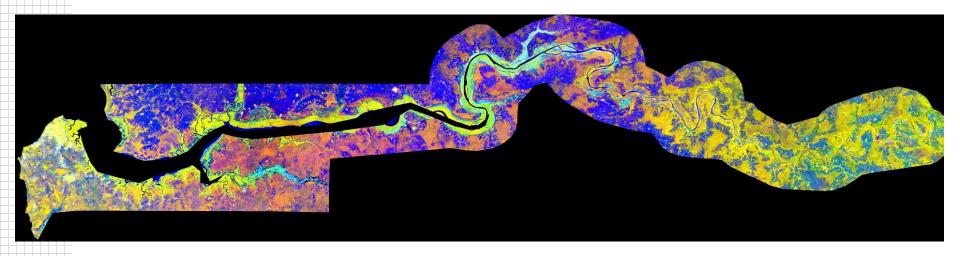


Agricultural area at 1 hectare





Multi-annual, multi-sensor mosaic at 15m



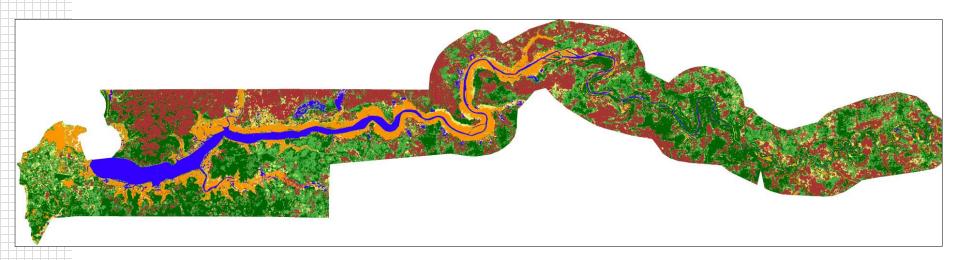
ALOS PALSAR-1 mean L-HV pre-crop season

ENVISAT ASAR mean C-HH pre-crop season

ENVISAT ASAR C-HH difference crop and pre-crop season



Multi-annual, multi-sensor Land Cover Map at 15m



Agricultural area

Mangrove - Sandbanks

Water

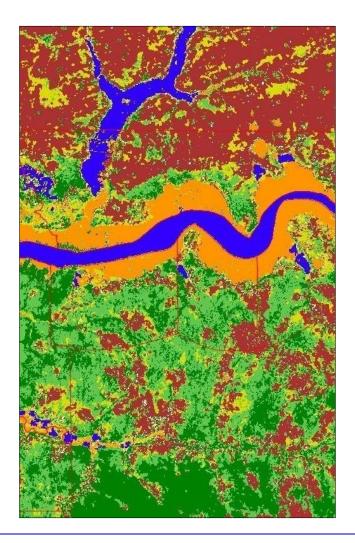
Bare soil-weak vegetation (low biomass)

Medium vegetation (medium biomass)

Strong vegetation (high biomass)



Multi-annual, multi-sensor Land Cover Map at 15m, detail



Agricultural area

Mangrove - Sandbanks

Water

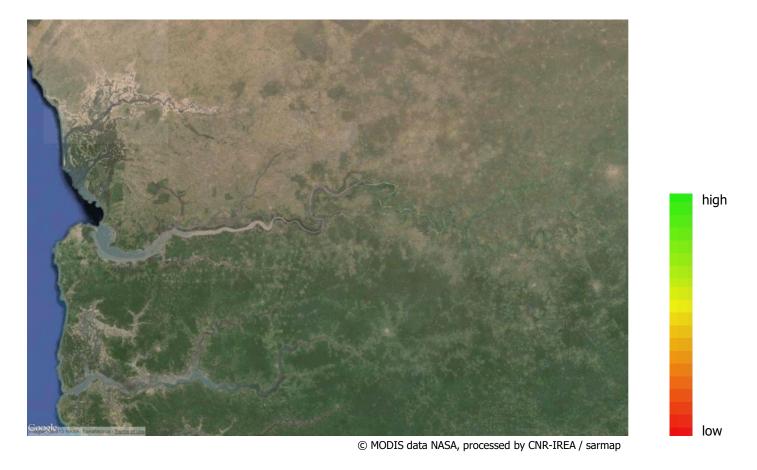
Bare soil-weak vegetation (low biomass)

Medium vegetation (medium biomass)

Strong vegetation (high biomass)



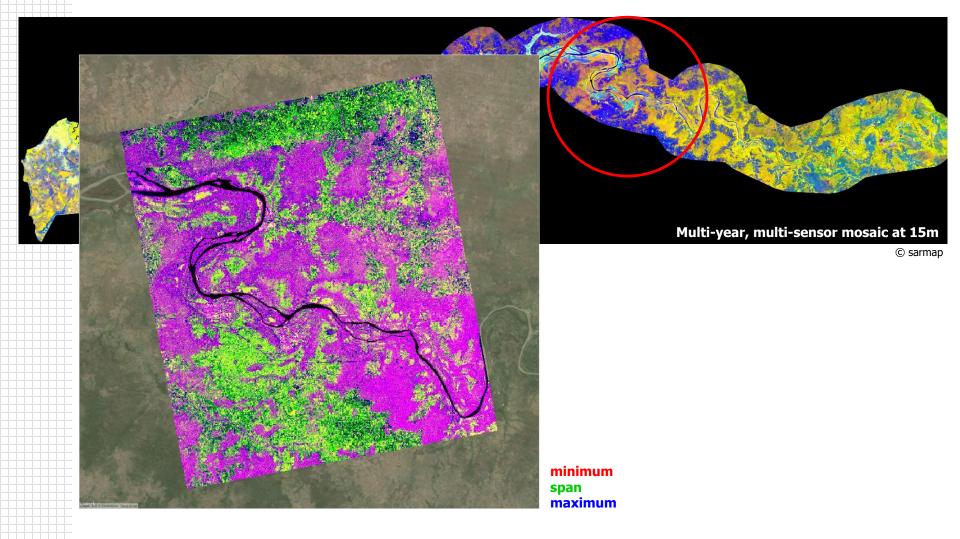
2002-12 Vegetation Productivity Index for agricultural area at 250 m



- The VPI has been derived from Aqua and Terra MODIS 250m every 8 days from 2002 to 2012
- It is relative to Mid September (approximately peak of season) of each year

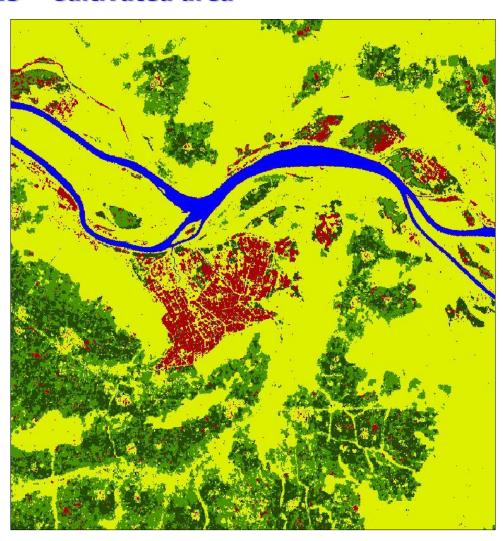


2013 - Seasonal Cosmo-SkyMed data at 3m





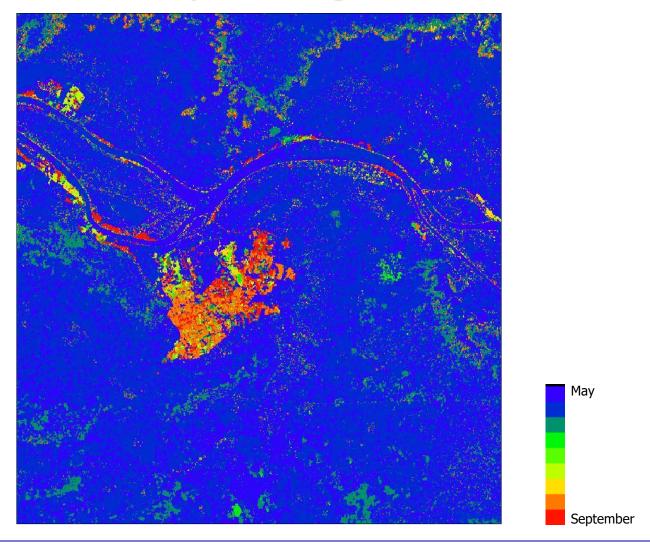
2013 - Cultivated area



Rice Crop 1 Crop 2 Water Forest

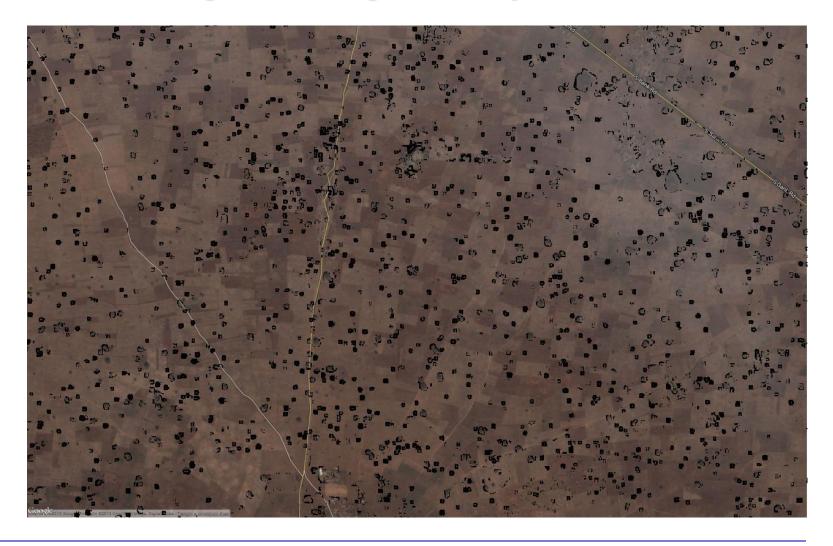


2013 - Date of crop season begin



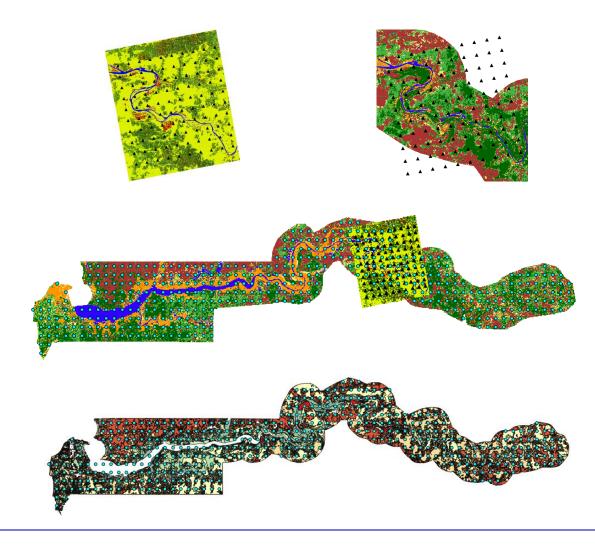


Detection of single trees using Cosmo-SkyMed 3m





Validation





Validation

		Мар		
		crop	non-crop	accuracy
Survey	crop	17	6	73.9%
Sur	non-crop	5	54	91.5%
	reliability	77.3%	90.0%	87.0%

		Map		
		crop	non-crop	accuracy
Survey	crop	18	5	78.3%
Sur	non-crop	8	54	87.1%
	reliability	69.2%	91.5%	85.0%

		Map		
		crop	non-crop	accuracy
Survey	crop	85	29	74.6%
Sur	non-crop	29	277	90.5%
	reliability	74.6%	90.5%	86.2%

Confusion matrices relative to the class agriculture for (top) seasonal LCM 2013; (centre) national baseline LCM 15m same area as seasonal LCM 2013; (bottom) national baseline LCM 15m. Accuracy is defined as 100%-omission error, reliability as 100%-commission error.



Lessons learned

- Understanding of crop practices and environmental conditions is essential for the provision of useful remote sensing products.
- Don't think just on pixels, resolution, frequency, algorithms ...
- The use of multi-year multi-sensor data (and how to combine them) is fundamental.

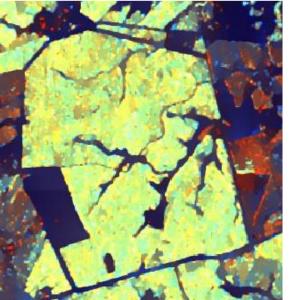


Content

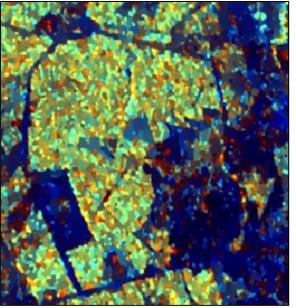
- 1. Key SAR basics
- 2. Past, existent, forthcoming SAR systems
- 3. SAR data processing
- 4. Agriculture
 - Rice in Asia
 - Small plot agriculture in Africa
- 5. Agriculture and other land covers in Africa
- 6. Forestry
 - Natural forest
 - Forest plantation
 - Bio-physical parameters
- 7. Digital Elevation Model
 - Fusion SAR interferometry-Optical stereo



Forest and SAR



ALOS PALSAR, Aug 2008 L-band



ENVISAT ASAR, Feb 2010 C-band

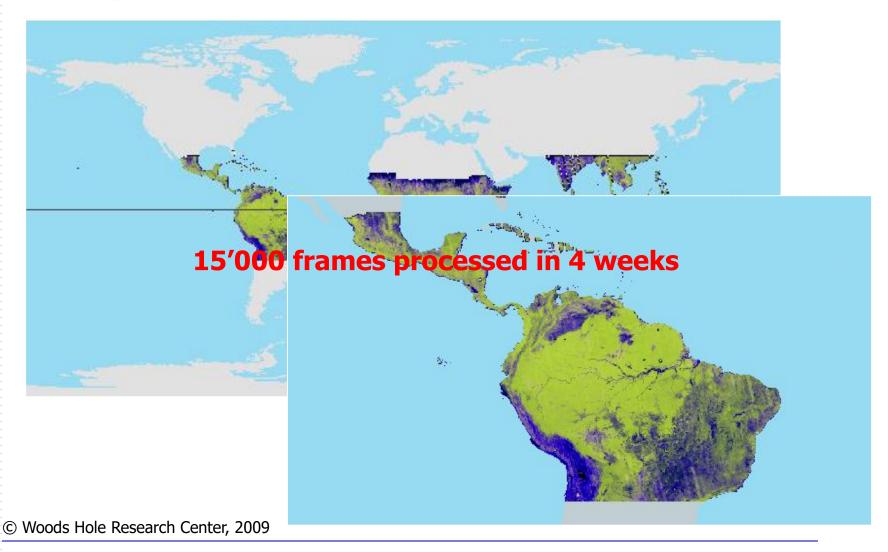


Cosmo-SkyMed, Dec 2009

X-band



Pan-tropical PALSAR-1 mosaic, 15m





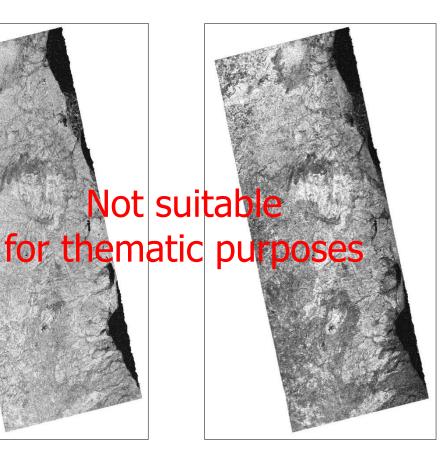
L-band Intensity vs. Coherence



Multi-year PALSAR-1 HH-HV intensity during dry season



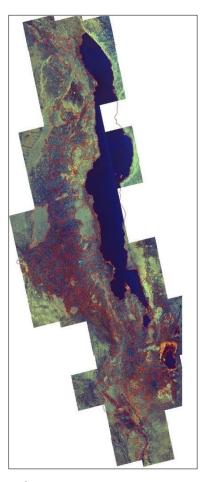
PALSAR-1 HH coherence during dry season



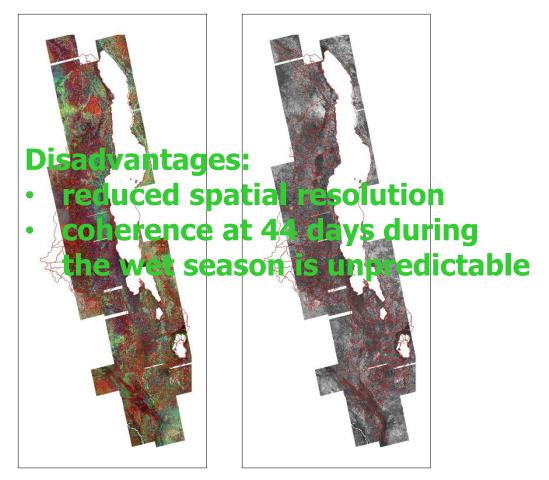
PALSAR-1 HV coherence during dry season



L-band Intensity vs. Coherence



Multi-year PALSAR-1 HH-HV during dry season

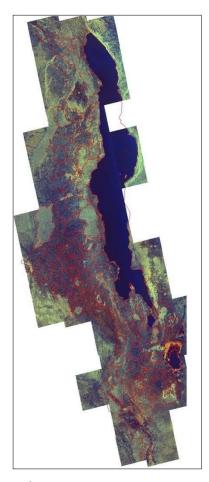


PALSAR-1 HH coherence & intensity during wet (crop) season

PALSAR-1 HH coherence during wet (crop) season



Forest area

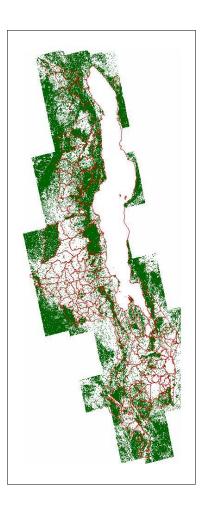


Multi-year PALSAR-1 HH-HV during dry season

Input data:
All PALSAR-1 HH/HV
data acquired during
the dry season from 2006

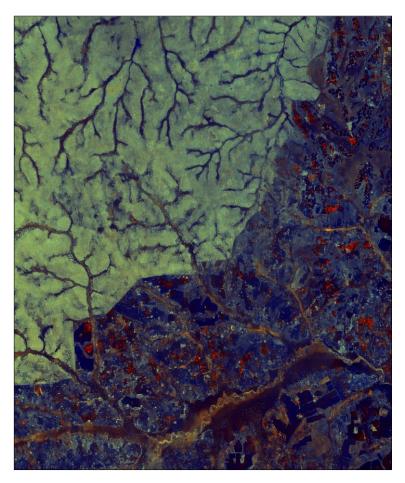
Temporal descriptors:

- Mode
- Span
- Maximum

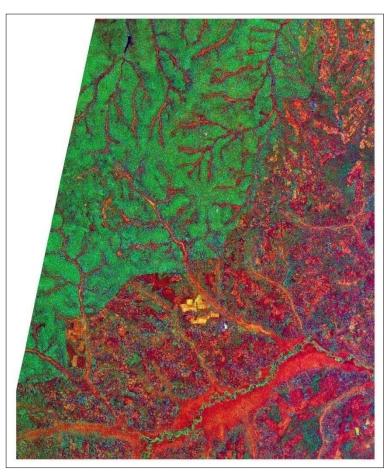




L-band vs. 1-day interferometry X-band data



Multi-year PALSAR-1 HH-HV (15m) during dry season



1 day InSAR CSK StripMap (3m) during dry season



Tropical (Malawi) – L-band vs. 1-day interferometry X-band data



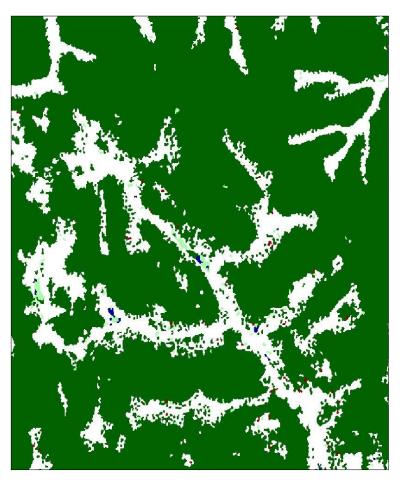


Multi-year PALSAR-1 HH-HV (15m) during dry season

1 day InSAR CSK StripMap (3m) during dry season



Tropical (Malawi) — L-band vs. 1-day interferometry X-band data

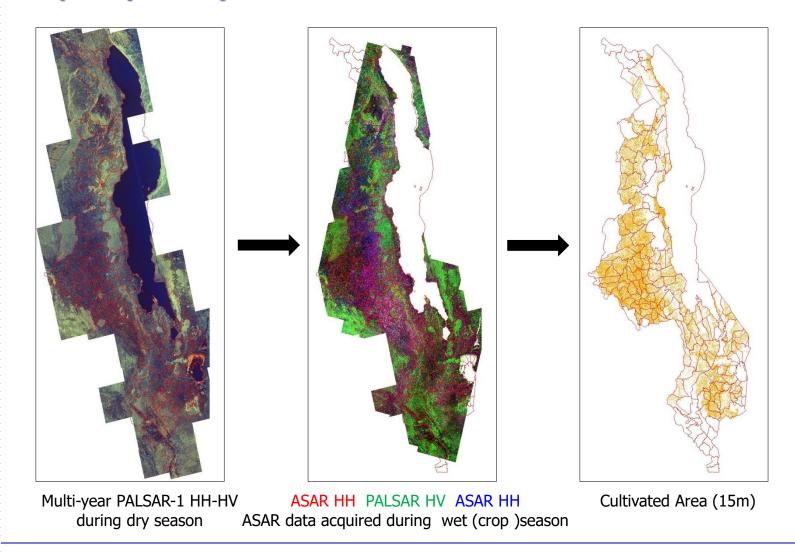


Multi-year PALSAR-1 HH-HV (15m) during dry season

1 day InSAR CSK StripMap (3m) during dry season

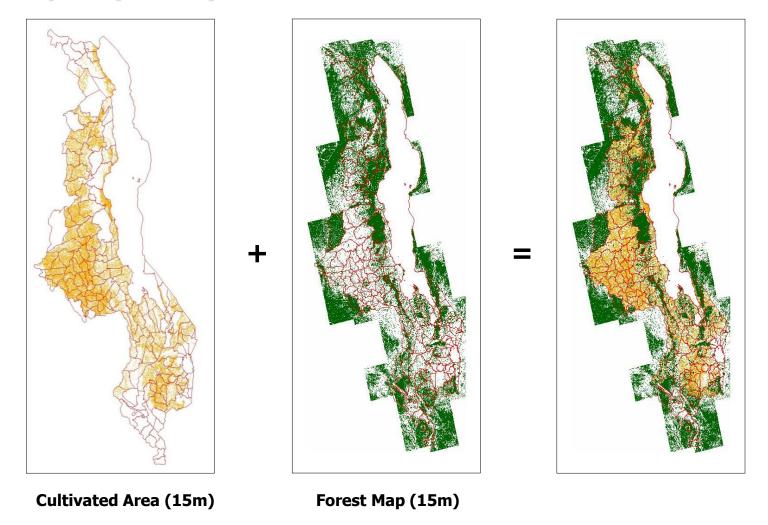


Tropical (Malawi) — Cultivated Area: L- and C-band data





Tropical (Malawi) – Cultivated and Forest Area





Tropical (Malawi) – Forest Area validation

	forest	sparse veg	other	Total	Omission error	
Urban	10	0	10	20	50	
Sugarcane	19	3	7	29	76	
Crop	42	0	347	389	11	
Forest	365	0	37	402	9	
Other	1	0	27	28	4	
Total	437	3	428	868	K-coeff 0.75	
Commission error (%)	16	0	9	overall accuracy 87%		
	forest	sparse veg	other	Total	Omission error	
Urban	10	0	10	20	50	
Sugarcane	10	3	16	29	45	
Crop	12	0	377	389	3	
Forest	357	0	45	402	11	
Other	1	0	27	28	4	
Total	390	3	475	868	K-coeff 0.82	
Commission error (%)	8	0	9	overall accuracy 91%		
	forest	sparse veg	other	Total	Omission error	
Urban	2	0	18	20	10	
Sugarcane	10	3	16	29	45	
Crop	12	0	377	389	3	
Forest	357	0	45	402	11	
Other	1	0	27	28	4	
Total	382	3	483	868	K-coeff 0.84	
Commission error (%)	7	0	9 overall accuracy 92%			

PALSAR-1 HH-HV

PALSAR-1 HH-HV Crop Map (ASAR HH-HV)

PALSAR-1 HH-HV Crop Map (ASAR HH-HV) ASAR HH-HV



Lessons learned

- The use of <u>multi-year</u> ALOS PALSAR-1 intensity data provide a <u>high data quality</u> (in terms geometry and radiometry) if compared to single-date intensity or interferometric SAR data.
- Multi-year ALOS PALSAR-1 intensity data are doubtless valuable for forest and environmental applications. However:
 - o depending on the geographical area, environmental conditions, and period of the year, data must be selected, processed, and used accordingly;
 - o SAR data synergy is conditio sine qua non to enhance the product quality.
- The products, at country-level, have been generated in an almost automated way. Today information at this level of detail is not available in Malawi.



PALSAR HH/HV, PALSAR HH InSAR, CSK HH InSAR

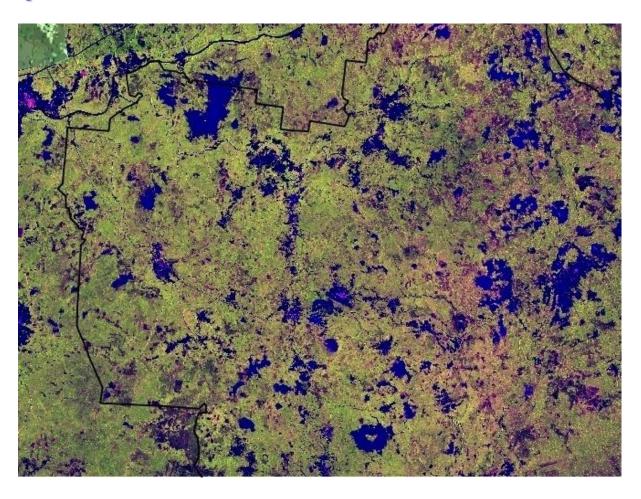


PALSAR HH/HV (15m) October 2009

PALSAR HH InSAR (8m) Dec 2008-Feb 2009

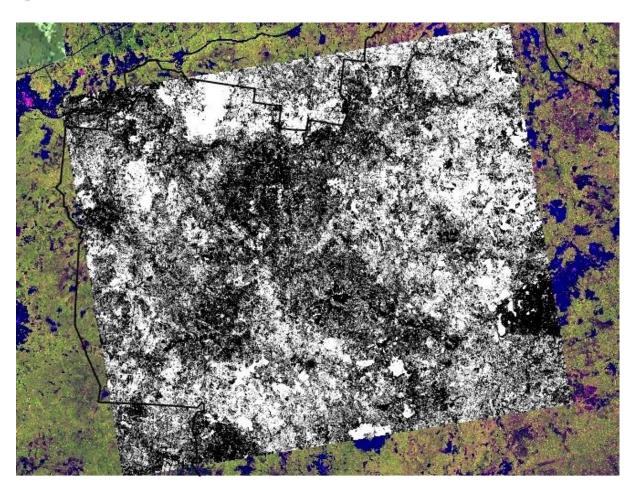
CSK HH InSAR (3m) September 24-25 2010





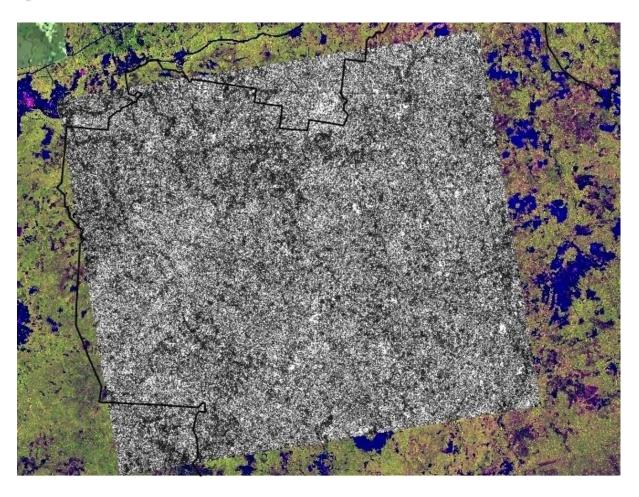
Multi-year PALSAR-1 **HH-HV Intensity**





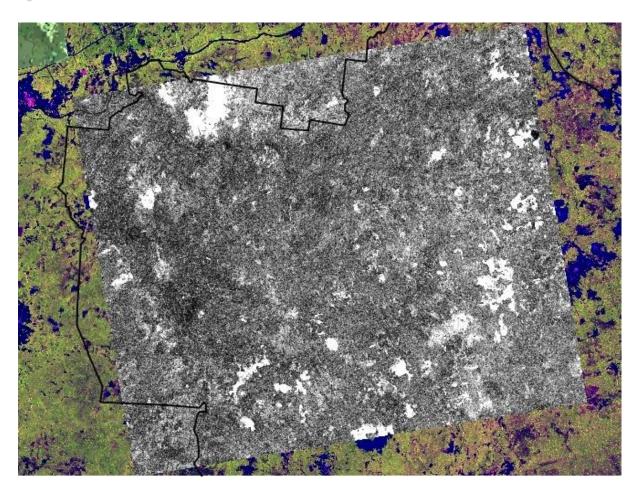
Coherence – 15 August 2007-30 September 2007





Coherence – 15 August 2007-17 August 2008



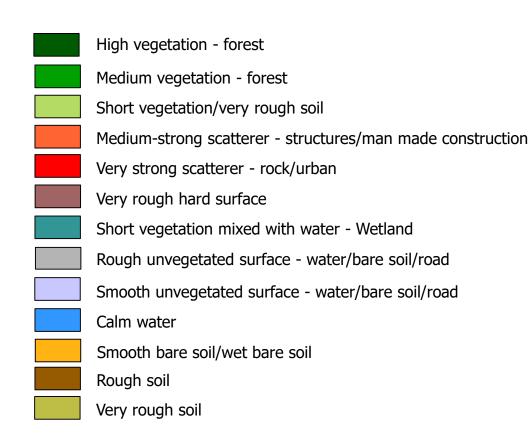


Coherence – 8 July 2010-25 August 2010



Forest area including land cover in non-forest areas

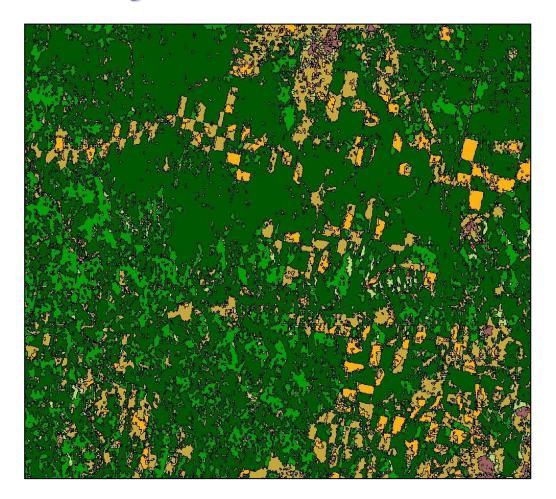




ALOS PALSAR-1 FBD, 15 meter - October 2009



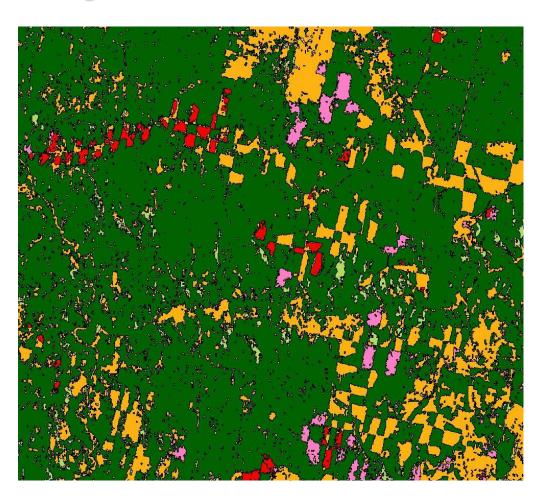
Forest area including land cover in non-forest areas



ALOS PALSAR-1 FBD, 15 meter - October 2009



Forest area changes



before 2007

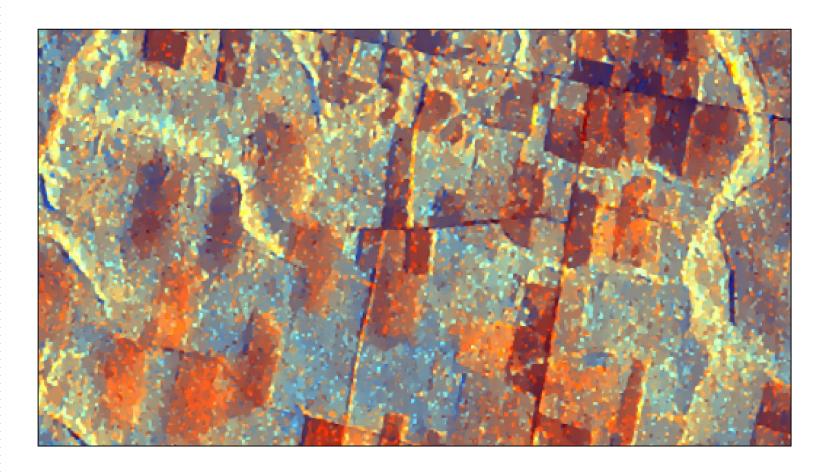
2007 - 2008

2008 - 2009

ALOS PALSAR-1 FBD, 15 meter



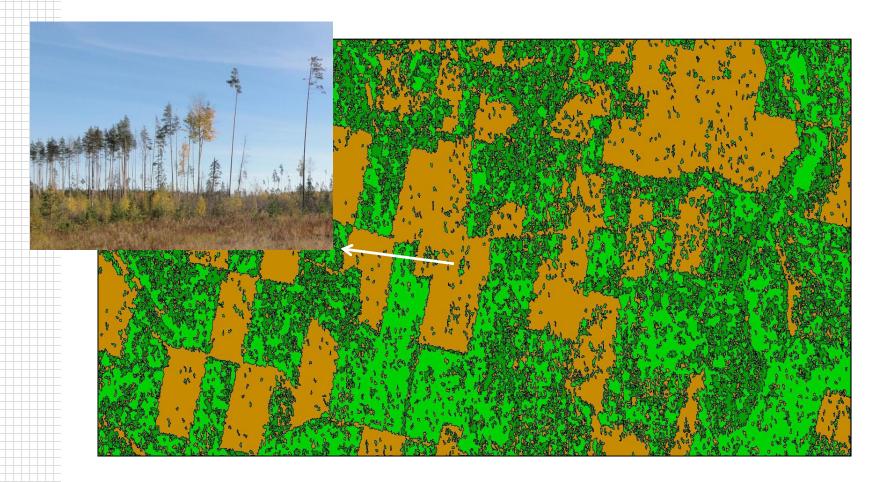
Clear fell areas



ALOS PALSAR-1 FBD, 15 meter - October 2009



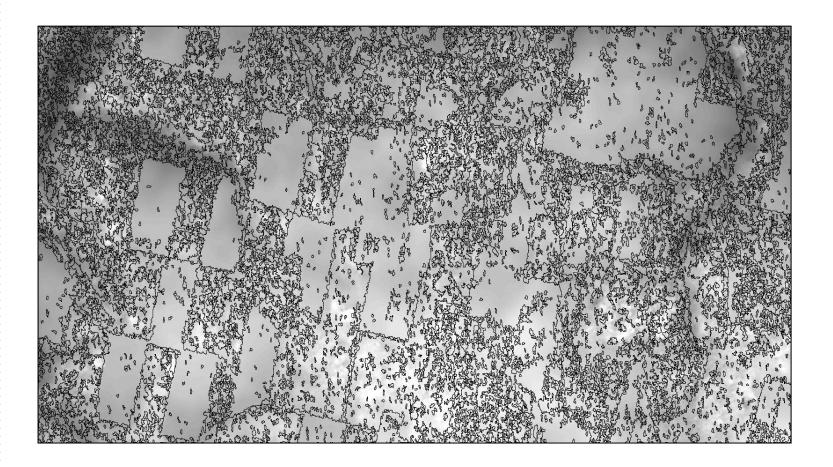
Clear fell areas and seed trees



1-day interferometric Cosmo-Skymed Stripmap, 3 meter - November 2010



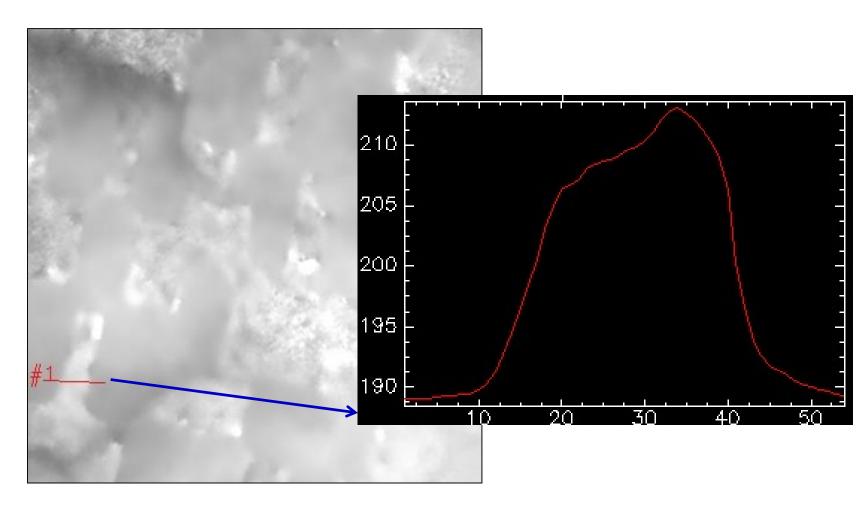
Clear fell areas and forest height estimation



1-day interferometric Cosmo-Skymed Stripmap, 3 meter - November 2010



Clear fell areas and forest height estimation

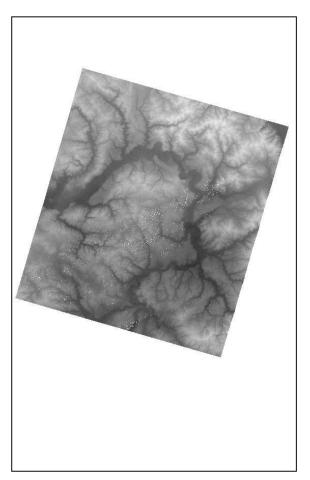


1-day interferometric Cosmo-Skymed Stripmap, 3 meter - November 2010



Digital Elevation Model, GTOPO vs. ERS-Tandem



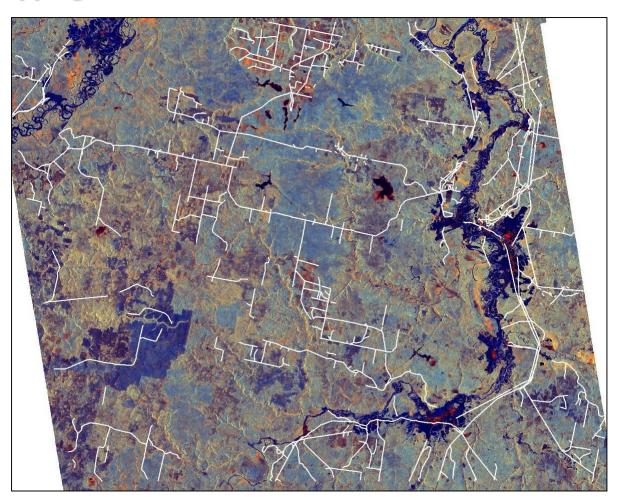


1 km

25 m



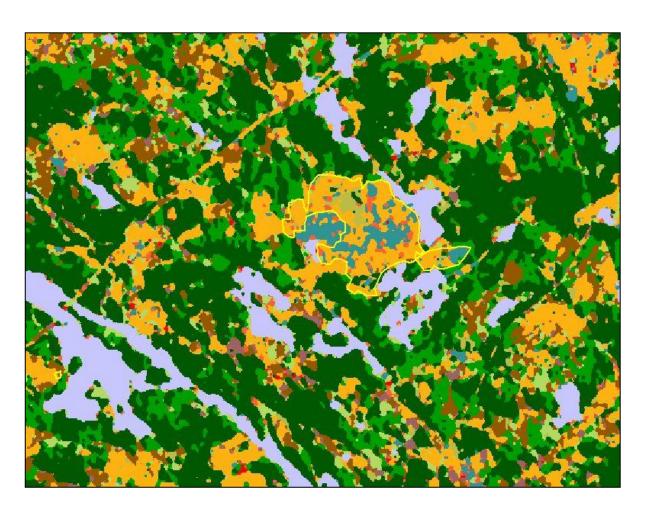
Road mapping



ALOS PALSAR-1 FBD, 15 meter - October 2009



Burnt areas



20070611

20070911

20080729

20080913

20090616

20090801

ALOS PALSAR-1 FBD, 15 meter



Lessons learned

- The use of multi-year (hence not single-date) intensity significantly improves the radiometric and geometric quality of the data and therefore of the product.
- At short wavelenghts, i.e. X-band, the use of 1-day coherence is mandatory to obtain an appropriate differentiation between forest and non-forest (but ofen still not sufficient). However, it is assumed that within the two acquistions meteorological events (e.g. rain, frost, wind, etc.) do not occur.
- In general, the use of repeat-pass coherence is not easy, because it is:
 - 1. very sensitive to the object status;
 - 2. the meteorological conditions/events. This is particularly true for long repeat-passes, as for instance with ALOS PALSAR-1 (46 days or a mutliple of 46 days).
 - 3. strongly dependent on the baseline; in orther words coherence should be calibrated accordingly. In general, it can be stated that Ithe correction factor is not linear: lower coeherence values must are more afficated than high ones.
- In summary, repeat-pass coherence is highly unpredictable.

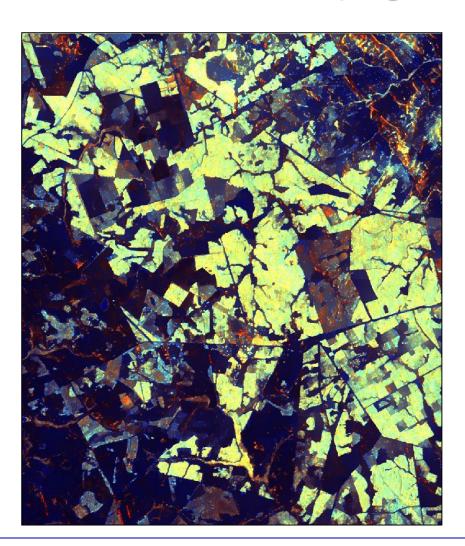


Content

- 1. Key SAR basics
- 2. Past, existent, forthcoming SAR systems
- 3. SAR data processing
- 4. Agriculture
 - Rice in Asia
 - Small plot agriculture in Africa
- 5. Agriculture and other land covers in Africa
- 6. Forestry
 - Natural forest
 - Forest plantation
 - Bio-physical parameters
- 7. Digital Elevation Model
 - Fusion SAR interferometry-Optical stereo



ALOS PALSAR-1 Fine Beam Dual, August 2008

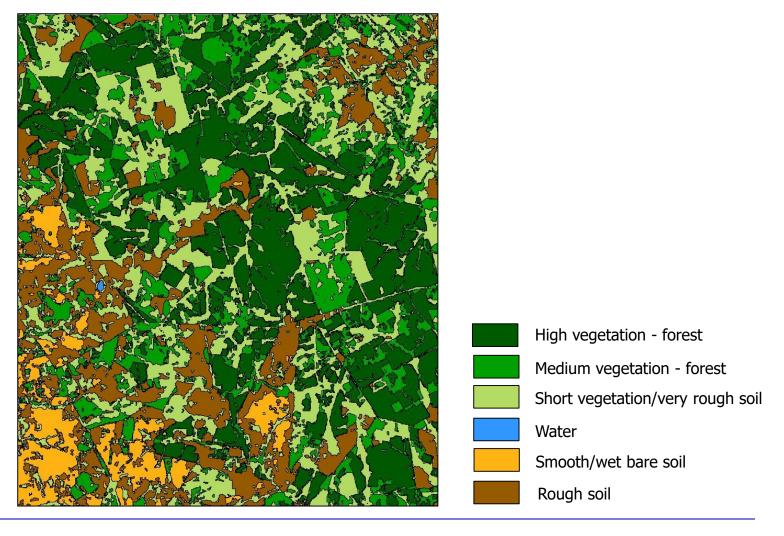


Processing

- Multi-looking
- Gamma DEMAP filtering
- Terrain geocoding including radiometric calibration and normalization
- ANLD filtering

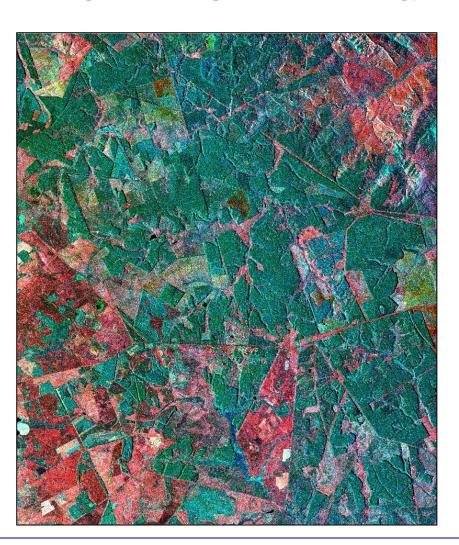


Land Cover Map





Cosmo-SkyMed 1-day Interferometry, Dec 2009

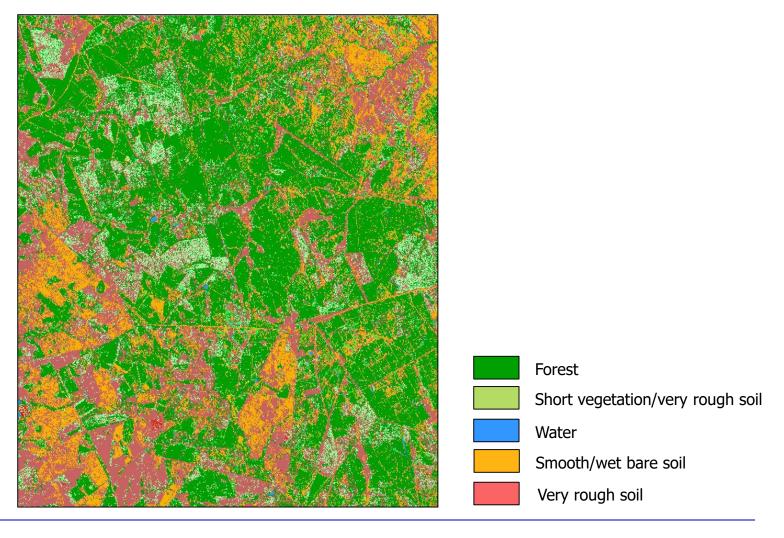


Processing

- SLC Gaussian DEMAP filtering
- Co-registration
- Coherence generation
- Terrain geocoding including radiometric calibration and normalization
- ANLD filtering

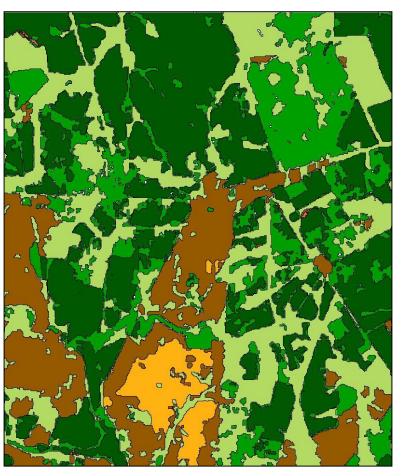


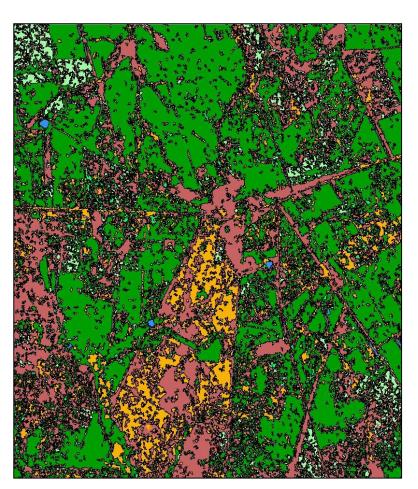
Land Cover Map





Land Cover Map comparison



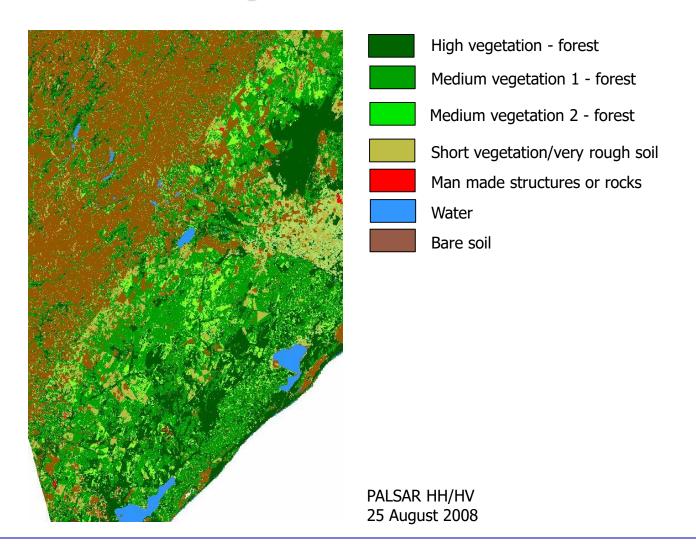


L-band HH-HV

1-day InSAR X-band

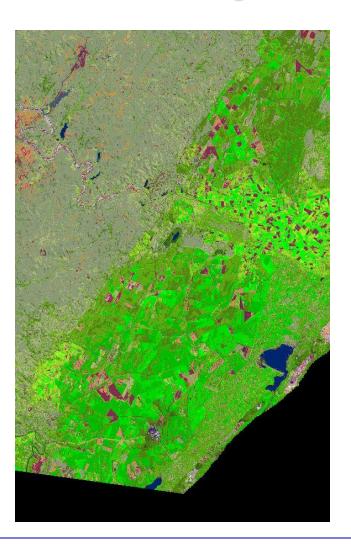


Forest area including land cover in non-forest areas





Forest area including land cover in non-forest areas



vegetation

rangeland

barren land

water

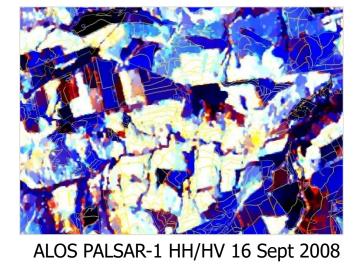
SPOT-4 30 May 2008



Genera detection – Eucalyptus, Pine, Amea



QuickBird 10 Sept 2008

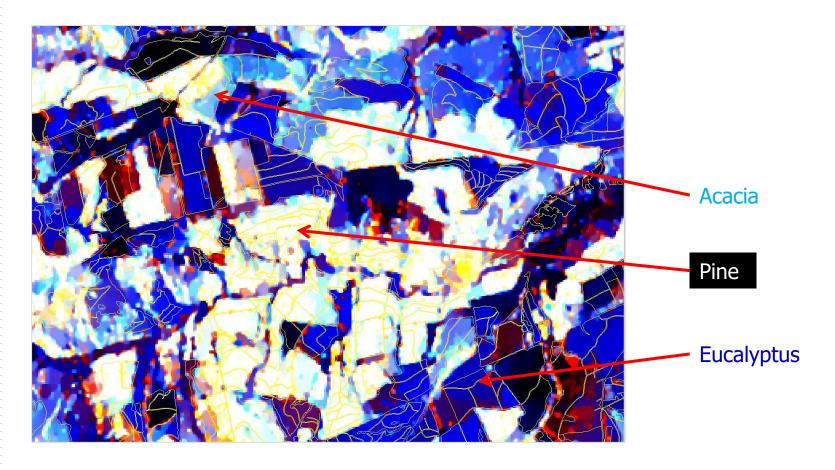




SPOT-4 6 Sept 2009



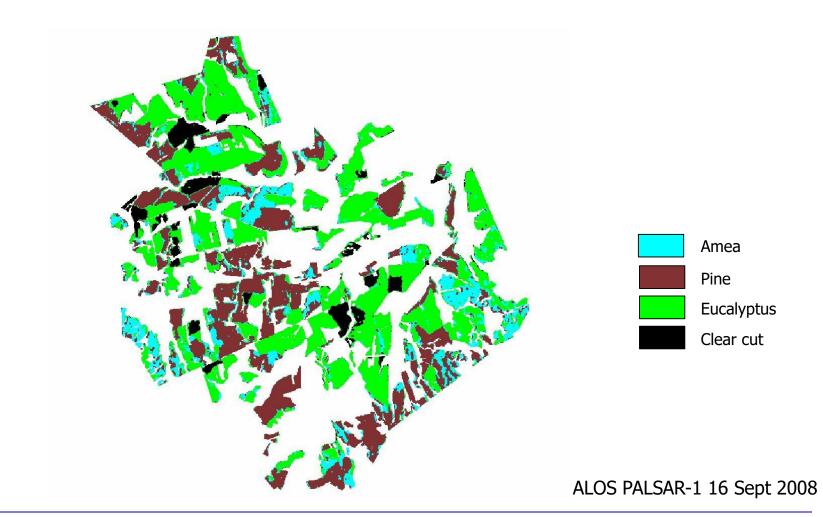
Genera detection – Eucalyptus, Pine, Amea



ALOS PALSAR-1 HH/HV 16 Sept 2008



Genera detection – Eucalyptus, Pine, Amea





Content

- 1. Key SAR basics
- 2. Past, existent, forthcoming SAR systems
- 3. SAR data processing
- 4. Agriculture
 - Rice in Asia
 - Small plot agriculture in Africa
- 5. Agriculture and other land covers in Africa
- 6. Forestry
 - Natural forest
 - Forest plantation
 - Bio-physical parameters
- 7. Digital Elevation Model
 - Fusion SAR interferometry-Optical stereo



Today's main approaches

- 1. By using low frequency VHF band, 20-90 MHz the attenuation is significantly reduced, and the large scale structures (of the order of the wavelength) dominate the backscatter.
- 2. Tree height can be inferred using airborne single-pass Interferometric SAR (InSAR) dual frequency (X -and P-band) data, or alternatively, LIght Detection And Ranging (LIDAR) systems. AGB is subsequently retrieved by species using allometric equations.
- 3. Forest biomass is estimated through regressions based on exponential function exclusively derived from single frequency single/dual polarizations, ensemble regression models at eco-regions level are developed by considering multi-sensor data and bio- and geo-physical gradient data (elevation, slope, aspect, canopy density, and land cover).

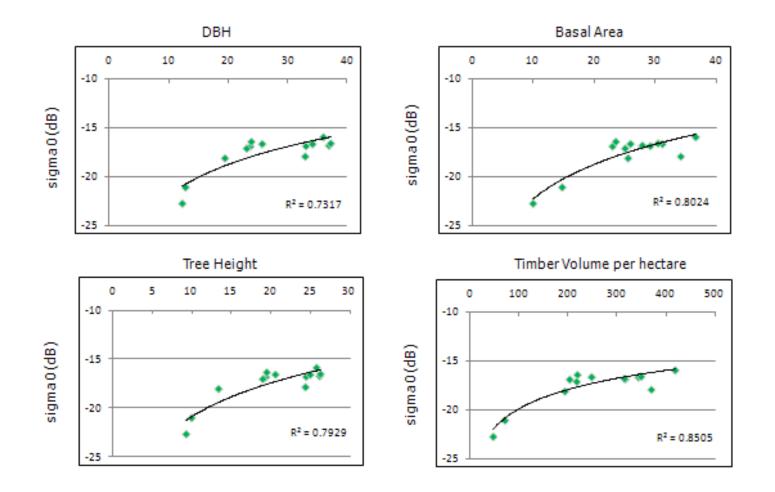


Today's main approaches

Key requirement is that a large stack of observations at C-band is available. The estimation of the GSV (Growing Stock Volume) is carried out by means of an algorithm, which combines hyper-temporal C-band data stacks, the inversion of a water-cloud model relating the GSV to the forest backscatter, and a multi-temporal combination of GSV estimates from each image. Traditionally, model training is based on in situ measurements for unvegetated and dense forest areas and corresponding forest backscatter measurements. The novel aspect is that these are identified by means of the MODIS Vegetation Continuous Fields (VCF) product, where corresponding measures are computed. The hyper-temporal combination exploits the different sensitivities of the forest backscatter to GSV, which can be retrieved from the estimates of the a priori unknown model parameters.

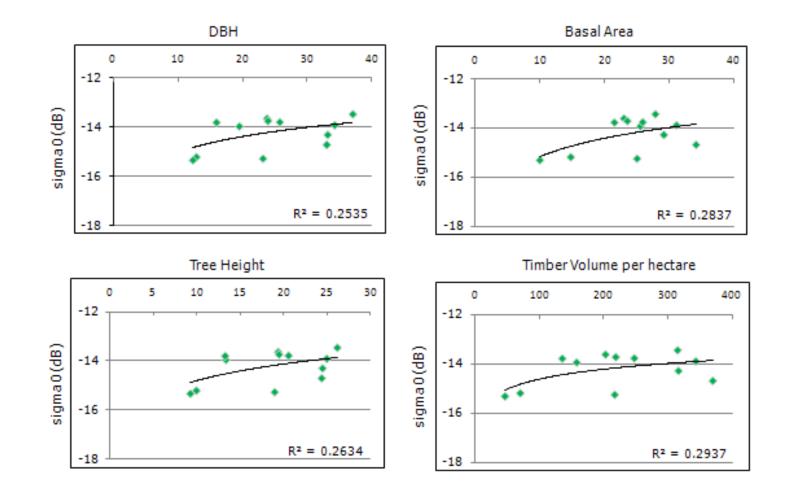


L-band HV vs. biophysical parameters



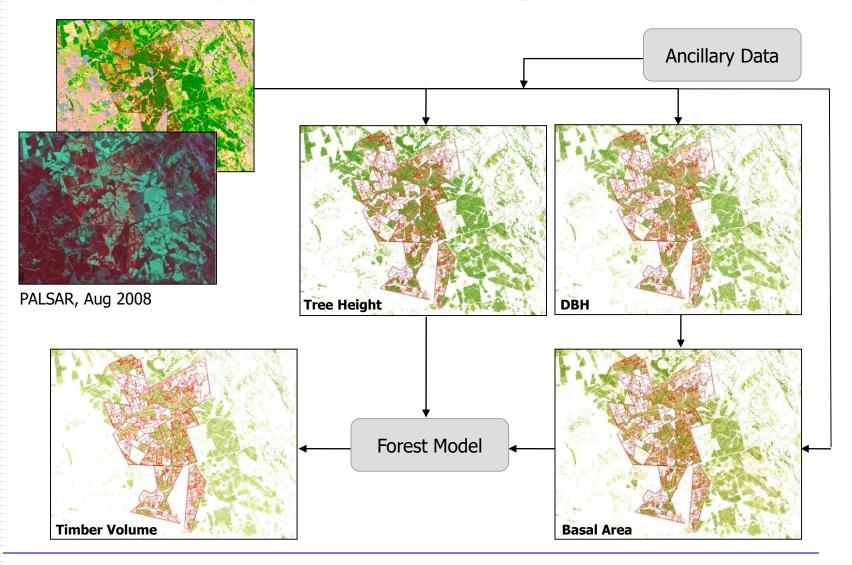


C-band HV vs. biophysical parameters





Estimation of biophysical parameters using PALSAR-1 HH/HV





Assessment

Variable	Route	Difference %
BA based on PALSAR-1	Extrapolation	-7.9
TH based on PALSAR-1	Extrapolation	-3.3
DBH based on PALSAR-1	Extrapolation	-1.3
TPH using PALSAR-1 BA, PALSAR-1 DBH		+2.7
TPH using PALSAR-1 BA and measured DBH	Hybrid	-10.0
Modeled TV using PALSAR-1 BA, PALSAR-1 TH, PALSAR-1 DBH	Volume equation	-11.1
Modeled TV using PALSAR-1 TH, PALSAR-1 BA, with calculated TPH using measured DBH	Hybrid	-11.7

BA = Basal Area

DBH = Diameter at Breast Height

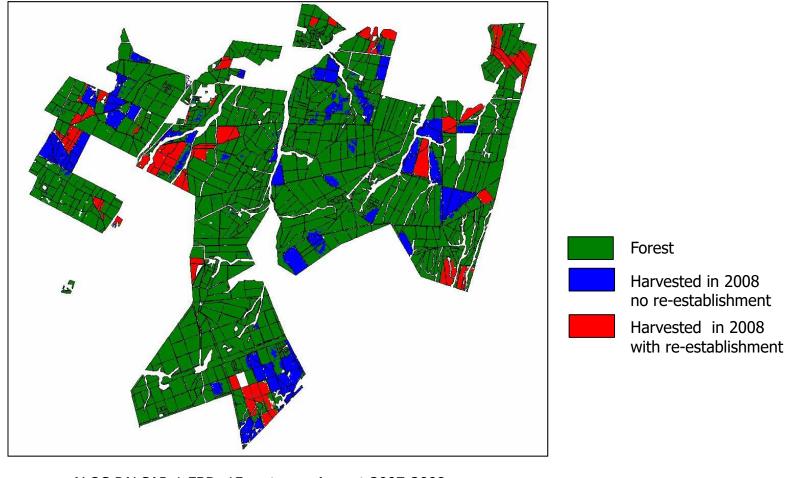
TH = Tree Height

TPH = Tree Per Hectare (derived from BA and DBH)

TV = Timber Volume

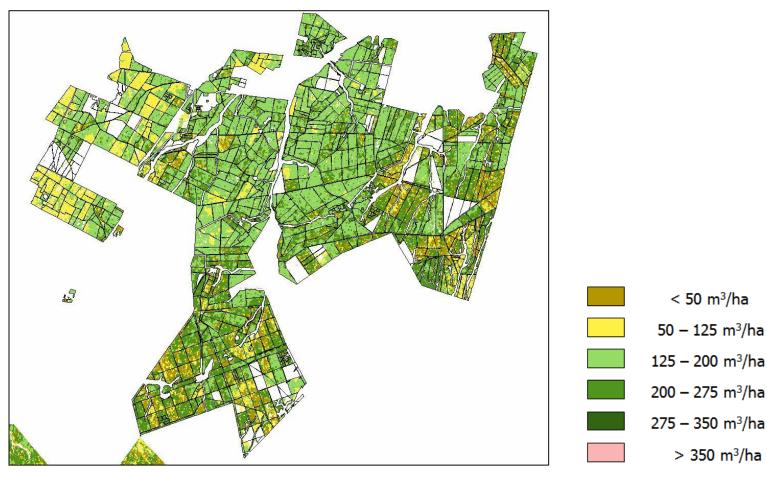


Forest area including harvested and re-established areas



ALOS PALSAR-1 FBD, 15 meter - August 2007-2008

Timber Volume Estimation



ALOS PALSAR-1 FBD, 15 meter - August 2007-2008

> 350 m³/ha

 $< 50 \text{ m}^{3}/\text{ha}$



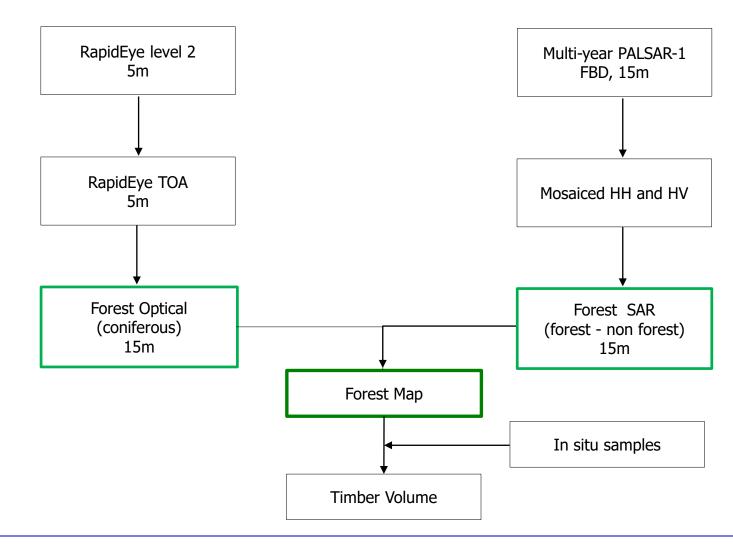
Lessons learned

In **forest plantation** in South Africa, the estimated bio-physical parameters are more than satisfactory. Specifically:

- <u>The SAR obtained results</u> for DBH and Height are very good, so much so that supplanting the SAR DBH measurement with the field-measured DBH degraded the accuracy of the results.
- <u>Using SAR derived variables</u> as inputs into standard volume equations showed good results for standing volume estimation. This implies that only DBH, TH and BA need to be estimated from SAR data in order to obtain acceptably accurate volume estimates.
- <u>The hybrid approach</u> (combining SAR with field-measured data) did not result in improved results for either volume or number of trees per hectare.

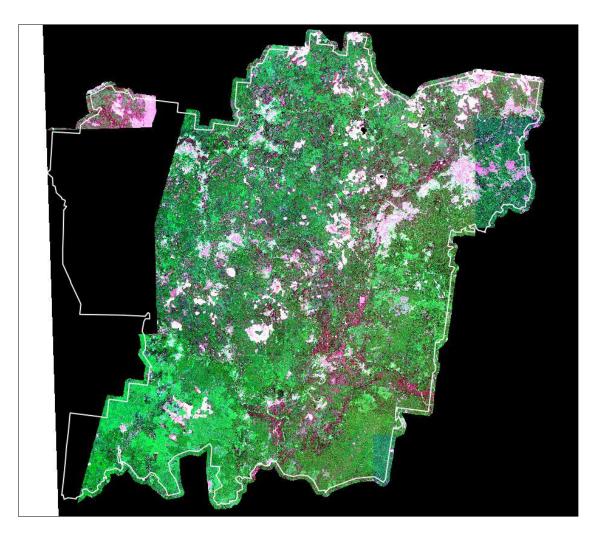


Forest Area and Timber Volume





RapidEye mosaic, June-August 2010



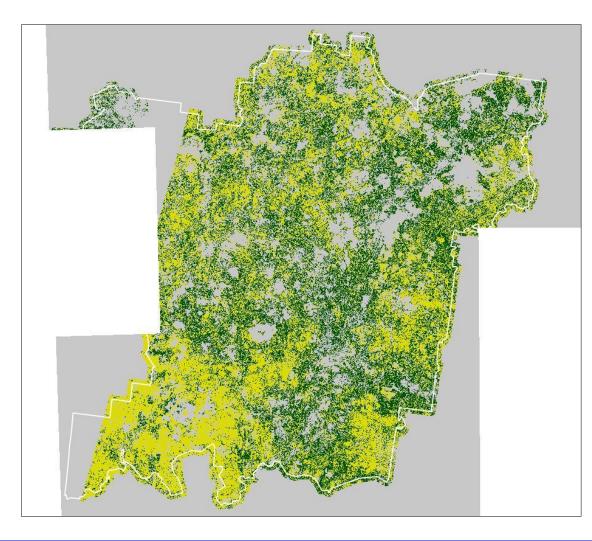
Red

Green

NIR



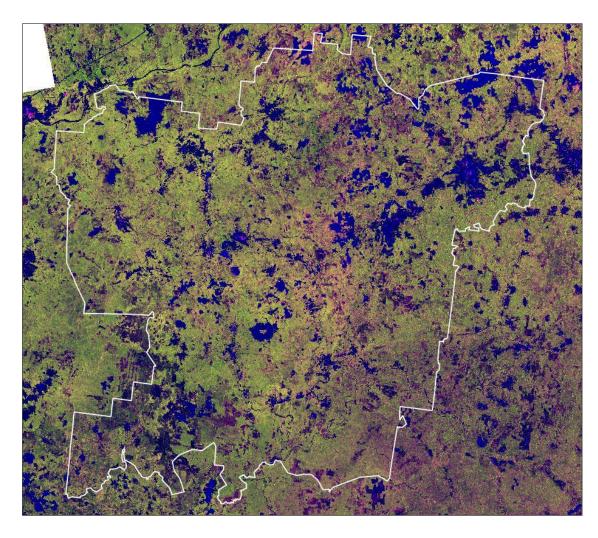
Forest area based in RapidEye



Deciduous & grassland Coniferous



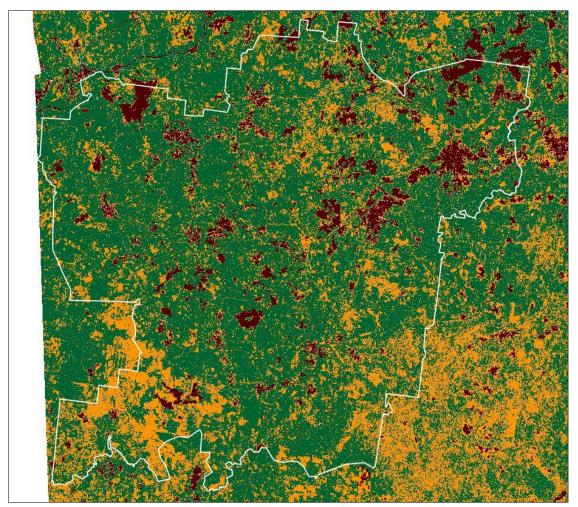
PALSAR-1 HH/HV data, August 2009 and 2010



HH HV HH/HV



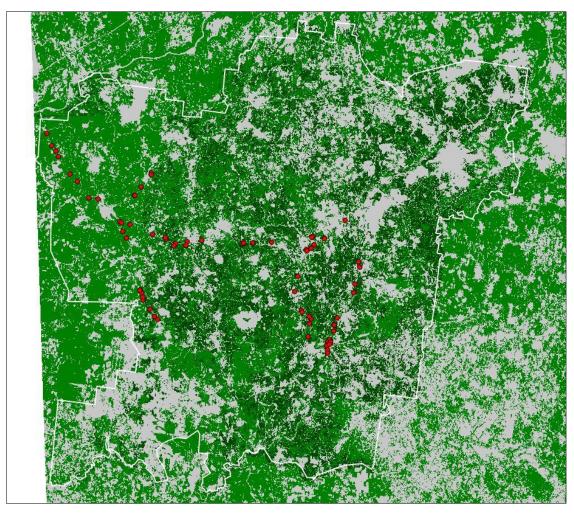
Forest area based in PALSAR-1 HH/HV



Forest



Forest area

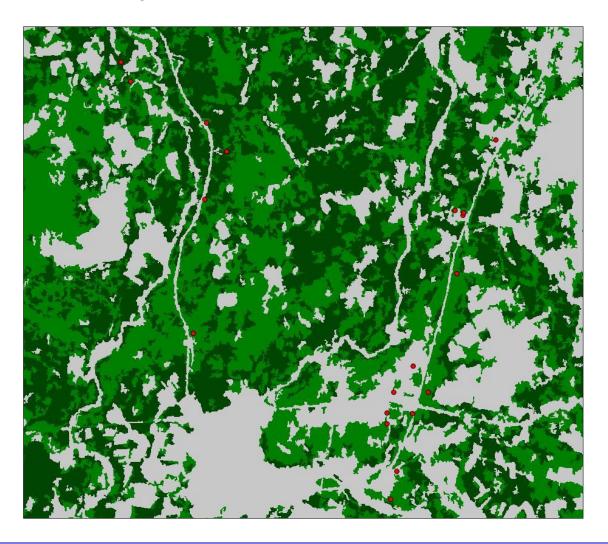


Forest - coniferous

Forest – non-coniferous

Sarmap your information gateway

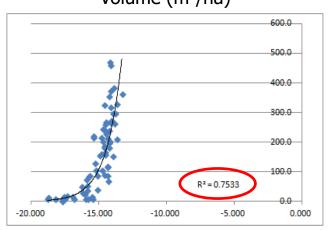
Forest area, detail



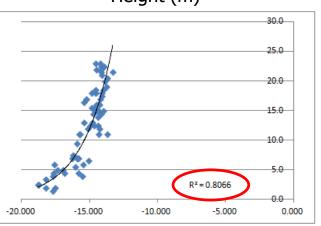


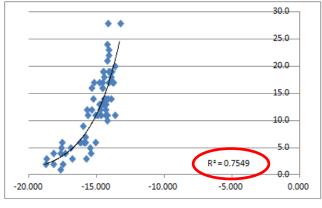
Relationship between σ^{o}_{HV} and forest bio-physical parameters





Height (m)

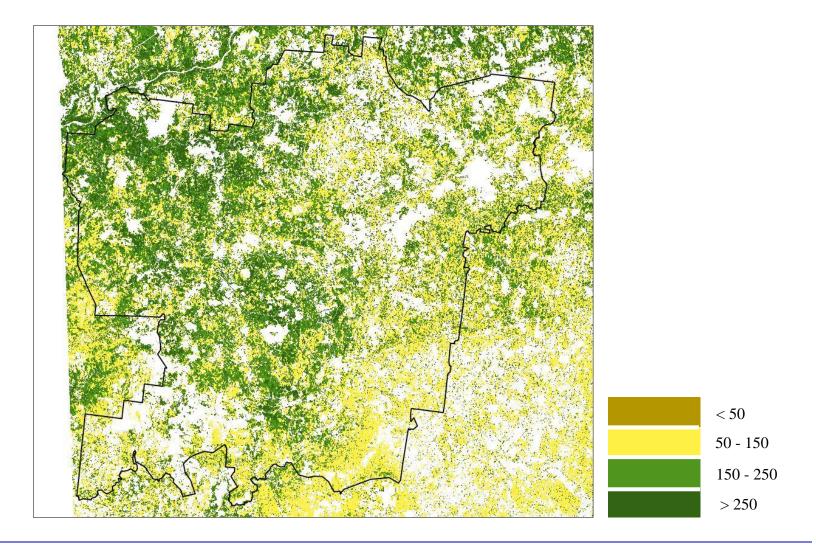




DBH (cm)

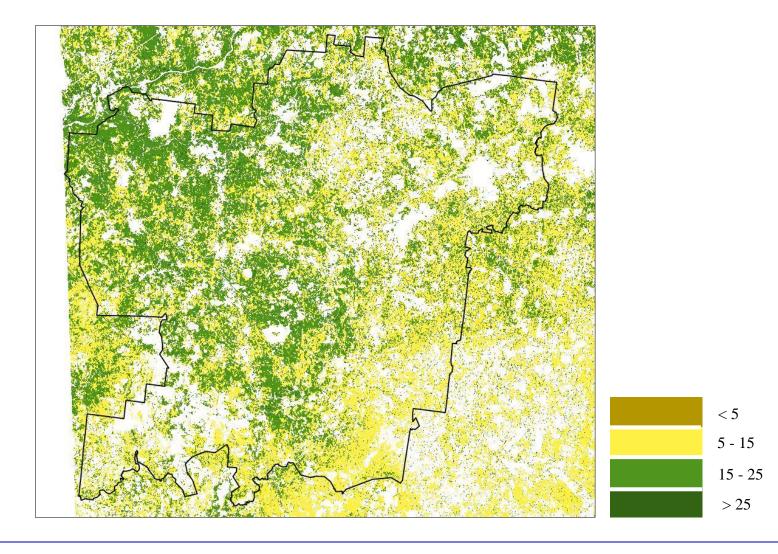
Sarmap your information gateway

Estimated forest volume (m³/ha)



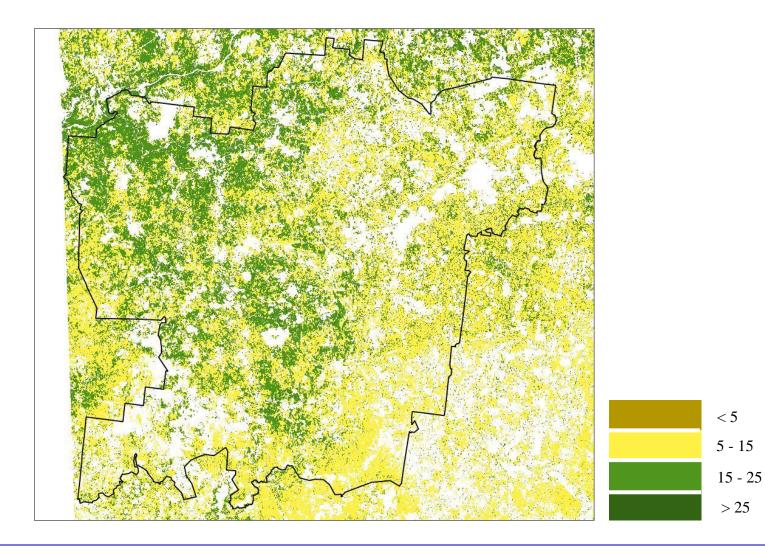


Estimated forest height (m)



Sarma your information gateway

Estimated forest DBH (cm)



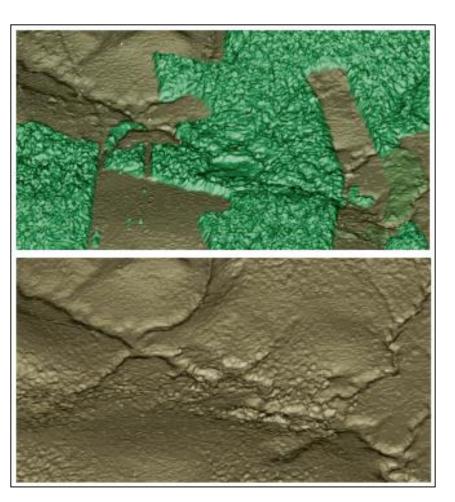


Lessons learned

- In **natural forest**, the estimated bio-physical parameters are more than satisfactory.
- The use of multi-annual SAR data is crucial, in order to obtain reliable relationships backscattering coefficient bio-physical parameter.
- However, due to the existence of different forest types, firstly, a forest type differentiation should be carried out and subsequently the different relationships backscattering coefficient - bio-physical parameter correspondingly applied.



Forest height estimation using dual frequency InSAR system



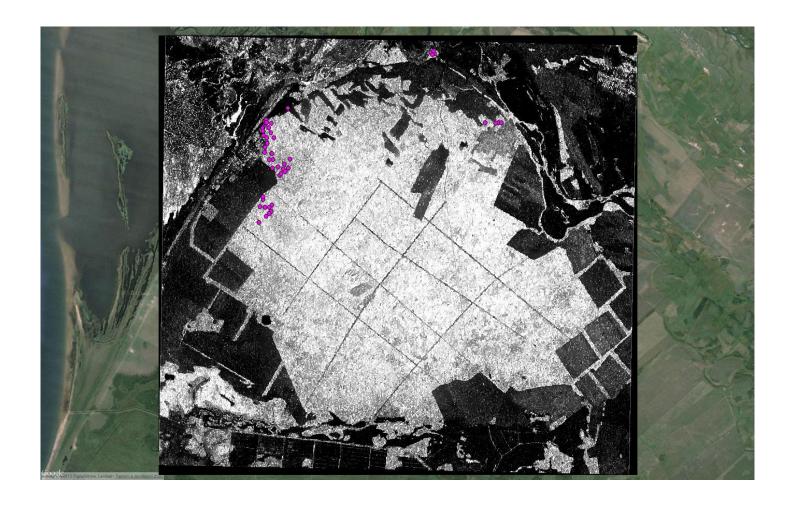
X-band

P-band

OrbiSAR-1 system, 5m

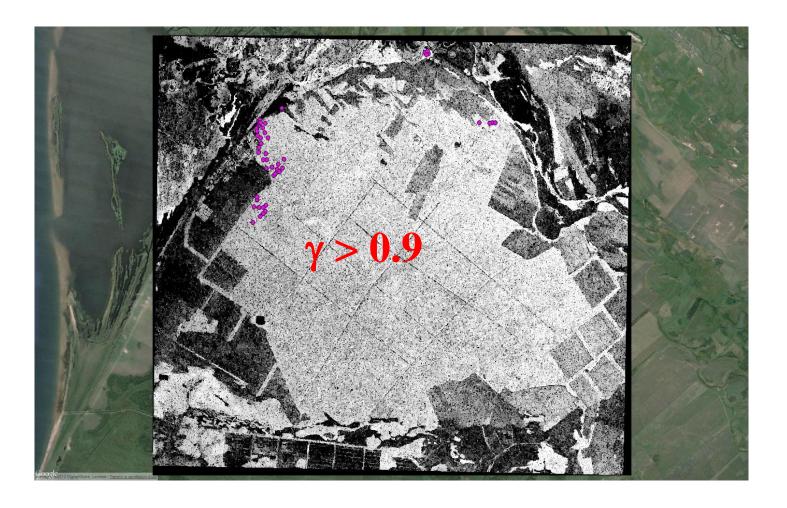
Sarma your information gateway

TanDEM-X σ⁰



Sarmap your information gateway

TanDEM-X coherence





TanDEM-X – InSAR data characteristics

•	Spatial re	esolution	5 m
---	------------	-----------	-----

- 2π phase ambiguity 125 m
- Average coherence forest > 0.9
- Theoretical height std dev at 1 look
 6.7 m
- Theoretical height std dev after processing
 4 m
- Acquisition time February 2012



TanDEM-X – Estimated forest height, February 2012





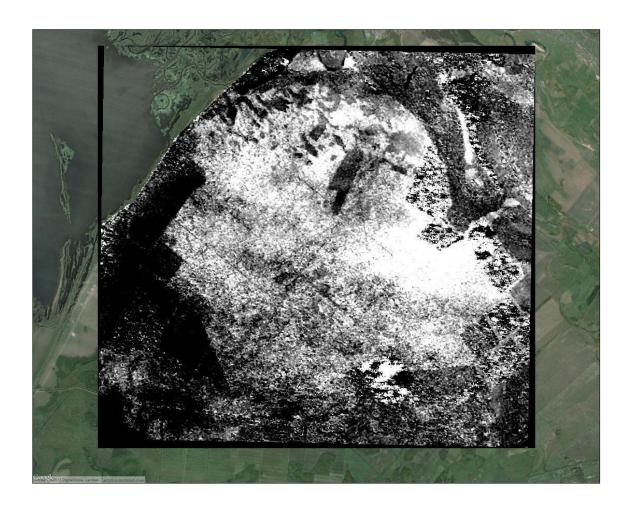
PALSAR-1 FBS – InSAR data characteristics

•	Spatial resolution	10 m
---	--------------------	------

- 2π phase ambiguity 25 m
- Average coherence forest > 0.7
- Theoretical height std dev at 1 look
 4 m
- Theoretical height std dev after processing
 2.5 m
- Acquisition time August-October 2006



PALSAR-1 FBS – Estimated forest height, August-October 2006





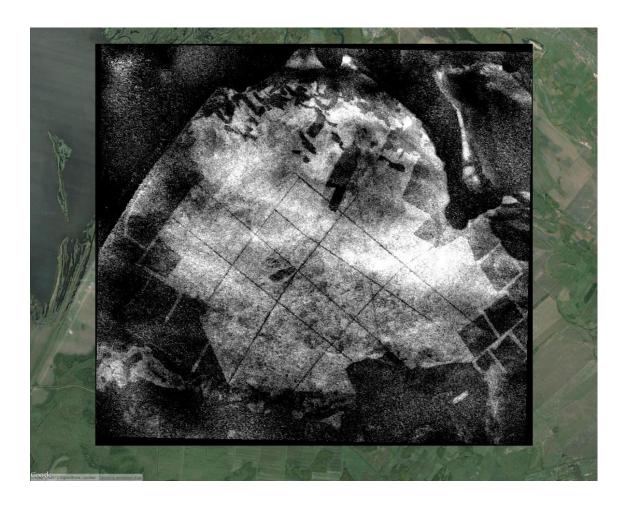
TanDEM-X – InSAR data characteristics

•	Spatial	resolution	5 m
---	----------------	------------	-----

- 2π phase ambiguity 285 m
- Average coherence forest > 0.85
- Theoretical height std dev at 1 look
 15 m
- Theoretical height std dev after processing
 12 m
- Acquisition time
 May 2012

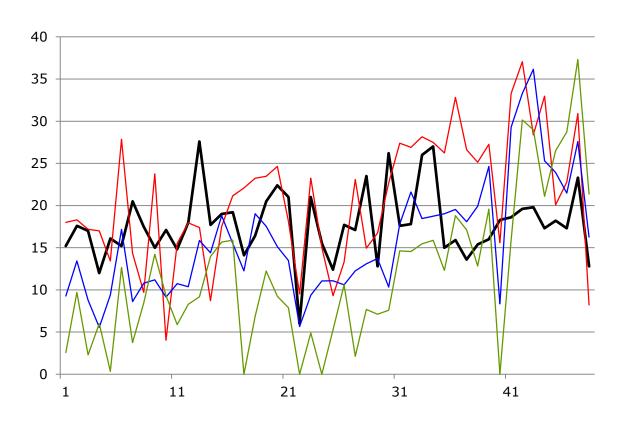
Sarma your information gateway

TanDEM-X – Estimated forest height, May 2012





Estimated forest height – Comparison



in situ TSX May 12 TSX February 12 PALSAR-1 Aug-Oct



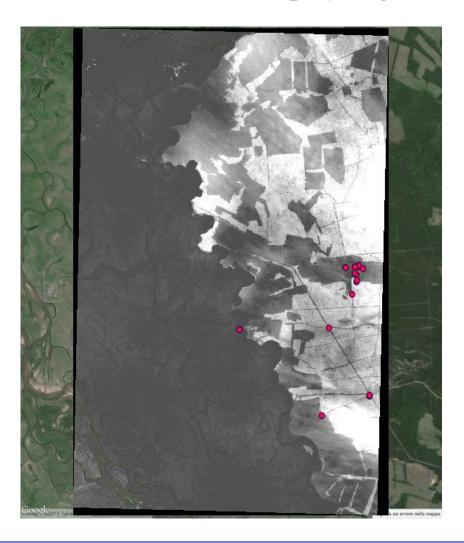
TanDEM-X – InSAR data characteristics

•	Spatial resolution	5 m
---	--------------------	-----

- 2π phase ambiguity 26 m
- Average coherence forest > 0.85
- Theoretical height std dev at 1 look 2 m
- Theoretical height std dev after processing > 1 m
- Acquisition time
 May 2013

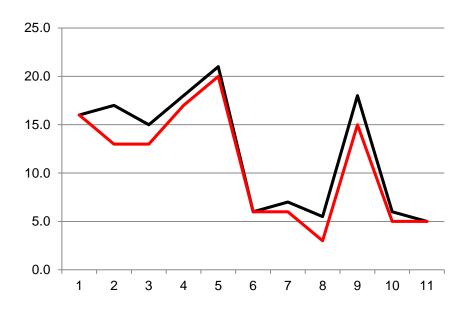


TanDEM-X – Estimated forest height, May 2013





Estimated forest height – Comparison



in situ TSX May 2013



Lessons learned

- **Baseline** and particularly **acquisition date** (winter acquisitions) play a key role, especially if the forest consists of deciduous and coniferous trees.
- A final consideration is on the accuracy of the **terrestrial measurements**: these are still unknown. It is, however, well known that:
 - In forestry, in particular in dense close canopy, the GPS X-Y location is typically inaccurate (several tens of meters): this depends upon the foliage coverage, device, amount of available GPS, atmosphere, and processing software. All this information is not available. Moreover, human errors may occur as shown in the next slide (note that this location is where the inferred TSX height is higher than the GCP one).
 - In (simple) dense close canopy in deciduous forest conditions (as in this case), terrestrial forest height estimations are typically overestimated by 10 to 20%.



Content

- 1. Key SAR basics
- 2. Past, existent, forthcoming SAR systems
- 3. SAR data processing
- 4. Agriculture
 - Rice in Asia
 - Small plot agriculture in Africa
- 5. Agriculture and other land cover in Africa
- 6. Forestry
 - Natural forest
 - Forest plantation
 - Bio-physical parameters
- 7. Digital Elevation Model
 - Fusion SAR interferometry-Optical stereo



Relevance of precise DEM

Remote Sensing sector

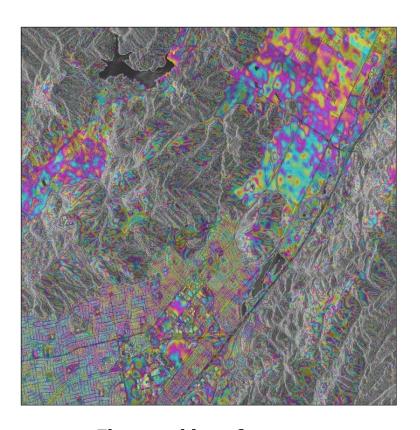
- Improvement of geo-referencing (ortho-rectification)
- Improvement of co-registration
- Improvement of phase unwrapping quality
- Improvement of land motion estimations
- Improvement of focusing quality

Geographic Information System sector

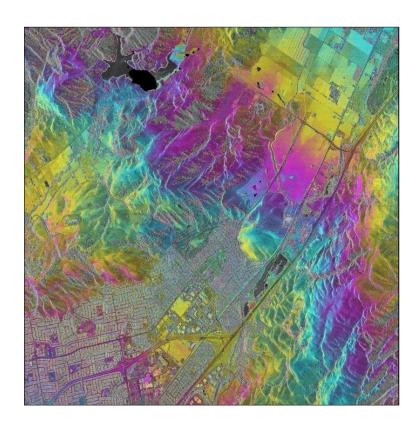
- Hydrology
- Risk assessment
- Telecommunication
- Visualization
- Forestry
- Planning and Construction
- Coastline



Relevance of precise DEM



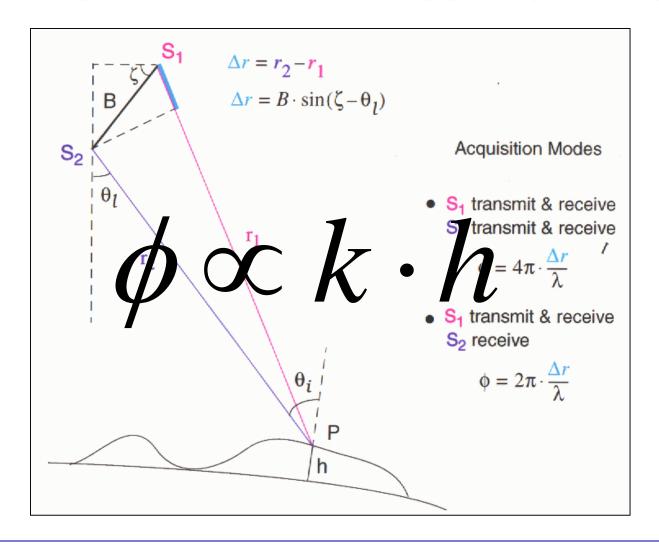
Flattened interferogram based on SRTM DEM



Flattened interferogram based on Laser DSM



Synthetic Aperture Radar Interferometry (InSAR) — Principle



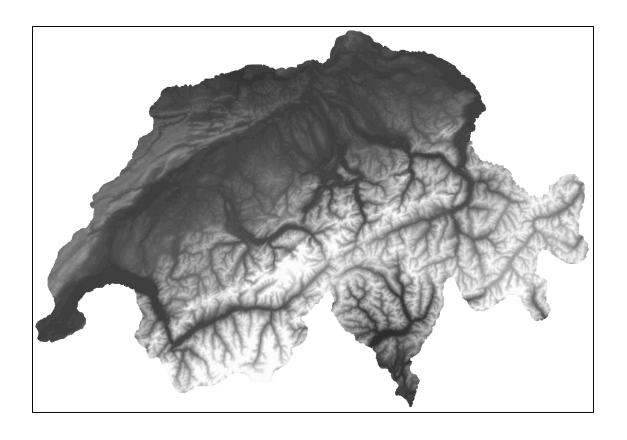


Interferometric Processing

- Interferogram generation
- DEM Interferogram flattening
- Adaptive filter and coherence generation
- Phase unwrapping
- Orbital refinement
- Phase to map

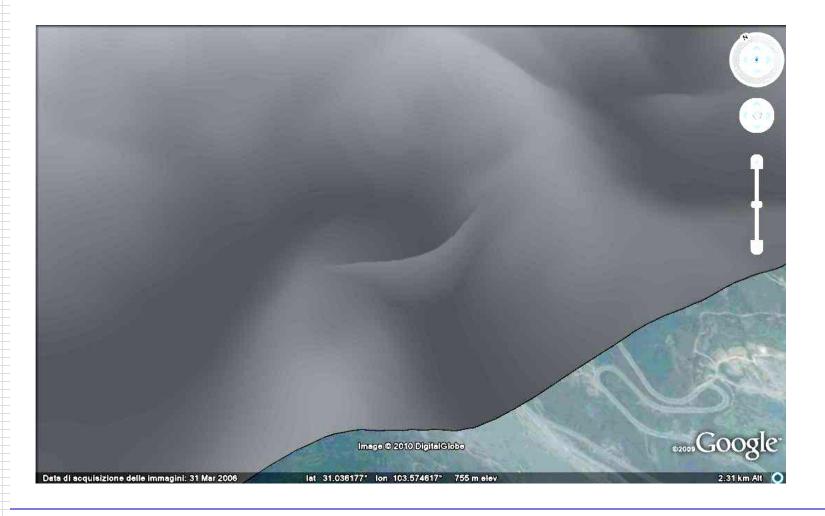


Spaceborne SAR Interferometry – ERS-Tandem, 25m



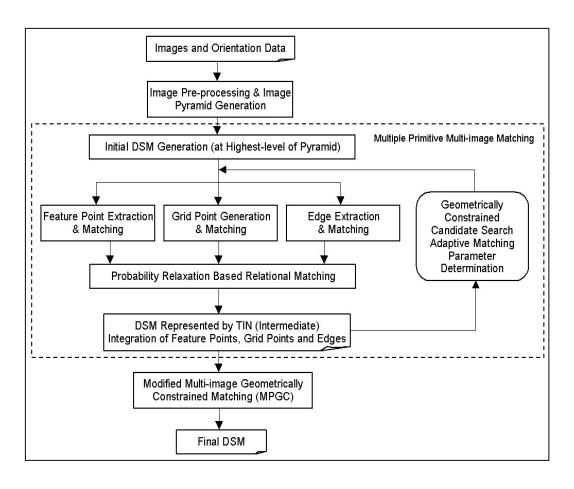


Spaceborne SAR Interferometry — Cosmo-SkyMed-1/2, 1m





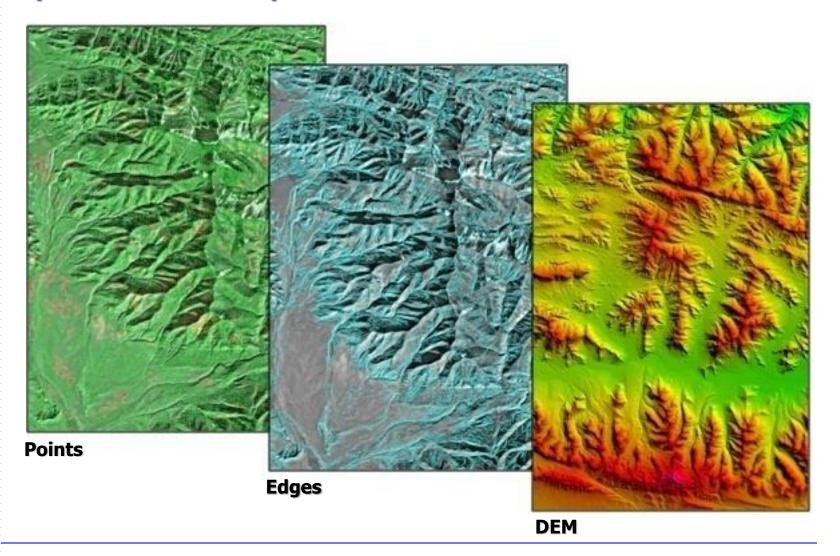
Stereo-optical processing chain*



^{*} Former SAT-PP, ported, streamlined, and extended by sarmap

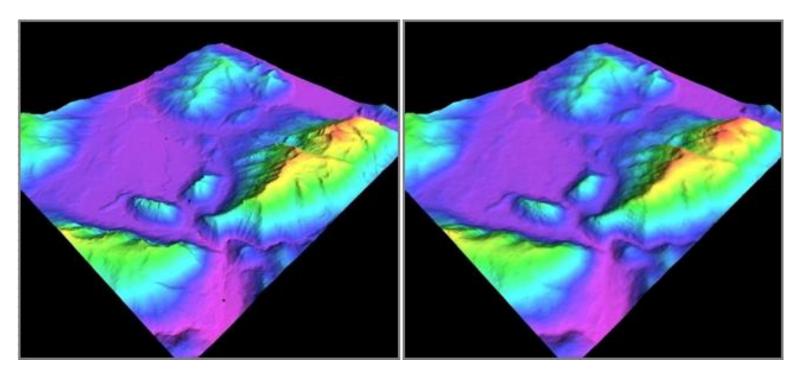


Spaceborne stereo-optical – SPOT-5 HRS





Spaceborne stereo-optical – SPOT-5 HRS

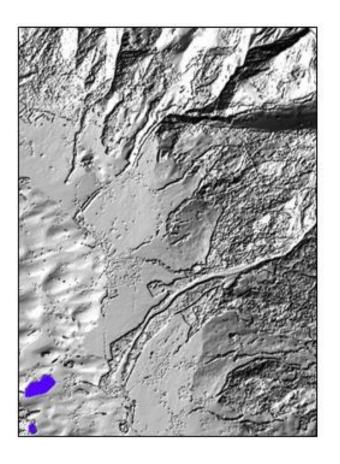


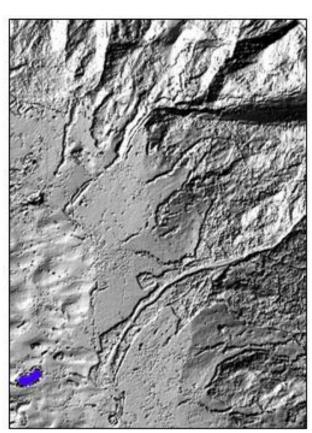
Reference DSM (5 m)

SPOT-5 DSM (25 m)



Spaceborne stereo-optical — IKONOS and comparison with LIDAR





LIDAR DSM (2 m)

IKONOS DSM (5 m)



SAR interferometry versus stereo-optical

	interferometry	stereo-optical
Influenced by clouds	NO	YES
Influenced by atmospheric water vapour	YES	NO
Influenced by sun illumination	NO	YES
Reliable height estimation on poorly textured areas	YES	NO
Accurate on edge features	NO	YES
Layover effects	YES	NO
Surface height	YES	YES
Terrain height	YES	NO



Precision, Reliability, Weighting, Feature maps

Precision estimated by exploiting

- baseline
- wavelength
- interferometric coherence
- local incidence angle (slope and aspect wrt the sensor)
- spatial ground resolution

Reliability estimated by exploiting

- cross-correlation
- slope and aspect

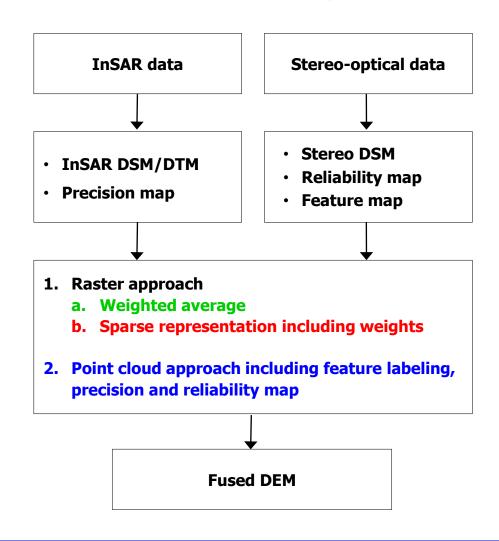
Weights a weighting factor ranging from 0 to 1 is otained by normalizing precision

and reliability.

Feature map features (edges in particular) detected and labeled in the point cloud.

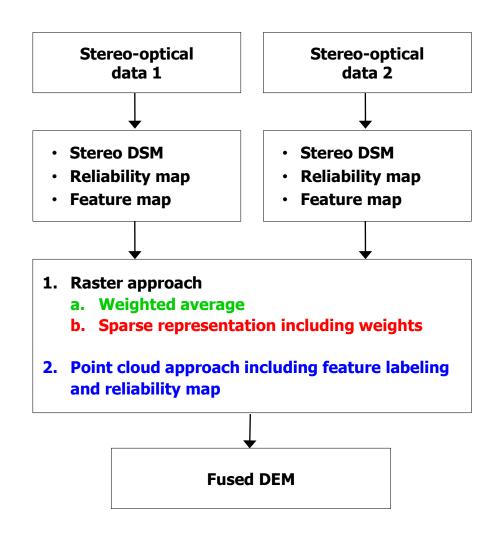


DEM fusion – Case 1: InSAR - stereo-optical



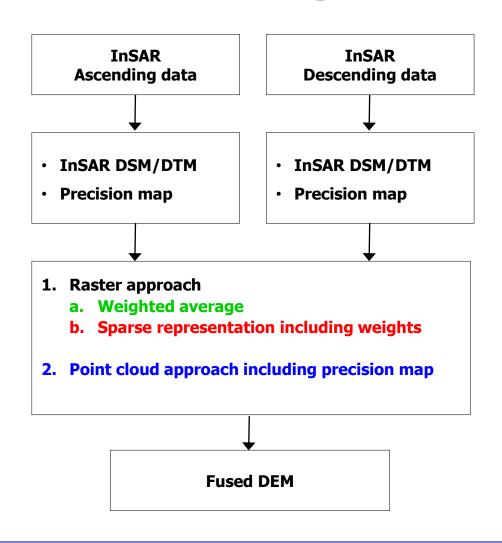


DEM fusion — Case 2: stereo-optical - stereo-optical



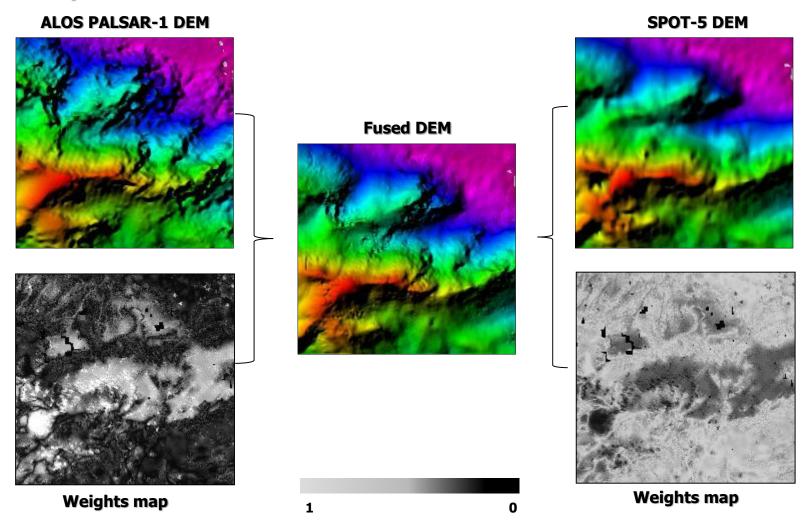


DEM fusion – Case 3: InSAR Ascending - InSAR Descending



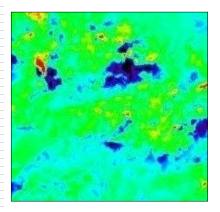


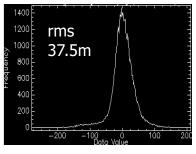
Example – DEM fusion based on ALOS-PALSAR-1 and SPOT-5

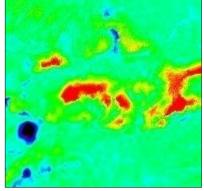


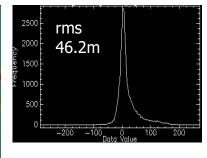


Example – Quantitative assessment



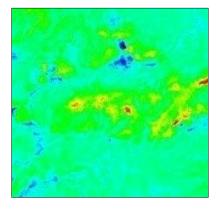


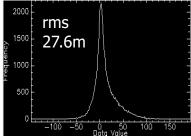




PALSAR-1 minus reference DSM

SPOT-5 minus reference DSM





Fused DEM minus reference DSM



Lessons learned

- A rigorous data processing (SAR and optical) is doubtless fundamental, in particular:
 - the Wallis filtering (for edge enhancement for optical data);
 - the phase unwrapping;
 - the height derivation (absolute phase calibration, image orientation);
 - the DEMs geo-location (range-Doppler, image orientation).
- The use of SAR interferometry and stereo-optical data is essential for the provision of high quality elevation products.
- Point cloud DEM fusion is doubtless the most suitable approach, because the error propagation derived from the data interpolation is minimized.
- Sparse representation is an interesting approach, however of difficult use due to a suitable dictionary definition.



All data have been processed using









• Basic

It includes a set of processing steps for the generation of SAR products based on intensity. This module is complemented by a multi-purpose tool.

This module is complemented by:

Focusing

It supports the focusing of ERS-1/2 SAR, JERS-1 SAR, ENVISAT ASAR and ALOS PALSAR-1 data.

Gamma & Gaussian Filter

It includes a whole family of SAR specific filters. They are particularly efficient to reduce speckle, while preserving the radar reflectivity, the textural properties and the spatial resolution, especially in strongly textured SAR images. Developed in collaboration with Privateers.





Interferometry

It supports the processing of Interferometric SAR (2-pass interferometry, InSAR) and Differential Interferometric SAR (n-pass interferometry, DInSAR) data for the generation of Digital Elevation Model, Coherence, and Land Displacement/ Deformation maps.

This module is complemented by:

ScanSAR Interferometry

It offers the capabilities to process InSAR and DInSAR data over large areas (400 by 400 km). Developed in collaboration with Aresys.

Interferometric Stacking

Based on Small Baseline Subset (SBAS) and Persistent Scatterers (PS) techniques this module enables to determine displacements of individual features on the ground.

Radargrammetry

It offers the capabilities to generate Digital Elevation Model from Stereo-SAR data.

• SAR Polarimetry / Polarimetric Interferometry

The PolSAR/PolInSAR module supports the processing of polarimetric and polarimetric interferometric SAR data.





Quality Assessment Tool

In order to quantitatively assess the geometric, radiometric, and polarimetric quality of SAR products, a Quality Assessment Tool (QAT) based on a solid methodology is proposed. The overall architecture of the QAT system supports the quality assessment for ENVISAT ASAR (IM,AP,WS) and RADARSAT-1 and -2 (FB,SB,WB,EB,ScanSAR) data.





This module - developed in collaboration with 4DiXplorer - supports the processing of **spaceborne and UAV stereo-optical data** from radiometric processing, image orientation to automatic Digital Elevation Model (DEM) and ortho-image generation.

Key features of this module are:

- **DEM generation**, which is based on an advanced matching algorithm. The approach uses a coarse-to-fine hierarchical solution with an effective combination of several image matching algorithms and automatic quality control. Moreover, the new characteristics provided by the latest imaging systems, i.e. the multiple-view terrain coverage and the high quality image data, are also efficiently utilized.
- The **DEM fusion** by considering sensor's characteristics. The proposed functionality supports the fusion of:
 - stereo-optical InSAR or stereo-SAR
 - InSAR stereo-SAR
 - stereo-optical stereo-optical
 - InSAR InSAR
 - stereo-SAR stereo-SAR



Acknowledgements

- The European Space Agency is acknowledged for the provision of ENVISAT ASAR data.
- The Japanese Aerospace Exploration Agency is acknowledged for the provision of ALOS PALSAR-1 data.
- The **Italian Space Agency** and **e-GEOS** are acknowledged for the provision of Cosmo-SkyMed data.
- Airbus Space Defence is acknowledged for the provision of TerraSAR-X data.
- The **US Geological Servey** is acknowledged for the provision of MODIS data.
- **RIICE** (www.rice.org) is acknowledged for the provision of RIICE product examples.



Thank you for your attention